



**A Review of Electrolyte Materials and Compositions for  
electrochemical supercapacitors**

Journal:	<i>Chemical Society Reviews</i>
Manuscript ID:	CS-REV-04-2015-000303
Article Type:	Review Article
Date Submitted by the Author:	13-Apr-2015
Complete List of Authors:	Zhong, Cheng; Tianjin University, School of Materials Science and Engineering Yida, Deng; Tianjin University, School of Materials Science and Engineering Hu, Wenbin; Tianjin University, School of Materials Science and Engineering Qiao, Jinli; Donghua University, School of Environmental Engineering Zhang, Lei; National Research Council of Canada, Zhang, JiuJun; Inst Fuel Cell Innovat, National Research Council Canada

# A review of electrolyte materials and compositions for electrochemical supercapacitors

Cheng Zhong,<sup>a</sup> Yida Deng,<sup>b</sup> Wenbin Hu,<sup>a,b,\*</sup> Jinli Qiao,<sup>c</sup> Lei Zhang,<sup>d</sup> Jiuju Zhang<sup>d,\*</sup>

<sup>a</sup> Key Laboratory of Advanced Ceramics and Machining Technology (Ministry of Education), School of Materials Science and Engineering, Tianjin University, Tianjin 300072, China

<sup>b</sup> Tianjin Key Laboratory of Composite and Functional Materials, Tianjin University, Tianjin 300072, China

<sup>c</sup> School of Environmental Engineering, Donghua University, Shanghai, China

<sup>d</sup> Department of Chemical & Biochemical Engineering, University of British Columbia, Vancouver, BC, Canada

**Abstract:** Electrolytes have been identified as one of the most influential components in the performance of electrochemical supercapacitors (ESs), which include: electrical double-layer capacitors, pseudocapacitors and hybrid supercapacitors. This paper reviews recent progress in the research and development of ES electrolytes. The electrolytes are classified into several categories, including: aqueous, organic, ionic liquids, solid-state or quasi-solid-state, as well as redox-active electrolytes. Effects of electrolyte properties on ES performance are discussed in detail. The principles and methods of designing and optimizing electrolytes for ES performance and application are highlighted through a comprehensive analysis of the literature. Interaction among the electrolytes, electro-active materials and inactive components (current collectors, binders, and separators) are discussed. The challenges of producing high-performing electrolytes are analyzed. Several possible research directions to overcome these challenges are proposed for future efforts, with the main aim to improve ESs' energy density without sacrificing existing advantages (e.g., high power density and long cycle-life). (507 references)

## 1. Introduction

Significant worldwide increases in the consumption of fossil fuels, resulting from the rapid growth of the global economy, are producing two major associated issues. The first is the accelerating depletion/exhaustion of existing fossil fuel reserves and the second is the affiliated environmental problems e.g., increasing greenhouse gas emissions and general air and water pollution. Taken together these items constitute the basis of an urgent, worldwide concern about the future, sustainable development and health of our society's ecosystem. The need to develop and scale up sustainable,

---

\* Corresponding authors. E-mails: wbhu@tju.edu.cn (W.B. Hu); [jiujun.zhang@nrc.gc.ca](mailto:jiujun.zhang@nrc.gc.ca) (J.J. Zhang).

clean energy sources and their associated technologies is recognized worldwide as an urgent priority. Most renewable clean energy sources are highly dependent on the time of day and regional weather conditions. Development of related energy conversion and energy storage devices is therefore required in order to effectively harvest these intermittent energy sources. In this regard, batteries, electrochemical supercapacitors (ESs) and fuel cells are all recognized as three kinds of the most important electrochemical energy storage/conversion devices.

The ES, also known as a supercapacitor or ultracapacitor, has attracted considerable interest in both academia and industry because it has some distinct advantages such as higher power density induced by a fast charging/discharging rate (in seconds) and a long cycle life (>100,000 cycles) when compared to batteries and fuel cells.<sup>1</sup> Depending on the charge storage mechanism, ESs can be briefly classified as electrochemical double-layer capacitors (EDLCs), pseudocapacitors and hybrid-capacitors. Compared to both pseudocapacitors and hybrid-capacitors, EDLCs constitute the majority of currently available commercial ESs, mainly due to their technical maturity.

In an evaluation of electrochemical energy devices, besides cycle-life (or lifetime), both their energy density and power density are the two most important properties. The relationship between these two important properties can be expressed by the Ragone plot. Fig. 1 shows the Ragone plots for several typical electrochemical energy storage devices.<sup>1</sup> It can be clearly seen from these Ragone plots that supercapacitors are currently located between the conventional dielectric capacitors and batteries/fuel cells. Despite the much lower energy density compared to the batteries/fuel cells, ESs can have much higher power densities. This makes them promising for applications in current stabilization when accessing intermittent renewable energy sources. In addition, ESs have also attracted considerable interest in a wide variety of applications requiring high power density, such as portable electronics, electric or hybrid electric vehicles, aircraft and smart grids. For example, in the case of both hybrid and electric vehicles including fuel cell ones, ESs could provide high power density for short-term acceleration and recovery of energy during braking, thus saving energy and protecting the batteries from the high-frequency rapid discharging and charging process (dynamic operation).

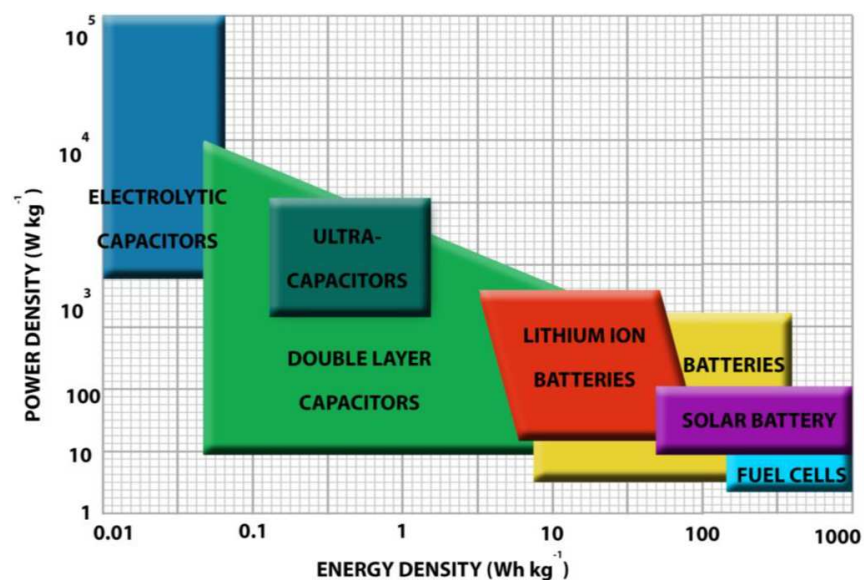


Fig. 1 Ragone plots for representative energy storage devices of batteries, fuel cells, and supercapacitors. Reprinted with permission from Ref. 2 (open access).

However, the major challenge for ESs, when compared to both batteries and fuel cells, is their insufficient energy density (for example, EDLCs commonly have an energy density of  $<10 \text{ Wh kg}^{-1}$ ; even for both pseudocapacitors and hybrid-capacitors, their energy densities are generally less than  $50 \text{ Wh kg}^{-1}$ ),<sup>11</sup> which cannot fully meet the growing demand of the applications where high energy density is required. To overcome this challenge, extensive work has been devoted to increase the energy density of ESs,<sup>3,4</sup> in order to widen their application scope. Since the energy density ( $E$ ) of ESs is proportional to the capacitance ( $C$ ) and the square of the voltage ( $V$ ), that is:

$$E = \frac{1}{2} CV^2$$

increasing either or both of the capacitance and the cell voltage are effective ways to increase the energy density. This can be achieved through the development of electrode materials with high capacitance, electrolytes (electrolyte salt + solvent) with wide potential windows, and integrated systems with new and optimized structure. To date, these developments can be briefly summarized as follows: (1) increasing the specific capacitance of carbon-based electrodes through the development of a novel carbon structure with a highly effective specific surface area and a high packing density;<sup>5</sup> (2) developing pseudocapacitors based on pseudocapacitive materials (e.g., some electroactive transition-metal oxides and conducting polymers) with high specific capacitance contributed from the pseudo-capacitance;<sup>6</sup> (3) enlarging the cell voltage via the development of a new electrolyte; and (4) exploring ESs with novel structures or new concepts, such as the hybrid (or asymmetric) capacitors, especially the lithium ion capacitors (LICs).<sup>3</sup> Note, these developments are all closely related with each other. Although it is relatively simple to fabricate the individual components (e.g., electrode material, electrolyte and structure) of the ESs, their interaction must be considered to promote the synergetic effect. For example, design and preparation of the porous carbon electrode materials should consider the matching between the pore structure and the size of the electrolyte ions in order to make a high capacitive electrode.<sup>7</sup> The development of some electrolytes should consider their possible interaction with the electrode materials

such as in the case of hybrid capacitors.

Regarding the development of ES electrolytes, widening the potential window of an electrolyte solution, that is, enlarging the cell voltage ( $V$ ), can effectively increase the energy density as seen from the equation of  $E = \frac{1}{2}CV^2$ . It is worth noticing that increasing the cell voltage would be more efficient than increasing the electrode capacitance in terms of energy density improvement. This is because the energy density is proportional to the square of the cell voltage. Therefore, developing new electrolytes/solutions with wide potential windows should be given even higher priority efforts than the development of new electrode materials.

As discussed above, the operating cell voltage of the ESs is largely dependent on the electrochemical stable potential window (ESPW) of the electrolytes if the electrode materials are stable within the working voltage range. For example, aqueous electrolyte-based ESs usually have an operating potential window of about 1.0–1.3 V because the aqueous electrolyte's potential window is about 1.23 V (the potential window of  $H_2/O_2$  evolution reactions at 1.0 atm and room temperature), while the organic electrolyte-based and ionic liquid (IL) based ESs generally have potential windows of 2.5–2.7 and 3.5–4.0 V, respectively. In addition to the determining role of the operating voltage window in ES energy density, electrolytes/solutions also play a critical role in establishing other important properties such as the power density, internal resistance, rate performance, operating temperature range, cycling lifetime, self-discharge and toxicity (as seen in Fig. 2), which are also important in the practical use of ESs.

Besides the property of the electrolyte potential window, the interaction between the electrolyte and the electrode materials also plays an important role in ES performance. For instance, the matching between the electrolyte ion size and the pore size of carbon electrode material has a profound influence on the achievable specific capacitance. The pseudocapacitances from the carbon-based materials and transition metal oxides are also strongly dependent on the nature of the electrolytes.<sup>8</sup> The ionic conductivity of electrolytes plays a significant role in the internal resistance of ESs especially for organic and IL electrolytes. The viscosity, boiling point and freezing point of the electrolytes can also largely affect the thermal stability and thereby the operating temperature range of ESs. As identified, the aging and failure of ESs are also related to the electrochemical decomposition of the electrolytes. Interestingly, the development of some new types of ESs such as flexible or solid-state ESs and micro-ESs also rely heavily on new electrolytes (e.g., solid-state electrolytes).

With respect to the development of ES electrolytes, a large variety of electrolytes, such as aqueous electrolytes, organic electrolytes, IL electrolytes, redox-type electrolytes and solid or semi-solid electrolytes have been explored and great progress has been made during the past several decades. For example, the operating potential window of aqueous electrolyte-based ESs has been reported to be greatly increased to about 2 V by using neutral aqueous electrolytes.<sup>9</sup> A wide variety of new organic electrolytes with wider operating potential windows and less toxicities when compared to the commercial organic electrolytes have been developed for ESs. With the development of IL electrolytes, the operating cell voltage of the corresponding ESs was further increased to 4 V although they suffered from low ionic conductivity and high viscosity.<sup>10</sup> Furthermore, the exploration for solid or semi-solid electrolytes has led to the the invention of flexible or solid-state ESs which are claimed to have no potential leakage issue like the liquid electrolyte-based ESs.<sup>11, 12</sup> Recently, redox-type electrolytes have also been suggested as electrolytes for ESs due to the additional

pseudocapacitance contribution from the redox reaction of the electrolyte at the electrode/electrolyte interface.<sup>13</sup>

In general, the requirements for an ideal electrolyte are as follows: (1) wide potential window; (2) high ionic conductivity; (3) high chemical and electrochemical stability; (4) high chemical and electrochemical inertness to ES components (e.g., electrodes, current collectors and packaging); (5) wide operating temperature range; (6) well-matched with the electrolyte materials; (7) low volatility and flammability; (8) environmentally friendly; and (9) low cost. Actually, it is very difficult for an electrolyte to meet all of these requirements, and each electrolyte has its own advantages and shortcomings. This has motivated tremendous research to improve the overall performance of electrolytes and their associated ESs.

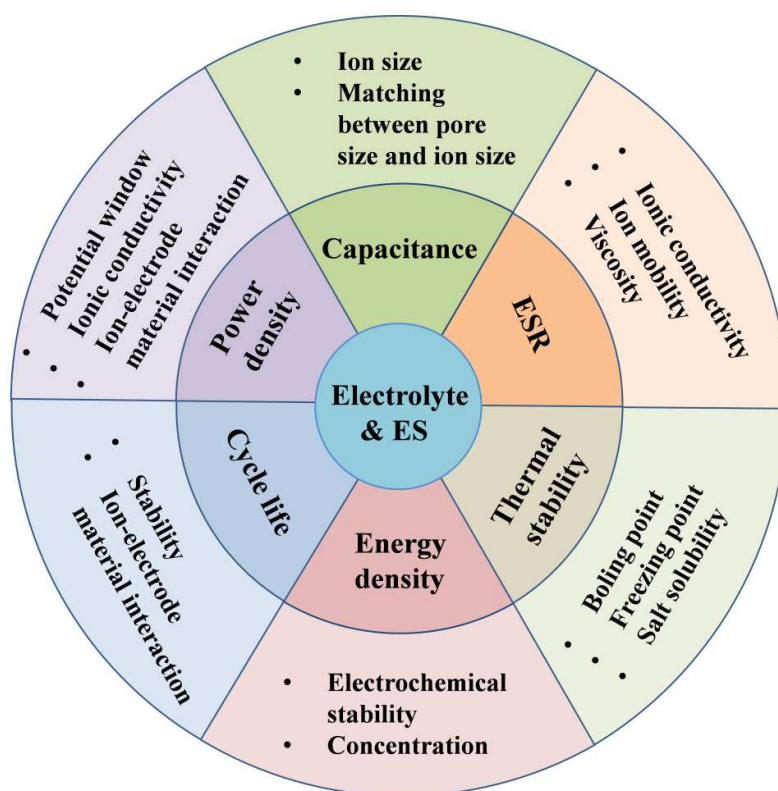


Fig. 2 Effects of the electrolyte on the ES performance.

While there have been many excellent reviews concerning electrode materials,<sup>6, 14-19</sup> reviews focusing on the electrolytes of ESs are rather limited.<sup>10-12, 15, 20, 21</sup> Although several excellent reviews concerning solid polymer electrolytes for ESs have been made previously,<sup>11, 12, 20, 21</sup> it is believed a review covering the latest achievements in this field and providing an insight into the electrolytes development is still necessary. In this review, the first section will give the general performance metrics of ESs and their relationship with electrolytes. This is followed by a comprehensive overview of all kinds of ES electrolytes/solutions, their performance comparisons, and the interactions between electrolytes and electrode materials. The effects of electrolytes on the ES performance will be highlighted to aid understanding

of the performance-affecting factors in design and optimization of electrolytes. Furthermore, the interplay between electrolytes and inactive components of ESs (such as current collectors, binders, and separators) are also discussed. In the final section, the major challenges and perspectives in ES electrolyte/solution research and development are documented and possible research directions in overcoming the challenges are proposed to facilitate efforts in this area.

## 2. Fundamentals of electrochemical supercapacitors

The fundamentals of electrochemical supercapacitors have been reviewed and discussed by many excellent reviews<sup>6, 14-19</sup> and books,<sup>22, 23</sup> which will not be discussed in detail in the present review. Basically, the ES is a special type of capacitor, which is different from the classical electrostatic capacitors (Fig. 3A). ESs can be distinguished in several ways such as the charge storage mechanism, the electrolyte, the electrode material and the cell structure. Depending on the charge storage mechanism, ESs can be classified into three categories:

(1) Electric double-layer capacitors (EDLCs), where the capacitance is produced by the electrostatic charge separation at the interface between the electrode and the electrolyte (Fig. 3B). To maximize the charge storage capacity, the electrode materials are usually made from highly porous carbon materials.

(2) Pseudocapacitors, which rely on fast and reversible faradaic redox reactions to store the charges (Fig. 3C).

(3) Hybrid ESs, which refer to ones using both electrical double-layer (EDL) and faradaic mechanisms to store charges. With the latest developments in this area, some new battery-type hybrid devices, such as LIC (Fig. 3D), and carbon//PbO<sub>2</sub>, have been developed. These devices are regarded as hybrid ESs since they have one EDL or pseudocapacitive electrode combined with the other rechargeable battery-type electrode. The hybrid ESs reviewed in this paper include: a) those based on composite electrodes made from both EDL capacitive materials and pseudocapacitive materials; b) those of asymmetric design with one EDL electrode and the other pseudocapacitive or battery-type electrode; as well as, c) those of asymmetric structure with one pseudocapacitive electrode and the other rechargeable battery-type electrode.

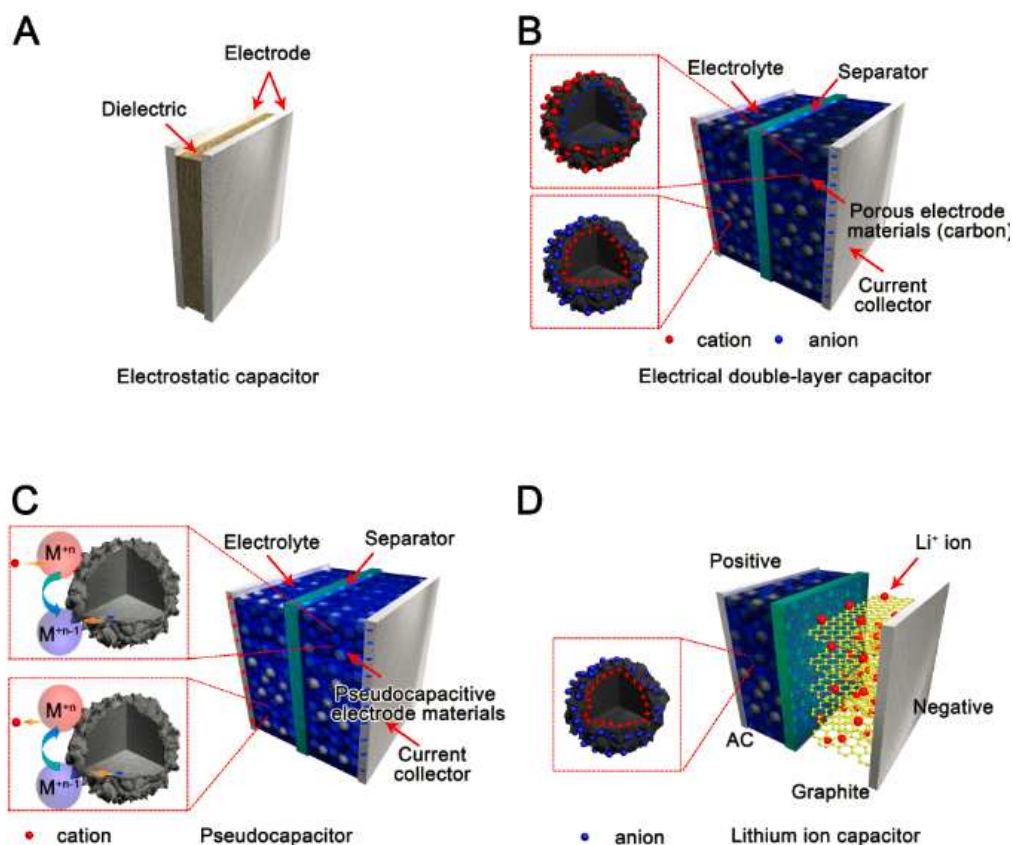


Fig. 3 Schematic diagram for (A) electrostatic capacitor, (B) electric double-layer capacitor, (C) pseudocapacitor, and (D) hybrid-capacitor.

## 2.1. Technical specifications of electrochemical supercapacitors and their relationships with the electrolytes

### 2.1.1. Capacitance

As shown in Fig. 3B, the entire ES can be treated as two capacitors in series since both electrode/electrolyte interfaces represent a capacitor. If the capacitances of the two electrodes are expressed as  $C_1$  and  $C_2$ , respectively, the overall capacitance ( $C_T$ ) can be expressed as:

$$\frac{1}{C_T} = \frac{1}{C_1} + \frac{1}{C_2} \quad (1)$$

For a symmetric ES, since  $C_1 = C_2$ , the total capacitance ( $C_T$ ) would be half of either electrode's capacitance. In the case of the asymmetric ES, the  $C_T$  is mainly dominated by the electrode with smaller capacitance. To evaluate the capacitance of an electrode material, a specific capacitance is often used, which can be expressed either as the mass specific capacitance (sometimes also called gravimetric specific capacitance) ( $C_s$ ), or the volumetric capacitance ( $C_V$ ). Generally,  $C_s$  is the most frequently used one to



characterize an electrode material, with a unit of Faraday per gram ( $F\ g^{-1}$ ) and can be expressed as:

$$C_s = \frac{C_i}{W_{em}} \quad (2)$$

where  $W_{em}$  is the weight of the electrode material in the electrode layer (g), and  $C_i$  is its corresponding electrode capacitance (anode or cathode) (F). A comparison between different electrode materials can be made based on their values of  $C_s$ . For an ES, its total special capacitance ( $C_{TS}$ ) should be the device's total capacitance ( $C_T$ ) normalized by the device's weight  $W_{TM}$  ( $W_{TM}$  is the sum weight of all necessary components including anode, cathode, electrolyte solution, current collector and others), which can be expressed as:

$$C_{TS} = \frac{C_T}{W_{TM}} \quad (3)$$

Normally, Equation (3) indicates the weight of the electrolyte solution can have a negative effect on the ES's capacitance because it can increase the weight of the entire device. Therefore, the lighter weight and smaller volume of electrolyte solution used in the device is most desirable.

It should also be noted that although the  $C_s$  in Equation (2) does not contain the weight of electrolyte, the electrolyte solution can also affect its capacitance value through affecting the capacitance of the electrode ( $C_i$  in Equation (2)). For example, if the electrolyte solution has better contact with the electrode material, the area of the double-layer will be increased, leading to a larger electrode capacitance. Therefore, developing an electrolyte which fills pore areas inside the electrode material layer well--thereby maximizing the material utilization for capacitance generation--is a critical aspect in improving ES performance.

### 2.1.2. Energy density and power density

When an ES is charged, a cell voltage ( $V$ ) will be built up across the two electrodes. The theoretical (or maximum) energy density of the ES cell ( $E$ ), and the power density ( $P$ ) can be expressed as Equations (4), and (5), respectively:<sup>18</sup>

$$E = \frac{1}{2} C_{TS} V^2 \quad (4)$$

$$P = \frac{1}{4W_{TS} R_{cell}} V^2 \quad (5)$$

Where in Equation (5),  $R_{cell}$  is the equivalent series resistance (ESR) of the ES cell ( $\Omega$ ). The energy density (Equation (4)) generally has a unit of  $Wh\ kg^{-1}$ , and the power density (Equation (5)) has a unit of  $W\ kg^{-1}$ .<sup>24, 25</sup> These two equations show that  $V$ ,  $C_{TS}$ ,  $W_{TS}$ , and  $R_{cell}$  are four important variables determining the performance of an ES. In order to improve both the energy and power densities of an ES, increasing the values of both  $V$  and  $C_{TS}$  and simultaneously reducing the values of both  $W_{TS}$  and  $R_{cell}$  are necessary. Since both energy and power densities are proportional to the square of the operating voltage, a cell voltage increase would have a greater contribution to the

improvement of the ES's energy and power densities than increasing the capacitance or reducing resistance. In general, the maximum operating voltage of an ES is strongly dependent on the electrochemical stable potential window (ESPW) or potential window of the electrolyte.

### 2.1.3. Equivalent series resistance

The equivalent series resistance (ESR) is an important parameter determining the ES's power density as indicated by Equation (5), which shows the power density increases with a decreasing ESR value. Similar to other electrochemical energy storage devices, a high ESR limits the charging/discharging rate, leading to low power density. Therefore, for some pulse power applications, the ESR value of an ES is even more important than the capacitance value. Normally, ESR is the sum of various types of resistances including intrinsic resistance of the electrode material and electrolyte solution, mass transfer resistance of the ions, and contact resistance between the current collector and the electrode.<sup>18</sup> As identified, the resistances of the bulk electrolyte solution and the electrolyte inside the electrode layer pores tend to dominate the ESR, especially when non-aqueous electrolytes such as organic, IL and solid-state electrolytes are used in the ESs. Therefore, in order to achieve a high power density from the ES, it is necessary to use an electrolyte with high ionic conductivity. However, there is often a trade-off between the ionic conductivity and the operating potential window of the electrolytes. Aqueous electrolytes, such as H<sub>2</sub>SO<sub>4</sub> and KOH, have high ionic conductivities, but the operating potential window is low. On the contrary, although non-aqueous electrolytes, such as organic and IL, can offer the advantage of high operating voltages, their ionic conductivities are generally at least one order of magnitude lower than that of the aqueous electrolytes,<sup>26</sup> leading to a higher ESR, and thereby limiting the power density. Therefore, for ESs to achieve both high energy and power densities, it is essential to develop electrolytes with a wide operating voltage and a small ESR (or high ion conductivity). This requirement will be the subject of a detailed discussion in Section 3.

### 2.1.4. Cycle-life

Cycle-life, a necessary indicator of the stability of the ES, is also one of the important parameters measuring overall ES performance. General test procedures for stability analysis involve the electrode undergoing charge and discharge cycling in a certain electrolyte to compare the initial and final capacitance. For example, EDLCs using carbon electrodes generally have a very high cycling stability.<sup>24</sup> However, when pseudocapacitive reactions are introduced, the cyclic stability is generally reduced due to the non-ideal electrochemical reversibility resulting from the interactions between the electrolyte ions and the electrode materials. Actually, the cycle-life of the ES depends on many factors such as the cell type, electrode material, electrolyte, charging/discharging rate and operating voltage and temperature, all of which will be discussed below.

### 2.1.5. Self-discharge rate

Another issue concerning the ES performance is self-discharge rates, which are related to potential losses of a charged electrode over a period of storage time.<sup>27, 28</sup> During the self-discharge process, current leakage leads to a decrease of the cell voltage, which in turn may limit the use of ESs for some applications requiring a fixed amount of energy retention for a relatively long time. Several mechanisms have been identified to explain the potential change during the self-discharge process.<sup>22</sup> As will be discussed more completely later, the ES self-discharge rate and its mechanism are dependent on the type of electrolyte, its impurities and residual gases.

### 2.1.6. Thermal stability

Most potential applications for ESs occur in the temperature range of  $-30$  to  $70^{\circ}\text{C}$ ,<sup>4</sup> therefore expanding the current working temperature range of ESs can further widen the scope of applications. For example, most electronics related to space avionics applications are required to operate at temperatures as low as  $-55^{\circ}\text{C}$ .<sup>4</sup> Fuel cell vehicles, on the other hand, may require a high working temperature for ESs. The application working temperature can affect several properties of ESs such as the energy and power densities, rate performance, ESR, cycle life and self-discharge rate. In particular, the temperature-dependent performance of ESs is strongly dependent on the nature of the electrolyte such as the concentration and type of conducting salt, and the specific properties of the solvent (e.g., freezing point, boiling point and viscosity). This subject will be discussed in greater detail for specific electrolytes throughout this review.

In summary, based on the above comments, it can be seen the primary characteristics of ESs are strongly dependent on the specific electrolytes employed.

The following sections, provide a focussed overview of recent developments concerning many different kinds of electrolytes and their associated ESs, used in a wide variety of applications.

## 3. Electrolytes (materials and compositions) for electrochemical supercapacitors

The electrolyte, meaning the electrolyte salt + solvent, is one of the key components of ESs, providing ionic conductivity and thus facilitating charge compensation on each electrode in the cell. The electrolyte within an ES not only plays a fundamental role in the EDL formation (in EDLCs) and the reversible redox process for the charge storage (in pseudocapacitors) but also determines the ES performance (Fig. 2). Currently, the majority of commercial ESs use organic electrolytes with a cell voltage of  $2.5$ – $2.8$  V.<sup>25</sup> Most organic electrolyte-based ESs use the acetonitrile (ACN) solvent while others employ the propylene carbonate (PC) solvent.

The electrolyte nature, including: a) the ion type and size; b) the ion concentration and solvent; c) the interaction between the ion and the solvent; d) the interaction between the electrolyte and the electrode materials; and e) the potential window, all

have an influence on the EDL capacitance and pseudocapacitance, the energy/power densities as well as the ES cycle-life. For example, the electrochemical stable potential window (ESPW) of the electrolyte directly determines the ES's operational cell voltage, through which both the energy and power densities are affected (Equations (4) and (5)). The ESR of an ES, is directly related to the electrolyte's ion conductivity and can have a strong effect on the power density. Furthermore, the interactions between the ion and solvent, and between the electrolyte and the electrode material can affect the life-time and self-discharge of ESs.

In general, various types of electrolytes have been developed and reported in the literature to date. As shown in Fig. 4, these electrolytes are mainly classified as liquid electrolytes and solid/quasi-solid-state electrolytes.

In general, liquid electrolytes can be further grouped into aqueous electrolytes, organic electrolytes and ion-liquids (ILs), while solid or quasi-solid state electrolytes can be broadly divided into organic electrolytes and inorganic electrolytes. To date, there has been no perfect electrolyte developed, meeting all the requirements discussed previously. Each electrolyte has its own advantages and disadvantages. For example, ESs using aqueous electrolytes possess both high conductivity and capacitance, but their working voltage is limited by the narrow decomposition voltage of aqueous electrolytes. Although organic electrolytes and ILs can operate at higher voltages, they normally suffer from much lower ionic conductivity. Solid-state electrolytes may avoid the potential leakage problem of the liquid electrolytes, but they also suffer from low conductivity. To overcome the drawbacks of targeted electrolytes, extensive efforts have been devoted to exploring new electrolyte materials to improve overall ES performance. In this regard, several different approaches have been undertaken, including: (1) development of new and high-performing electrolytes to make a wider operating potential window, higher ionic conductivity/viscosity, wider working temperature range, and so on; (2) exploration of the positive effects of given electrolytes on the ES properties such as capacitance, energy and power densities, thermal stability and self-discharging process; and (3) establishing a fundamental understanding of the role of the electrolyte on the ES performance through advanced experimental, modeling and simulation methods.

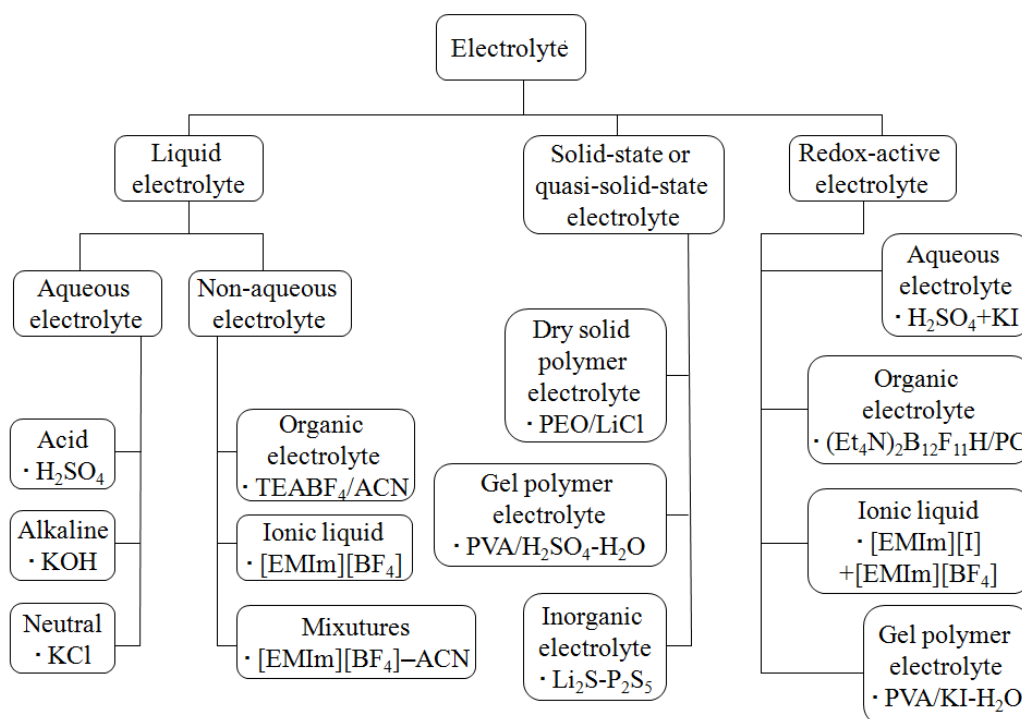


Fig. 4 Classification of electrolytes for electrochemical supercapacitors.

### 3.1. Aqueous electrolytes

Generally, in consideration of energy density, aqueous electrolytes are a low choice for commercial ES products due to their narrow voltage windows. This may be one of the major reasons why most commercial ESs use organic electrolytes instead of aqueous electrolytes. However, aqueous electrolytes have been used extensively in research and development in the reported literature from 1997 to 2014

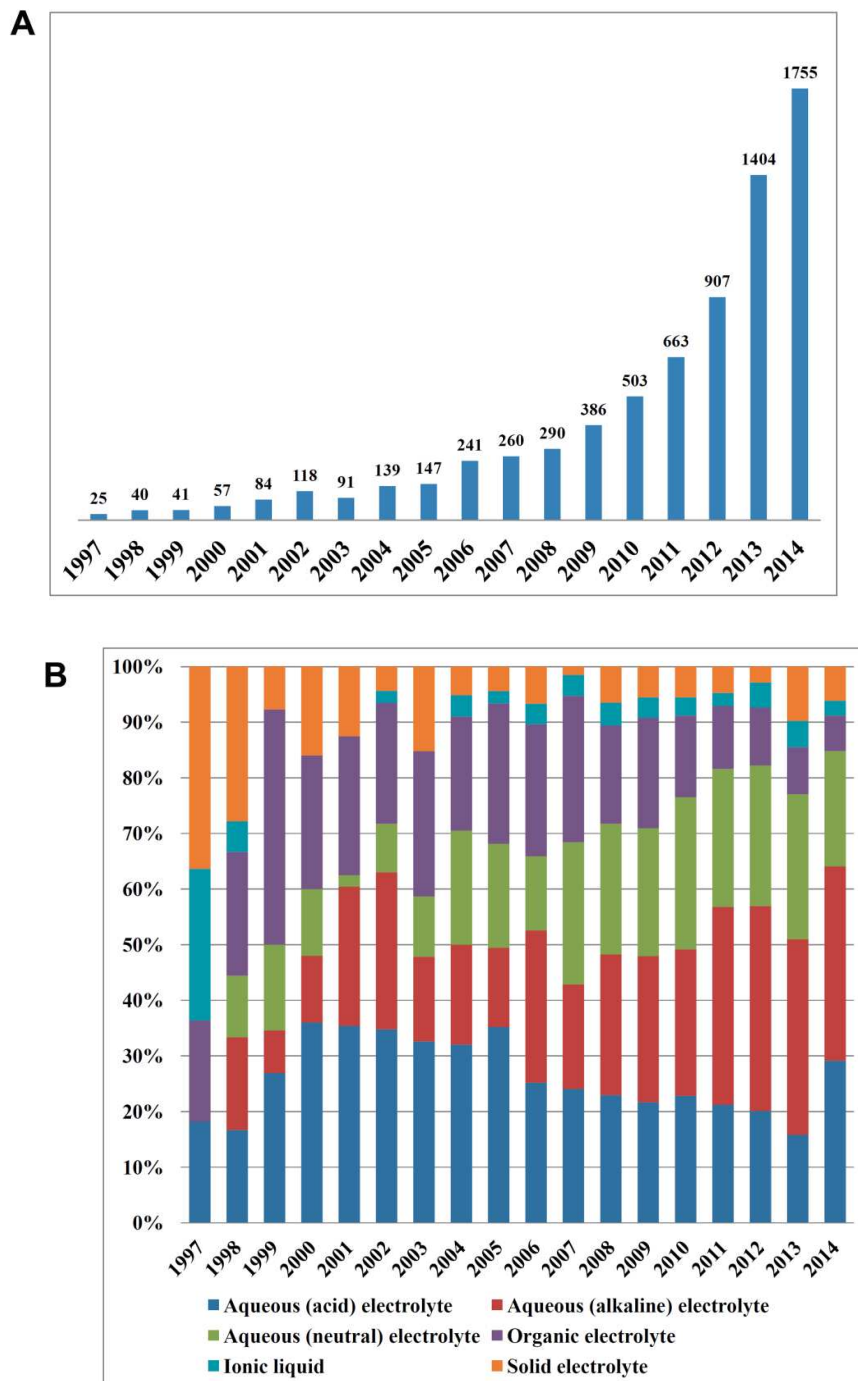


Fig. 5B). For example, in 2014, about 84.8% of the published literature employed aqueous electrolytes for ESs. This is mainly due to the fact aqueous electrolytes are inexpensive and can be easily handled in the laboratory without needing special conditions thus greatly simplifying the fabrication and assembly processes. Organic electrolytes and ILs, on the other hand, generally require complicated purification procedures under a strictly controlled atmosphere to avoid introduction of moisture.

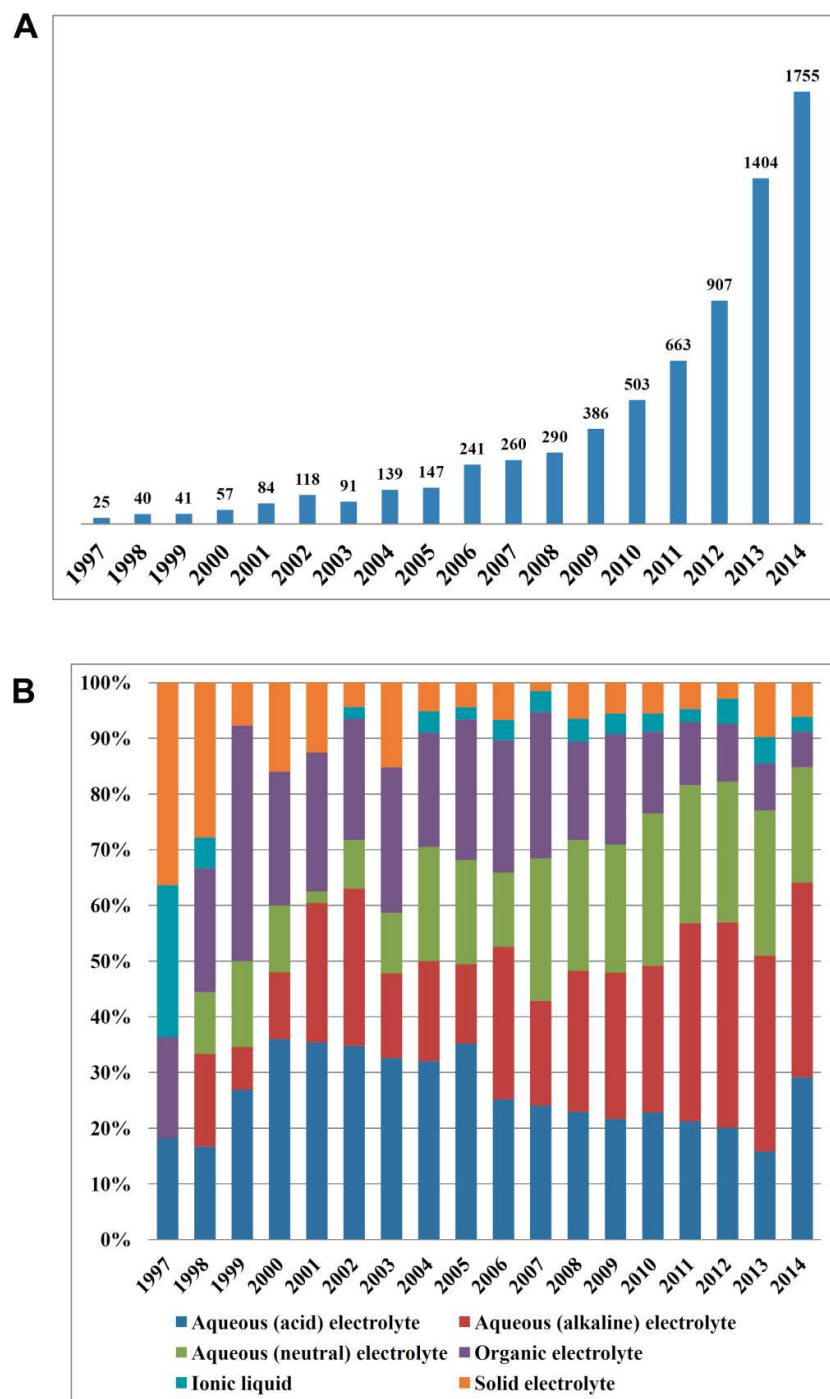


Fig. 5 (a) Total amount of the reported literature related to electrochemical supercapacitors from 1997 to 2014, (b) percentage of different electrolytes from 1997 to 2014. Search formulation for ESs: (“Electrochemical capacitor\*” or “supercapacitor\*” or “ultracapacitor\*” or “ pseudocapacitor\*” or “double layer capacitor\*”); Search from Web of Science; Search time: 28, Feb, 2015.

Normally, aqueous electrolytes exhibit high conductivity (for example, about  $0.8 \text{ S cm}^{-2}$  for  $1 \text{ M H}_2\text{SO}_4$  at  $25^\circ\text{C}$ ), which is at least one order of magnitude higher than that of organic and IL electrolytes.<sup>29</sup> This is beneficial for lowering the ESR, leading to a better power delivery of ESs. The selection criteria for aqueous electrolytes generally considers the sizes of bare and hydrated cations and anions and the mobility of ions (Table 1), which affects not only the ionic conductivity but also the specific capacitance value. In addition, an electrolyte's ESPW and the corrosive degree should also be taken into account.

In general, aqueous electrolytes can be grouped into acid, alkaline, and neutral solutions in which  $\text{H}_2\text{SO}_4$ ,  $\text{KOH}$  and  $\text{Na}_2\text{SO}_4$  are representatives and also the most frequently used electrolytes (Fig. 4). As previously mentioned, the main disadvantage of aqueous electrolytes is their relatively narrow ESPW, restricted by the decomposition of water. For example, hydrogen evolution occurs at a negative electrode potential of around  $0 \text{ V}$  vs. SHE, and oxygen evolution at a positive electrode potential of around  $1.23 \text{ V}$ , the resulting ES has a cell voltage about  $1.23 \text{ V}$ .<sup>23</sup> The gas evolution would potentially cause the rupture of the ES cells, threatening the safety and decreasing the performance. To avoid the gas evolution, the cell voltage of ESs with aqueous electrolytes is commonly restricted to about  $1.0 \text{ V}$ . Table 2 lists the typical aqueous electrolyte-based ESs and their performance. It can be seen that for acid and alkaline electrolytes, the cell voltages are all limited within  $1.3 \text{ V}$  no matter what electrode material is used. For neutral electrolytes, the highest cell voltages reported in Table 2 is  $2.2 \text{ V}$ .<sup>9</sup> Besides, the operating temperature range of ESs with aqueous electrolytes has also to be restricted to above the water freezing point and below boiling point.

Table 1 The sizes of bare and hydrated ions, and ionic conductivity values

Ion	Bare ion size (Å)	Hydrated ion size (Å)	Ionic conductivity ( $\text{S cm}^2 \text{ mol}^{-1}$ )
$\text{H}^+$	0.115 <sup>b</sup>	2.80 <sup>b</sup>	350.1 <sup>a</sup>
$\text{Li}^+$	0.60 <sup>c</sup>	3.82 <sup>bc</sup>	38.69 <sup>a</sup>
$\text{Na}^+$	0.95 <sup>c</sup>	3.58 <sup>bc</sup>	50.11 <sup>a</sup>
$\text{K}^+$	1.33 <sup>c</sup>	3.31 <sup>bc</sup>	73.5 <sup>a</sup>
$\text{NH}_4^+$	1.48 <sup>bc</sup>	3.31 <sup>bc</sup>	73.7 <sup>a</sup>
$\text{Mg}^{2+}$	0.72 <sup>ab</sup>	4.28 <sup>bc</sup>	106.12 <sup>a</sup>
$\text{Ca}^{2+}$	1.00 <sup>b</sup>	4.12 <sup>bc</sup>	119 <sup>a</sup>
$\text{Ba}^{2+}$	1.35 <sup>c</sup>	4.04 <sup>c</sup>	127.8 <sup>a</sup>
$\text{Cl}^-$	1.81 <sup>ac</sup>	3.32 <sup>bc</sup>	76.31 <sup>a</sup>
$\text{NO}_3^-$	2.64 <sup>c</sup>	3.35 <sup>c</sup>	71.42 <sup>a</sup>
$\text{SO}_4^{2-}$	2.90 <sup>c</sup>	3.79 <sup>c</sup>	160.0 <sup>a</sup>
$\text{OH}^-$	0.176 <sup>c</sup>	3.00 <sup>bc</sup>	198 <sup>a</sup>
$\text{ClO}_4^-$	2.92 <sup>c</sup>	3.38 <sup>c</sup>	67.3 <sup>a</sup>
$\text{PO}_4^{3-}$	2.23 <sup>d</sup>	3.39 <sup>d</sup>	207 <sup>a</sup>
$\text{CO}_3^{2-}$	2.66 <sup>c</sup>	3.94 <sup>c</sup>	138.6 <sup>a</sup>

Sources: <sup>a</sup> from Ref. 30; <sup>b</sup> from Ref. 31; <sup>c</sup> from Ref. 32; <sup>d</sup> from Ref. 33.



Table 2 Aqueous electrolyte-based supercapacitors and their performance

Aqueous Electrolyte/ Concentration	Electrode materials	Specific capacitance (F g <sup>-1</sup> )	Cell voltage (V)	Energy density (Wh kg <sup>-1</sup> )	Power density (W kg <sup>-1</sup> )	Temp. (°C)	Ref.
<b>Strong acid electrolyte:</b>							
H <sub>2</sub> SO <sub>4</sub> /2 M	MMPGC	105 at 4 mV s <sup>-1</sup>	0.8	4	20	RT	34
H <sub>2</sub> SO <sub>4</sub> /1 M	AC fibers	280 at 0.5 A g <sup>-1</sup>	0.9	–	–	RT	35
H <sub>2</sub> SO <sub>4</sub> /1 M	GQD/3DG composite	268 at 1.25 A g <sup>-1</sup>	0.8	–	–	RT	36
H <sub>2</sub> SO <sub>4</sub> /1 M	Microporous carbon 3D heteroatom-doped	~100 at 0.2 A g <sup>-1</sup>	1	~3.8	~100	RT	37
H <sub>2</sub> SO <sub>4</sub> /2 M	carbon nanofiber networks	204.9 at 1 A g <sup>-1</sup>	1	7.76	~100	RT	38
H <sub>2</sub> SO <sub>4</sub> /1 M	phosphorus-enriched carbons	220 at 1 A g <sup>-1</sup>	1.3	16.3	33	–	39
H <sub>2</sub> SO <sub>4</sub> /1 M	ANS-rGO	375 at 1.3 A g <sup>-1</sup>	1	213	1328	RT	40
H <sub>2</sub> SO <sub>4</sub> /0.5 M	RuO <sub>2</sub> –graphene	479 at 0.25 A g <sup>-1</sup>	1.2	20.28	600	–	41
H <sub>2</sub> SO <sub>4</sub> /1 M	PANI-grafted rGO	1045.51 at 0.2 A g <sup>-1</sup>	0.8	8.3	60000	–	42
H <sub>2</sub> SO <sub>4</sub> /0.5 M	PPy thin films	510 at 0.25 mA cm <sup>-2</sup>	1	133	758	–	43
H <sub>2</sub> SO <sub>4</sub> /1 M	graphene/mPANI nitrogen and oxygen-containing	749 at 0.5 A g <sup>-1</sup>	0.7	11.3	106.7	–	44
H <sub>2</sub> SO <sub>4</sub> /1 M	hierarchical porous carbon frameworks	428.1 at 0.5 A g <sup>-1</sup>	0.8	37.4	197	–	45
<b>Strong alkaline electrolyte:</b>							
KOH/6 M	3D FHPC	294 at 2mV s <sup>-1</sup>	1	–	–	–	46
KOH/6 M	highly porous graphene planes	303 at 0.5 A g <sup>-1</sup>	1	6.5	~50	–	47
KOH/6 M	p-CNTn/CGBs	202 at 0.325 A g <sup>-1</sup>	0.9	4.9	150	RT	48
KOH/2 M	sub-3 nm Co <sub>3</sub> O <sub>4</sub> Nanofilms	1400 at 1 A g <sup>-1</sup>	0.47	–	–	RT	49
KOH/2 M	porous NiCo <sub>2</sub> O <sub>4</sub> nanotubes	1647.6 at 1 A g <sup>-1</sup>	0.41	38.5	205	–	50
LiOH/1 M	MnO <sub>2</sub> nanoflower	363 at 2mV s <sup>-1</sup>	0.6	–	–	–	51
<b>Neutral electrolyte:</b>							
Na <sub>2</sub> SO <sub>4</sub> /1M	3D FHPC	–	1.8	15.9	317.5	–	46
NaNO <sub>3</sub> /1 M	AC	116 at 2mV s <sup>-1</sup>	1.6	–	–	RT	52
Na <sub>2</sub> SO <sub>4</sub> /0.5 M	microporous carbon	~60 at 0.2 A g <sup>-1</sup>	1.8	~7	~40	–	37
NaNO <sub>3</sub> –EG/4 M	AC	22.3 at 2 mV s <sup>-1</sup> (0°C)	2	14–16 (RT)	~500	0 to 60	53
Na <sub>2</sub> SO <sub>4</sub> /0.5 M	seaweed carbons	123 at 0.2 A g <sup>-1</sup>	1.6	10.8	–	–	54
Na <sub>2</sub> SO <sub>4</sub> /0.5 M	AC	135 at 0.2 A g <sup>-1</sup>	1.6	~10	–	–	55

	MnCl <sub>2</sub> -doped						
KCl/1 M	PANI/SWCNTs nanocomposites	546 at 0.5 A g <sup>-1</sup>	0.8	194.13	~550	RT	56
Li <sub>2</sub> SO <sub>4</sub> /1 M	AC	180 at 0.2 A g <sup>-1</sup>	2.2	–	–	–	9
Na <sub>2</sub> SO <sub>4</sub> /1 M	mesoporous MnO <sub>2</sub>	278.8 at 1 mV s <sup>-1</sup>	1	~28.4	~70	RT	57
Li <sub>2</sub> SO <sub>4</sub> /1 M	mesoporous MnO <sub>2</sub>	284.24 at 1 mV s <sup>-1</sup>	1	~28.8	~70	RT	57
K <sub>2</sub> SO <sub>4</sub> /0.65 M	mesoporous MnO <sub>2</sub>	224.88 at 1 mV s <sup>-1</sup>	1	~24.1 (0.5 M K <sub>2</sub> SO <sub>4</sub> )	~70	RT	57
	well-ordered mesoporous						
Na <sub>2</sub> SO <sub>4</sub> /1 M	carbon/Fe <sub>2</sub> O <sub>3</sub> nanoparticle composites	235 at 0.5 A g <sup>-1</sup>	1	39.4	–	RT	58
Na <sub>2</sub> SO <sub>4</sub> /0.5 M	MnO <sub>2</sub> @carbon nanofibers composites	551 at 2 mV s <sup>-1</sup> (75 °C)	0.85	–	–	0 to 75	59
Na <sub>2</sub> SO <sub>4</sub> /1 M	hydrous RuO <sub>2</sub> CNFs with radially grown graphene sheets	52.66 at 0.625 A g <sup>-1</sup>	1.6	18.77	500	–	60
Na <sub>2</sub> SO <sub>4</sub> /1 M	grown graphene sheets	–	1.8	29.1	450	–	61

Abbreviations: Temp: temperature; RT: room temperature; MMPGC: macro/mesoporous partially graphitized carbon; GQD/3DG composite: graphene quantum dots/3D graphene composites; AC: activated carbon; PANI: polyaniline; ANS: 6-amino-4-hydroxy-2-naphthalenesulfonic acid; rGO: reduced graphene oxide; PPy: polypyrrole; mPANI: mesoporous PANI film on ultra-thin graphene nanosheet; 3D FHPC: 3D flower-like and hierarchical porous carbon material; p-CNTn/CGBs: porous CNT networks decorated crumpled graphene balls; EG: ethylene glycol; SWCNTs: single-walled carbon nanotubes; CNFs: carbon nanofibers.

### 3.1.1. Strong acid electrolytes

As listed in Fig. 5B and Table 2, acidic electrolytes are the choice in many ES studies. Among different acidic electrolytes, H<sub>2</sub>SO<sub>4</sub> is the most commonly used acid electrolyte for aqueous-based ESs mainly due to its very high ionic conductivity (0.8 S cm<sup>-1</sup> for 1 M H<sub>2</sub>SO<sub>4</sub> at 25°C). Of course, this conductivity is strongly dependent on the concentration of H<sub>2</sub>SO<sub>4</sub>. With respect to this, some optimum concentrations to achieve the maximum ionic conductivities of the H<sub>2</sub>SO<sub>4</sub> electrolytes at certain temperatures have been extensively studied. Generally, the ionic conductivity of the electrolyte can be decreased if the concentration is too low or too high. Since the maximum ionic conductivity of H<sub>2</sub>SO<sub>4</sub> electrolyte is achieved at 1.0 M concentration at 25°C, the majority of studies use 1.0 M H<sub>2</sub>SO<sub>4</sub> electrolyte solution, particularly, for those ESs using carbon-based electrode materials.

### 3.1.1.1. Acid electrolytes for electrical double-layer capacitors

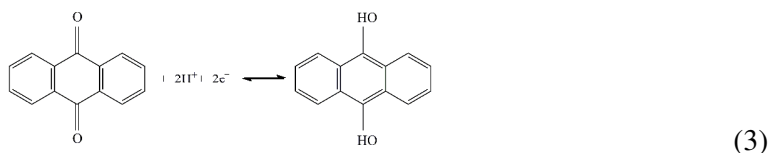
In a literature search, the majority of comparative studies found the specific capacitances of EDLCs, obtained in the H<sub>2</sub>SO<sub>4</sub> electrolyte, are higher than that in the neutral electrolytes.<sup>37, 62-64</sup> In addition, due to the higher ionic conductivity of the H<sub>2</sub>SO<sub>4</sub> when compared to the neutral electrolytes, the ESR of ESs with H<sub>2</sub>SO<sub>4</sub> as electrolyte is generally lower than that with the neutral electrolytes.<sup>37, 63, 64</sup> Previous studies have also found there is a relationship between the specific capacitance of the activated carbons and the electrolyte conductivity, i.e., the specific capacitance increased with increasing the electrolyte conductivity.<sup>62</sup> This can be understood by considering the ion mobility which is closely related to the electrolyte conductivity. For EDLCs with a strong acid electrolyte such as H<sub>2</sub>SO<sub>4</sub>, the reported specific capacitances in the literature published in the past several years are mainly in the range between 100 and 300 F g<sup>-1</sup> (e.g., Ref. 35-37), which are generally higher than those obtained in the organic electrolytes. Actually, the major contribution to the specific capacitance is made from the carbon-based electrode materials as reviewed by many excellent reviews,<sup>14-16, 18, 19</sup> and the electrolyte contribution to the capacitance value should be less than that of electrode materials.

As generally observed, the H<sub>2</sub>SO<sub>4</sub> electrolyte-based EDLCs have higher specific capacitances when compared to those of organic electrolyte-based ones, even using the same electrode materials. This may reflect the different interactions between the electrode materials and the electrolytes induced by different electrolytes.

### 3.1.1.2. Acid electrolytes for pseudocapacitors

Due to the low energy density of EDLCs, extensive efforts have been made to increase the value of the energy density by exploring other type of ESs, such as pseudocapacitors. For carbon-based electrode materials, it was found that the specific capacitance in aqueous H<sub>2</sub>SO<sub>4</sub> electrolyte also included some pseudocapacitance contributions besides the electrostatic EDL capacitance.<sup>22</sup> This was attributed to the fast redox reactions which occurred on the particular surface functionalities, such as oxygenated carbon species.<sup>22</sup> This pseudocapacitance could be further enhanced by introducing heteroatoms (e.g., oxygen,<sup>65</sup> nitrogen,<sup>66, 67</sup> and phosphorous<sup>39, 66</sup>) or certain surface functional groups (e.g., anthraquinone<sup>68</sup>) to the carbon material surfaces.

It should be emphasized that the nature of the electrolyte has a strong influence on the pseudocapacitive properties of carbon-based materials because the surface functionalities behave differently with different electrolytes. For example, surface quinone-type functionalities could produce pseudocapacitive effects in the presence of acidic aqueous electrolytes (e.g., H<sub>2</sub>SO<sub>4</sub>) since the protons were involved in the redox processes as shown in Equation (6).<sup>8, 68</sup> In alkaline electrolytes, this effect was hardly observed.<sup>8, 68</sup>



Therefore, generating favorite surface functionalities on the carbon-based electrode

materials using suitable electrolytes seems fairly important in achieving an optimum ES performance. However, the cycle-lives of pseudocapacitors are normally shorter than that of EDLCs because of the degradation of electrode functional materials in the presence of aqueous electrolytes. On the contrary, in the presence of organic electrolytes, the ES cycle-lives are much longer than those in aqueous electrolytes. This is because of the capacitances in organic electrolytes largely come from the electrostatic charge separation.<sup>69</sup> One of the approaches was the introduction of certain surface functional groups (e.g., phosphorus groups) into the carbon surface, which showed some improvement in the stability of electrode materials in aqueous electrolytes even at higher voltages.<sup>39</sup>

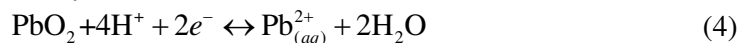
In addition, the pseudocapacitance could also be provided by other pseudocapacitive materials such as metal oxides, sulfides, and electrically conductive polymers (ECPs), which have much higher theoretical capacitances than carbon-based materials in aqueous electrolytes.<sup>6, 17</sup> However, these electrode materials are not normally stable in acidic aqueous electrolytes due to their sensitivity to the type and pH of the electrolytes. In this regard, few of the non-carbon materials could be suitable for the pseudocapacitors in strong acidic electrolytes except RuO<sub>2</sub>. As recognized, RuO<sub>2</sub> is one of the most extensively studied pseudocapacitive materials in H<sub>2</sub>SO<sub>4</sub> electrolytes. The capacitance of amorphous RuO<sub>2</sub> could give a very high value of ~1000 F g<sup>-1</sup> probably due to the relatively easy insertion of protons into the amorphous structure.<sup>70</sup> Unfortunately, the high cost and limited sources of Ru have limited their commercial usage. Some alternative materials such as α-MoO<sub>3</sub> with pseudocapacitive behaviour were tested for such in strong acidic electrolytes.<sup>71</sup>

### 3.1.1.3. Acid electrolytes for hybrid capacitors

To increase the energy densities of the aqueous electrolyte-based ESs, some efforts have been devoted to developing hybrid supercapacitors to make their cell voltage wider. As discussed previously, when a symmetric ES with the same type of electrode materials as both the electrodes in aqueous electrolytes (e.g., H<sub>2</sub>SO<sub>4</sub> or KOH), the maximum cell voltage is limited by the gas evolution reactions.<sup>4</sup> However, if an ES with asymmetric configurations (the anode materials are different from those of the cathode) are used, the resultant ESs could have a wider working potential window even in aqueous electrolytes.<sup>72</sup> The combination of two different electrodes in an ES can work complementary in separate potential windows, leading to a higher operating voltage in aqueous electrolytes. For example, the high overpotential for H<sub>2</sub> evolution at a carbon-based negative electrode and O<sub>2</sub> evolution at a battery-like (e.g., PbO<sub>2</sub>) or pseudocapacitive electrode (e.g., RuO<sub>2</sub>) could give an ES a working voltage window of aqueous electrolytes beyond the thermodynamic limit of water.<sup>72</sup> To date, several types of asymmetric ESs, such as carbon//PbO<sub>2</sub>,<sup>73</sup> carbon//RuO<sub>2</sub>,<sup>74</sup> carbon//ECPs<sup>75</sup> and carbon with different mass or properties in each electrode,<sup>69, 76</sup> have been tested in strong acid electrolytes, and demonstrated the feasibility for application.

For example, typical energy densities for a carbon/PbO<sub>2</sub> hybrid ESs with an H<sub>2</sub>SO<sub>4</sub> electrolyte were reported to have a value range of 25–30 Wh kg<sup>-1</sup>, which was much higher than that for symmetric carbon-based EDLCs with the same H<sub>2</sub>SO<sub>4</sub> electrolyte (3–6 Wh kg<sup>-1</sup>).<sup>77</sup> However, the chemical stability of the PbO<sub>2</sub> in the H<sub>2</sub>SO<sub>4</sub> electrolyte was found to be a concern. Perret et al.<sup>78</sup> found the structure of

PbO<sub>2</sub> nanowires could be changed during the electrochemical potential cycling in 1 M H<sub>2</sub>SO<sub>4</sub>, leading to poor cycling stability. To address this issue, they explored an alternative electrolyte composed of methanesulfonic acid (CH<sub>3</sub>SO<sub>3</sub>H) and lead methanesulfonate.<sup>73</sup> In this case, the redox process at the PbO<sub>2</sub> electrode was changed from a solid/solid couple in H<sub>2</sub>SO<sub>4</sub> electrolyte to a solid/solvated ion one in the methanesulfonic-based electrolyte:<sup>73</sup>



During the discharging process, PbO<sub>2</sub> was reduced into Pb<sup>2+</sup> (aq). During the charging process, Pb<sup>2+</sup> (aq) was oxidized and the PbO<sub>2</sub> formed was electrodeposited on the electrode surface. Therefore, sulfation of PbO<sub>2</sub> in H<sub>2</sub>SO<sub>4</sub> electrolytes was not a limitation and a much improved cycle-life was realized for this system. Although the energy densities could be improved, both the power density and cycle-life of the aqueous hybrid ESs would be compromised. To overcome this, other types of asymmetric/hybrid ESs with a combination of carbon-based material with pseudocapacitive materials, such as AQ-modified carbon//RuO<sub>2</sub>,<sup>74</sup> carbon//ECP,<sup>79</sup> and/or carbon//carbon (with different surface functionalities) were also explored.<sup>69, 76</sup>

It may be noted here that, there are other types of acid electrolytes that may be used for ESs, including perchloric acid, hexafluorosilicic acid and tetrafluoroboric acid. However, few of them have been studied for the application in ESs due to a concern for safety.<sup>73</sup> In addition, the self-discharge in the concentrated electrolytes, especially in the presence of contamination (e.g., metal ions) and oxygen is also a concern.<sup>80, 81</sup>

### 3.1.2. Strong alkaline electrolytes

Based on the statistics in Fig. 5 and also the list in Table 2 the alkaline electrolytes are one kind of the most widely used aqueous electrolytes in literatures application. In comparison with strong acidic electrolytes, some cost-effective metal materials (e.g., Ni) can be used as the current collectors for ESs. Among various alkaline electrolytes, KOH has been the most extensively used one due to its high ionic conductivity (maximum value of 0.6 S cm<sup>-1</sup> for 6 M at 25°C) although other base electrolytes, such as NaOH and LiOH, have also been investigated. These alkaline electrolytes can be used for carbon-based EDLCs, pseudocapacitors (e.g., Ni(OH)<sub>2</sub> and Co<sub>3</sub>O<sub>4</sub>) and hybrid ESs.

#### 3.1.2.1. Alkaline electrolytes for electrical double-layer capacitors

In the literature, reported values of EDLC specific capacitances and energy densities with an aqueous KOH electrolyte are generally similar to that reported with an H<sub>2</sub>SO<sub>4</sub> electrolyte. Besides the efforts to use strong acid electrolytes for ESs, considerable effort has also been devoted to improving the ES energy densities using base electrolytes through increasing the capacitance and/or widening the operating voltage window. These developments can be briefly summarized as follows: (1) enhancing the capacitance of carbon-based electrode materials through the introduction of a pseudocapacitance contribution; (2) developing pseudocapacitive materials with high specific capacitance; (3) exploring composite materials that

combine the carbon-based materials and pseudocapacitive materials; and (4) increasing the operating voltage window of base electrolytes via the designing of asymmetric ESs.

### 3.1.2.2. Alkaline electrolytes for pseudocapacitors

As discussed, the pseudocapacitance of carbon-based electrode materials is contributed from the carbon surface functionalities which are closely related to the faradaic interactions between the ions in the electrolyte and surface functional groups.<sup>67</sup> In this regard, studies found the KOH electrolyte was beneficial for the nitrogen-doped carbon electrode materials, suggesting that the corresponding pseudocapacitance was strongly dependent on the nature of electrolytes (e.g., type and pH).<sup>82, 83</sup> Wang et al.<sup>84</sup> reported that co-doping the porous carbons with phosphorus and nitrogen could achieve a higher specific capacitance, wider potential window and enhanced stability compared to phosphorus-free counterparts, resulting in a further improvement in ES performance. In addition, it was observed that hydrogen could be stored through negative polarization at potentials lower than the thermodynamic value of water reduction.<sup>76, 85</sup> This behaviour was also strongly dependent on the electrolyte type and was more favorable to occur in alkaline electrolytes.<sup>85</sup>

In alkaline electrolytes, some transition metal oxides (e.g., NiO<sub>x</sub>,<sup>86</sup> CoO<sub>x</sub>,<sup>49</sup> MnO<sub>2</sub>,<sup>87</sup> and NiCo<sub>2</sub>O<sub>4</sub>,<sup>50</sup>), hydroxides (e.g., Ni(OH)<sub>2</sub>,<sup>88</sup> Co(OH)<sub>2</sub>,<sup>49</sup>), sulfides (e.g., cobalt sulfide<sup>89</sup>) and nitrides (e.g., VN<sup>90</sup>) have also been explored due to their high theoretical capacitances. It is recognized that the interaction between ions in the electrolytes and the electrode materials plays an important role in the pseudocapacitive behaviour of these materials. As discussed, the charge-storage mechanism of pseudocapacitive electrode materials normally involves the adsorption/desorption or insertion/extraction of electrolyte ions into/from the electrode materials.<sup>86, 91</sup> For example, Feng et al.<sup>49</sup> prepared sub-3 nm Co<sub>3</sub>O<sub>4</sub> nanofilms, and obtained a specific capacitance as high as 1400 F g<sup>-1</sup> in 2 M KOH electrolyte. Mefford et al.<sup>92</sup> recently demonstrated the anion intercalation-based charge storage mechanism for LaMnO<sub>3</sub> perovskite pseudocapacitive electrodes in KOH electrolyte, which may provide a new strategy to obtain high specific capacitance of the pseudocapacitive materials. It needs to be noted that the possible electrochemical reaction between the electrode materials and the electrolytes might also have a strong influence on the pseudocapacitive behaviour. For example, some metal sulfides, such as CoS<sub>x</sub> and NiS, showed poor pseudocapacitive performance in KOH electrolytes,<sup>93, 94</sup> however, when they were electrochemically transformed into new electroactive phases (e.g., Co(OH)<sub>2</sub> and Ni(OH)<sub>2</sub>) in the KOH electrolytes, a large increase in the pseudocapacitance was observed.<sup>93, 94</sup>

Normally, the electrolyte properties, such as ion type, concentration, and the operating temperature can affect the performance of ESs. For example, it was observed the alkaline electrolyte concentration can affect the value of ESR,<sup>95</sup> specific capacitance<sup>95, 96</sup> as well as the oxygen evolution reaction.<sup>95</sup> One drawback when using a concentrated electrolyte is the corrosion at the electrode substrate surface, which may lead to the electrode material peeling off from the substrate.<sup>96</sup> Therefore, it is necessary to optimize the electrolyte concentration with respect to the overall ES performance. An increase in the electrolyte temperature can usually result in a decrease in ESR and then an increase in the specific capacitance due to the enhanced

ion diffusion process in the electrolyte.<sup>95,97</sup> However, the oxygen evolution reaction at the positive electrode was found to be facilitated with increasing temperature, leading to a decrease in the onset potential of oxygen evolution.<sup>4,98</sup> Furthermore, the elevated temperatures were reported to decrease the cycling stability of activate carbons due to the material degradation caused by the surface oxidation in KOH electrolytes.<sup>95</sup>

Since the intercalation and deintercalation of alkaline electrolyte ions generally involves pseudocapacitive materials, the bare (unsolvated) ionic size is expected to have a pronounced influence on the pseudocapacitive behaviour. Normally, the effect of the electrolyte ion type on the ES performance is relatively complicated. For example, some researchers found the specific capacitance of  $\text{MnO}_2$ <sup>51,87</sup> was higher in LiOH electrolyte than that in KOH or NaOH electrolyte. The authors attributed this to the relatively easy intercalation/deintercalation of the  $\text{Li}^+$  ion due to its smaller ionic radius compared to that of the  $\text{K}^+$  or  $\text{Na}^+$  ion. Inamdar et al.<sup>99</sup> found the specific capacitance of NiO in NaOH electrolyte was nearly two times more than in KOH electrolyte, and they attributed this to a higher intercalation rate of  $\text{Na}^+$  ions into the electrode material surface. However, other comparative studies with different alkaline electrolytes for electrode materials such as  $\text{Co}_2\text{P}_2\text{O}_7$ ,<sup>100</sup>  $\text{MnFe}_2\text{O}_4$ <sup>101</sup> and  $\text{Bi}_2\text{WO}_6$ <sup>102</sup> showed higher specific capacitances could be achieved in KOH electrolytes than those in NaOH or LiOH electrolyte. Since comparative studies of various alkaline electrolytes have been rather limited, it still remains unclear whether this phenomenon is related to the electrolyte, or the type of electrode materials, or the preparation procedure and the resultant material structure.

As mentioned before, pseudocapacitive materials usually have less cycling stability when compared to those non-pseudocapacitive ones. This instability could be partially caused by the repeated ion intercalation/deintercalation in alkaline electrolytes. Besides that, the dissolution of electrode materials in alkaline electrolytes might also be responsible for the decrease of capacitive performance after long-term charging/discharging cycling.<sup>91</sup>

Similar to those ES studies in acidic electrolytes, widening the operation voltage window of ESs with alkaline electrolytes is a current research trend in order to significantly improve energy density. In the case of symmetric ESs, this can be generally achieved through modification of the electrode materials to increase the electrode stability at wide/large potential windows and/or inhibit the side reaction in the electrolytes.<sup>39,103</sup>

### 3.1.2.3. Alkaline electrolytes for hybrid capacitors

According to the literature, to improve energy density, a series of alkaline electrolyte-based asymmetric ESs with wide potential windows have been developed. Generally, for those asymmetric ESs, the positive electrodes are different from the negative electrode. The positive electrode is a battery-type one (e.g.,  $\text{Ni}(\text{OH})_2$ )<sup>77</sup> or pseudocapacitive one (e.g.,  $\text{RuO}_2$ )<sup>104</sup> where charge is stored through faradaic reactions, and the negative electrode is a carbon-based one where charge is primarily stored by the EDL.<sup>72</sup> The operating cell voltages of these asymmetric ESs were reported to be effectively increased in KOH electrolyte, e.g., 1.7 V for carbon// $\text{Ni}(\text{OH})_2$ ,<sup>105</sup> 1.4–1.6 V for carbon// $\text{Co}(\text{OH})_2$ ,<sup>106</sup> carbon// $\text{Co}_3\text{O}_4$ ,<sup>107</sup> and carbon// $\text{Co}_9\text{S}_8$ ,<sup>89</sup> 1.6 V for carbon// $\text{Ni}_3\text{S}_2$ ,<sup>108</sup> and 1.4 V for carbon// $\text{RuO}_2$ - $\text{TiO}_2$ .<sup>104</sup> Because of the larger operating voltage window and the usage of a high capacity faradaic-type electrode, most of these ESs could deliver higher energy densities ranging from 20 to 40  $\text{Wh kg}^{-1}$ , with

some even as high as  $140 \text{ Wh kg}^{-1}$ ,<sup>105</sup> which was comparable to rechargeable lithium-ion batteries. However, due to the usage of faradaic-type electrodes, the cycling stabilities of these asymmetric ESs are normally much lower than those of the EDLCs. For example, it was reported there were more than a 10% loss in the specific capacitance of some asymmetric ESs after a certain number of cycles (1000–5000).<sup>105</sup> Besides, these asymmetric ESs usually suffer from a slower charging/discharging process when compared to the EDLCs and their few-second response.

### 3.1.3. Neutral electrolytes

Besides the acidic and alkaline electrolytes, neutral electrolytes have also been widely studied for ESs, as shown in Fig. 5 and Table 2. This is due to their advantages such as larger working potential windows, less corrosion and greater safety. Typical conducting salts in the neutral electrolytes include Li (e.g., LiCl, Li<sub>2</sub>SO<sub>4</sub> and LiClO<sub>4</sub>), Na (e.g., NaCl, Na<sub>2</sub>SO<sub>4</sub> and NaNO<sub>3</sub>), K (e.g., KCl, K<sub>2</sub>SO<sub>4</sub> and KNO<sub>3</sub>), Ca (Ca(NO<sub>3</sub>)<sub>2</sub>) and Mg (e.g., MgSO<sub>4</sub>) salts. Among various neutral electrolytes, Na<sub>2</sub>SO<sub>4</sub> is the most commonly used neutral electrolyte, and has been shown to be a promising electrolyte for many pseudocapacitive materials (especially MnO<sub>2</sub>-based materials). These neutral electrolytes are mostly used in pseudocapacitors and hybrid ESs although some studies have also focused on EDLCs.

#### 3.1.3.1. Neutral electrolytes for electrical double-layer capacitors

Comparative studies have found the specific capacitances of EDLCs with neutral electrolytes were lower than those with H<sub>2</sub>SO<sub>4</sub> electrolyte or KOH electrolyte.<sup>37, 62-64</sup> Due to the lower ionic conductivities, the ESRs of ESs using neutral electrolytes are generally lower than those using H<sub>2</sub>SO<sub>4</sub> or KOH electrolyte.<sup>37, 63, 64</sup> However, carbon-based ESs with neutral electrolytes could give larger operating voltages due to the increased electrolyte stable potential windows (ESPWs) when compared to both the acidic and alkaline aqueous electrolytes.<sup>9, 54, 55</sup> As discussed, a neutral electrolyte has lower H<sup>+</sup> and OH<sup>-</sup> concentrations compared to acidic and alkaline electrolytes, therefore a higher overpotential for hydrogen and oxygen evolution reactions can be expected, suggesting an increased ESPW. For example, Demarconnay et al.<sup>55</sup> showed an excellent cycle-life with 10,000 charging/discharging cycles at a high cell voltage of 1.6 V for a symmetric active carbon-based ES with 0.5 M Na<sub>2</sub>SO<sub>4</sub> electrolyte. Using nitrogen and oxygen doping for carbon nanofiber electrodes, Zhao et al.<sup>61</sup> further increased the ES cell voltage to 1.8 V and achieved a high energy density of  $29.1 \text{ Wh kg}^{-1}$  at a power density of  $450 \text{ W kg}^{-1}$  with 1 M Na<sub>2</sub>SO<sub>4</sub> as the electrolyte. When using 1 M Li<sub>2</sub>SO<sub>4</sub> electrolyte, Fic et al.<sup>9</sup> obtained an even higher working voltage of 2.2 V for a carbon-based symmetrical ES. Their ES could be cycled for 15,000 cycles without any significant capacitance fade. To investigate the degradation of carbon-based ESs under high voltage operation in Li<sub>2</sub>SO<sub>4</sub> electrolyte, some accelerated ageing tests were performed by Ratajczak et al.<sup>110, 111</sup> They found that gases (e.g., CO<sub>2</sub> and CO) could start to evolve at a cell voltage higher than 1.5 V due to the oxidation of carbon electrode material. It was thus concluded the carbon-based ESs with aqueous 1 M Li<sub>2</sub>SO<sub>4</sub> could operate safely up to a cell voltage of 1.5 V, which was lower than that reported by other work.<sup>9, 61</sup> Noticeably, the current



collector in this study was stainless steel instead of a gold collector as reported in other studies,<sup>9, 61</sup> which may be the reason why the results were different. Since the operating voltages obtained for neutral electrolyte-based ESs are remarkably higher than those with KOH and H<sub>2</sub>SO<sub>4</sub> electrolytes (usually 0.8–1 V for carbon-based symmetrical ESs) and neutral electrolytes are generally less corrosive than the strong acidic and alkaline electrolytes, neutral electrolyte-based symmetric carbon ESs have been identified as the most promising candidates in terms of producing a lower environmental impact and higher energy density.

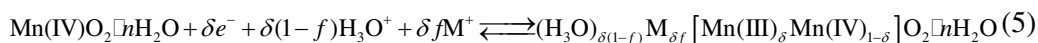
For neutral electrolytes, whether a high salt concentration can be obtained or not is an important concern. This is not an issue for acidic and alkaline electrolytes since they can achieve a high concentration (e.g., 6 M for KOH electrolyte). Normally, highly concentrated electrolytes are generally used for practical ESs to ensure a high performance. However, some salts (e.g., K<sub>2</sub>SO<sub>4</sub>) cannot achieve such a high concentration, especially when it is used in lower temperatures. In fact, the effect of a neutral electrolyte on ES performance is also dependent on the type of electrolyte.<sup>9, 112</sup>

To understand the effect of different ions on the performance of carbon-based ESs, some comparative studies for neutral electrolytes with different salts have been carried out. However, some controversial results have been noticed in this area. For example, for alkali metal sulfate electrolytes including Li<sub>2</sub>SO<sub>4</sub>, Na<sub>2</sub>SO<sub>4</sub> and K<sub>2</sub>SO<sub>4</sub>, several studies found that the ES specific capacitance values followed the order: Li<sub>2</sub>SO<sub>4</sub> > Na<sub>2</sub>SO<sub>4</sub> > K<sub>2</sub>SO<sub>4</sub>,<sup>9, 113</sup> while other research did not show such a behaviour.<sup>114</sup> There are other factors, such as the material preparation method and measurement conditions such as voltage scan rate/discharge rate that might also affect the results. In this regard, further work may be needed to further clarify the salt effect on the ES performance. As for the ESR, it was found that the ESR increase followed the order of the resistivity of bulk electrolytes, i.e., Li<sub>2</sub>SO<sub>4</sub> > Na<sub>2</sub>SO<sub>4</sub> > K<sub>2</sub>SO<sub>4</sub>,<sup>113, 114</sup> leading to increasing order of both power density and rate performance: Li<sub>2</sub>SO<sub>4</sub> < Na<sub>2</sub>SO<sub>4</sub> < K<sub>2</sub>SO<sub>4</sub>.<sup>114</sup>

Regarding the effect of anions in neutral electrolytes, Chae et al.<sup>113</sup> found that for electrolytes with the same cation and concentration, changing anion from SO<sub>4</sub><sup>2-</sup> ion to Cl<sup>-</sup> ion could increase the specific capacitance due to the smaller size of Cl<sup>-</sup> ion compared to that of SO<sub>4</sub><sup>2-</sup> ion. Most recently, some new types of electrolyte, such as lithium, sodium, and potassium salts of silicotungstic acid (Li-SiW, Na-SiW and K-SiW), were explored as aqueous neutral electrolytes for EDLCs by Gao et al.<sup>115</sup> These electrolytes exhibited much higher ionic conductivities when compared to their counterpart with Cl<sup>-</sup>, SO<sub>4</sub><sup>2-</sup> or NO<sub>3</sub><sup>-</sup> anion. This is because of the larger amount of dissociated cations and the much greater anion mobility of the Keggin anions. A cell voltage of 1.5 V was achieved for carbon-based EDLCs with these neutral electrolytes.

### 3.1.3.2. Neutral electrolytes for pseudocapacitors

In neutral electrolytes, MnO<sub>2</sub>- and V<sub>2</sub>O<sub>5</sub>-based electrode materials have shown to be promising pseudocapacitive materials for ESs.<sup>116</sup> So far, MnO<sub>2</sub> is the most extensively studied pseudocapacitive material in neutral electrolytes. When MnO<sub>2</sub> was used as the electrode material, during charging/discharging process, Mn oxidation state could be varied between III and IV, accompanied by surface adsorption/desorption or intercalation/deintercalation of electrolyte cations M<sup>+</sup> (e.g., K<sup>+</sup>, Na<sup>+</sup> and Li<sup>+</sup>) as well as proton (H<sup>+</sup>). The process can be described by Equation

(8):<sup>117</sup>

Since the electrolyte ions are directly involved in the charge storage process, the nature of the neutral electrolytes is expected to have a significant influence on the pseudocapacitive performance.

Various factors of the neutral electrolytes, such as pH, the types of cation and anion species,<sup>117</sup> salt concentrations,<sup>118-120</sup> additives,<sup>121, 122</sup> and solution temperatures, have been found to have influence on the ES performance. Regarding the cation species, various alkaline metal or alkaline-earth metal cations have different ionic sizes and hydrated ion sizes, and thus have different diffusion coefficients and ionic conductivities, which are expected to have strong influences on both the specific capacitance and ESR of the ESs. However, the dependence of specific capacitance on cation species has not been fully understood due to variations in preparation methods and electrode material structures. Li et al.<sup>57</sup> reported the specific capacitance values and the corresponding energy and power densities of mesoporous MnO<sub>2</sub> oxide-based electrode was in an electrolyte order: Li<sub>2</sub>SO<sub>4</sub> > Na<sub>2</sub>SO<sub>4</sub> > K<sub>2</sub>SO<sub>4</sub>. This behaviour seems to be related to the order of bare (unsolvated) ion size of these alkali metal ions, i.e., Li<sup>+</sup> < Na<sup>+</sup> < K<sup>+</sup> (Table 1), indicating that a smaller ionic size is beneficial for increasing the specific capacitance. On the contrary, several studies using MnO<sub>2</sub> as an electrode material showed that Na salts (e.g., Na<sub>2</sub>SO<sub>4</sub>,<sup>118, 119</sup> and NaCl<sup>123</sup>) gave higher specific capacitances than those of Li and K salts. When K<sub>x</sub>MnO<sub>2</sub>·nH<sub>2</sub>O was used as the electrode material, K<sub>2</sub>SO<sub>4</sub> salts could result in a higher specific capacitance than those of Na<sub>2</sub>SO<sub>4</sub> and Li<sub>2</sub>SO<sub>4</sub> salts.<sup>124</sup> Wen et al.<sup>120</sup> found no obvious change in specific capacitance when three different electrolytes (KClO<sub>4</sub>, NaClO<sub>4</sub>, and LiClO<sub>4</sub>) were used. It should be noted most studies used mass specific capacitance to compare the ES performances in different electrolytes. However, the mass specific capacitance value of an ES is also dependent on a series of factors, such as the structure (e.g., δ-MnO<sub>2</sub> or α-MnO<sub>2</sub>), morphology, preparation methods and the amount of the electrode materials. It is therefore not easy to identify the individual effect of cation species on the ES capacitance if mass specific capacitances are used for comparison. For example, different preparation methods can generally lead to electrode materials with different pore structure that may also affect the diffusion path of electrolyte ions and make the the whole process complicated. In this regard, further investigations using electrode materials with well-defined surfaces may be beneficial to understanding of the effect of cation species on the intrinsic capacitance of electrode materials. Furthermore, since the cation intercalation/deintercalation were involved in MnO<sub>2</sub>-based electrode materials, the scan rate of CV or charging/discharging current density might also have a pronounced influence on the obtained specific capacitance values.<sup>57, 125</sup> As identified, the ion intercalation/deintercalation are believed to be the rate-determining step during the charging/discharging process, and thus a lower scan rate or charging/discharging rate may favor the intercalation/deintercalation process. In this case, the bare cation size, which is closely associated with the intercalation/deintercalation process, may play a dominant role. For example, the electrolytes containing Li<sup>+</sup> ions would be beneficial to ES performance due to the smaller Li<sup>+</sup> ion size might favour the intercalation/deintercalation process.

Besides alkaline metal ions, the effect of alkaline-earth cations on ES performance has also been studied.<sup>119, 126</sup> For example, Xu et al.<sup>119</sup> reported that the specific capacitance of MnO<sub>2</sub> was doubled by replacing univalent cation (i.e., Li<sup>+</sup>, Na<sup>+</sup> and K<sup>+</sup>) with bivalent cation (i.e., Mg<sup>2+</sup>, Ca<sup>2+</sup> and Ba<sup>2+</sup>). This observation was

explained by the fact that when one bivalent alkaline-earth metal cation was intercalated into  $\text{MnO}_2$ , it could balance the valence change of two Mn ions from (IV) to (III), whereas one univalent alkaline metal cation could only balance the valence change of one Mn ion.

Regarding the anions, Boisset et al.<sup>127</sup> carried out in-depth research on the effect of anions on ES performance in neutral aqueous electrolytes containing different lithium salts, in which Birnessite-type and Cryptomelane-type  $\text{MnO}_2$  electrode materials were used. As shown in Fig. 6, ten different lithium salts based on mineral anions and organic anions are investigated in their study. The basicity and the volume of the anion in each aqueous lithium salt electrolyte were found to be the two key parameters in controlling the electrochemical properties (e.g., oxidation and reaction currents) of  $\text{MnO}_2$  electrodes (Fig. 7).

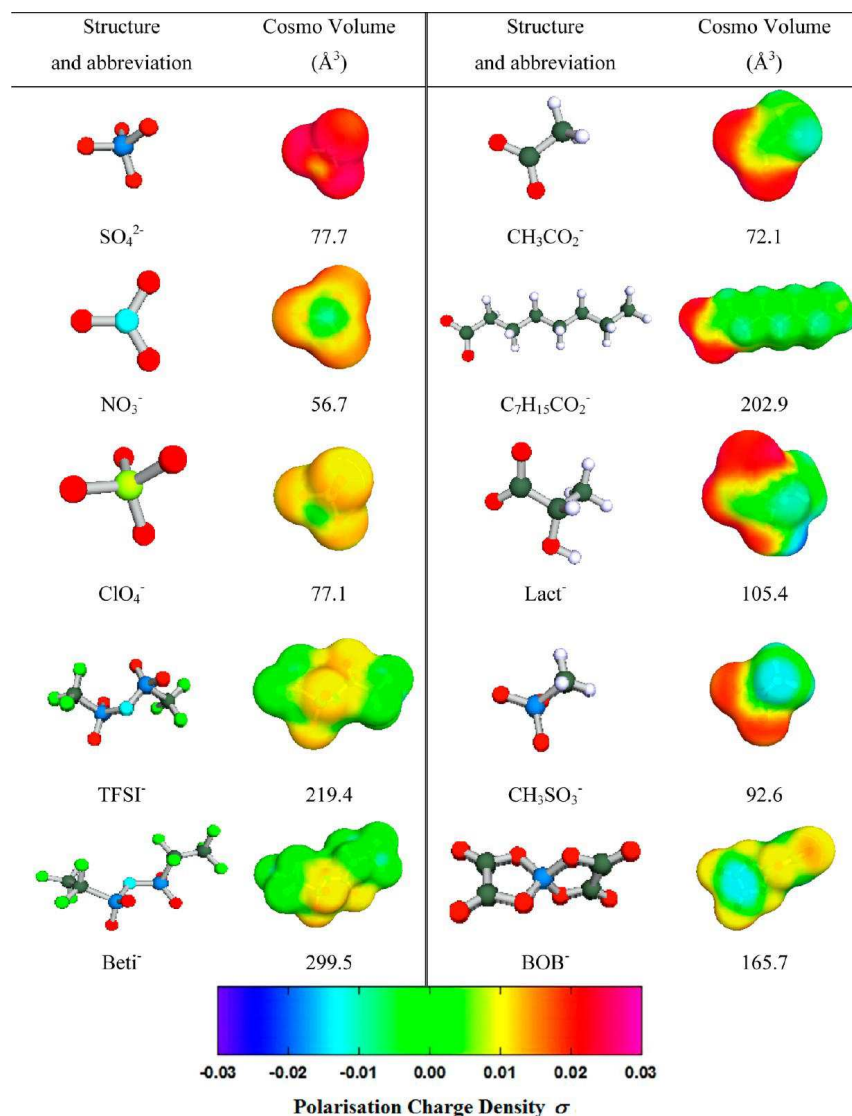


Fig. 6 Structure, abbreviation, and Cosmo volume evaluated by CosmothermX Interface of studied anion ( $\text{X}^-$ ) in Lithium salt ( $\text{LiX}$ ). Reprinted with permission from Ref. 127. Copyright 2013 American Chemical Society.

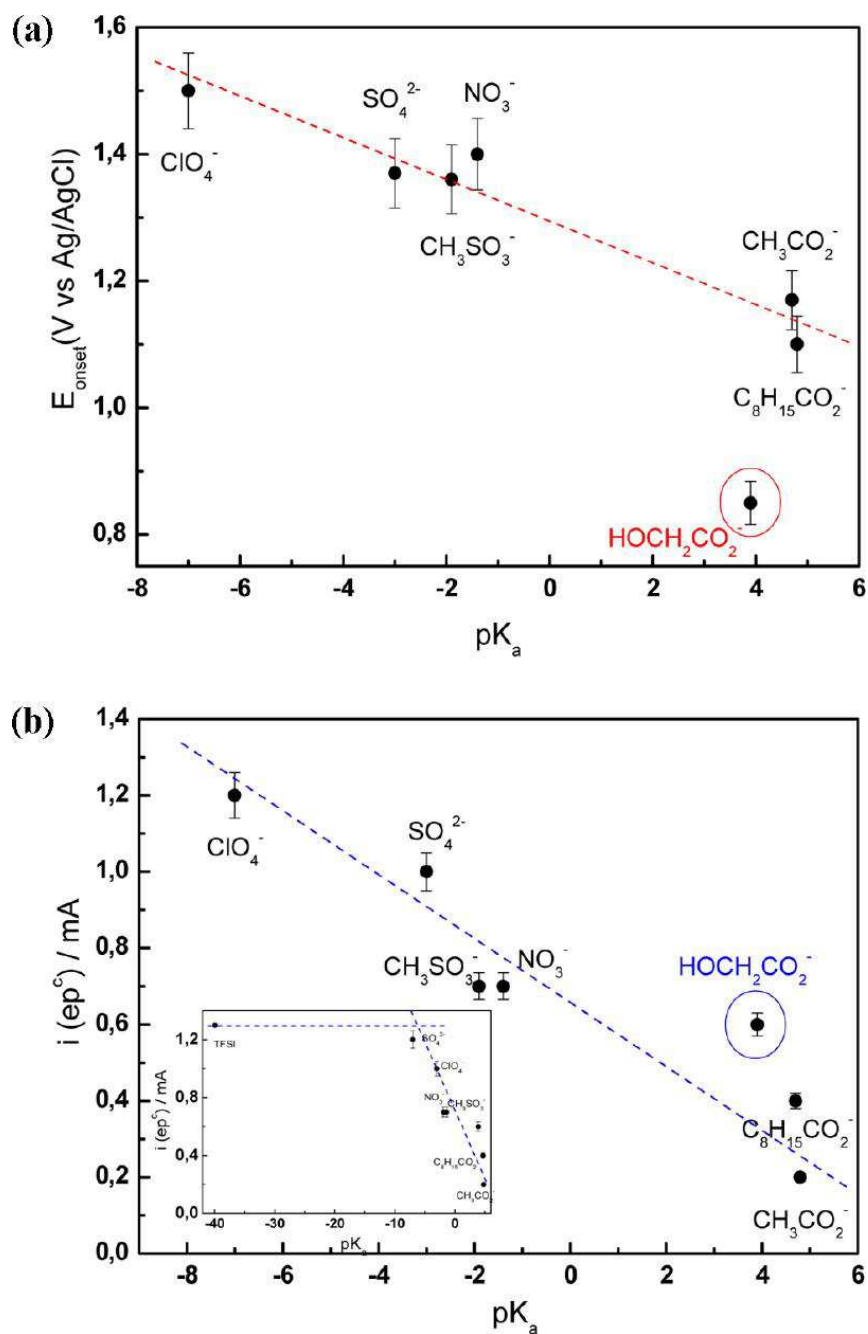


Fig. 7 Variation of the potential limit (a) on oxidation,  $E_{\text{onset}}$ , or (b) in reduction, expressed by  $i(\text{ep}^c)$  as a function of the anion (denoted  $\text{X}^-$ ) basicities expressed by their  $\text{pK}_a$  values ( $\text{HX}/\text{X}^-$ ). Reprinted with permission from Ref. 127. Copyright 2013 American Chemical Society.

Regarding the temperature effect, unlike carbonaceous materials that were generally stable at a wide temperature range,  $\text{MnO}_2$  electrode materials were found to undergo some structural change at high temperatures during the charging/discharging process, which could negatively affect the cycling stability.<sup>59</sup> Therefore, the effect of

electrolyte temperature on the pseudocapacitive behaviour especially the cycling stability of  $\text{MnO}_2$ -based ESs should be considered one of the important issues.

In the efforts to improve ES performance, other strategies such as adding additives into the neutral electrolytes have also been explored.<sup>121</sup> For example, Komaba et al.<sup>121</sup> found that upon addition of small amount of  $\text{Na}_2\text{HPO}_4$ ,  $\text{NaHCO}_3$ , or  $\text{Na}_2\text{B}_4\text{O}_7$  into  $\text{Na}_2\text{SO}_4$  electrolyte, the specific capacitance of the birnessite electrode could be increased from  $190 \text{ F g}^{-1}$  to  $200\text{--}230 \text{ F g}^{-1}$  at  $1.0 \text{ A g}^{-1}$ , and at the same time the cyclability was also significantly improved ( $>1000$  cycles). This was attributed to the formation of a protection layer on the birnessite, which could inhibit Mn dissolution due to the optimized pH buffer provided by the additives (Fig. 8).

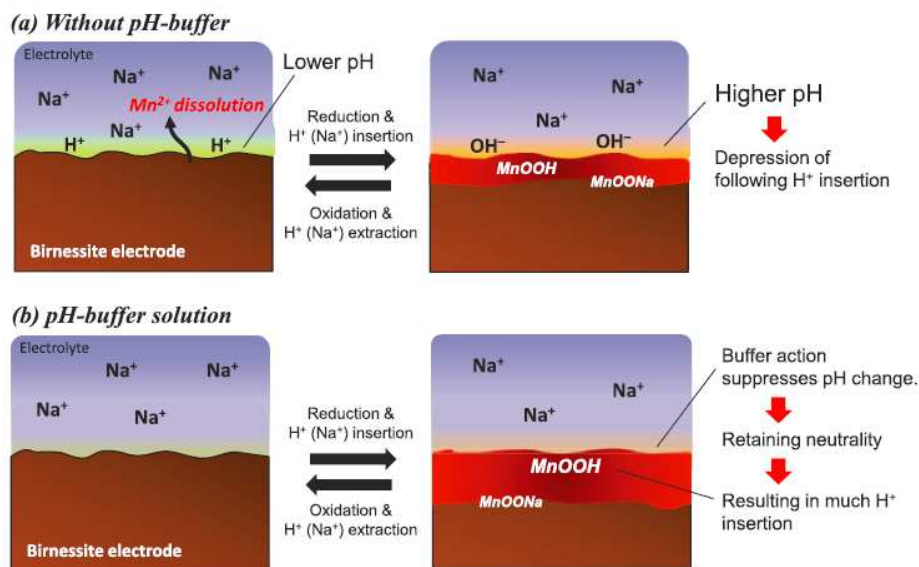


Fig. 8 Schematic illustration of electrode/electrolyte structure in aqueous electrolyte solutions (a) without and (b) with buffer action. Reproduced by permission of The Electrochemical Society from Ref. 121.

Regarding the ES cycle-life in neutral electrolytes, since the charge storage process of most pseudocapacitive materials (e.g.,  $\text{MnO}_2$ ) involves intercalation/deintercalation of ions from the electrolyte, the material structure change upon repeated charging/discharging process is considered as an important issue that could strongly affect the cycle life of the electrode materials.<sup>124</sup>

Besides  $\text{MnO}_2$ , the effect of electrolytes on other pseudocapacitive metal oxides (e.g.,  $\text{V}_2\text{O}_5$ ,<sup>128</sup>  $\text{Fe}_3\text{O}_4$ ,<sup>58</sup>  $\text{SnO}_2$ ,<sup>129</sup>  $\text{ZnO}$ ,<sup>130</sup> and  $\text{RuO}_2$ <sup>60</sup>) and ECPs<sup>131, 132</sup> have also been reported although they have not received as much attention as those with  $\text{MnO}_2$ . Actually, the electrolyte effect is strongly dependent on the type of electrode material. For example, although  $\text{RuO}_2$ -based electrodes were normally used in acid electrolytes, it was found that  $\text{RuO}_2$ -based ESs with a neutral aqueous electrolyte (i.e.,  $1 \text{ M Na}_2\text{SO}_4$ ) could also achieve a high operating voltage of  $1.6 \text{ V}$ , and thus a relatively high energy density of  $19 \text{ Wh kg}^{-1}$  at a power density of  $500 \text{ W kg}^{-1}$ .<sup>60</sup> In addition, the use of neutral electrolytes is also beneficial to various ECP-based ESs due to the mild pH condition.<sup>131</sup>

### 3.1.2.3. Neutral electrolytes for hybrid capacitors

Neutral electrolytes have also been extensively applied for asymmetric ESs, allowing for a larger operative voltage and thus a higher energy density. As identified, most pseudocapacitive materials (e.g.,  $\text{MnO}_2$ ) have high specific capacitances, although their potential windows are limited, which restricts the cell voltage and thus the energy density of symmetrical ESs if using these materials. For  $\text{MnO}_2$ -based symmetrical ESs, the cell voltage is about 1 V in most cases. By replacing the negative electrode with other different electrode material (e.g., activated carbons) which has a complementary potential window to that of  $\text{MnO}_2$ , the cell voltage can be significantly increased through extending to a more negative voltage.<sup>72</sup>

Compared with the previously mentioned asymmetric ESs using a battery-type positive electrode (e.g., AC// $\text{PbO}_2$  and AC// $\text{Ni(OH)}_2$ ) in the strong acidic or alkaline electrolyte, asymmetric AC// $\text{MnO}_2$  ESs in neutral electrolytes have a great advantage of long cycle life due to the pseudocapacitive behaviour of  $\text{MnO}_2$ . Since the early work on asymmetric AC// $\text{MnO}_2$  ESs using neutral electrolytes reported by Hong et al.<sup>133</sup> and Brousse et al.,<sup>134</sup> considerable efforts have been made to focus on the development of neutral electrolyte-based asymmetric ESs.<sup>135</sup> To date, various types of negative and positive electrode materials have been explored for asymmetric ESs using neutral aqueous electrolytes (mostly sulfate salt-based electrolytes).<sup>135-140</sup> These asymmetric ESs could reach an operative cell voltage range of 1.8–2.0 V,<sup>135-140</sup> which are higher than those reported for the asymmetric ECs with strong acidic or alkaline electrolytes. Because of the increased cell voltage, most of the reported energy densities could be achieved to high values above 20 Wh  $\text{kg}^{-1}$ ,<sup>135-140</sup> and some reported values could even be as high as 50 Wh  $\text{kg}^{-1}$ .<sup>138</sup> Excitingly, some of these reported energy density values can be comparable to or higher than those of the organic electrolyte-based EDLCs. Therefore, if other issues (e.g., cycle life and rate performance) could be further improved, these asymmetric ESs with neutral electrolytes should be very promising alternatives for commercial organic electrolyte-based EDLCs.

Recently, it was reported a very high cell voltage of about 4 V could be seen in neutral electrolytes such as  $\text{Li}_2\text{SO}_4$  and  $\text{LiCl}$  by using a battery-type Li negative electrode coupled with an appropriate positive electrode material (e.g. AC and  $\text{MnO}_2$ ).<sup>141</sup> Since the metallic Li electrode could not work directly in contact with aqueous electrolyte, a water-stable multilayered Li negative electrode (protected Li electrode) might be used.<sup>141</sup>

To conclude, using neutral aqueous electrolytes in ESs can not only solve the corrosion issues but also provide a cost effective and environmentally friendly way to increase the operating voltage and thereby the energy density. However, more improvement in ES performance with neutral electrolytes is still needed to further increase the energy density and cycle-life.

## 3.2. Organic electrolytes

Although extensive studies have focused on the aqueous electrolyte-based ESs in the academic research, organic electrolyte-based ESs are currently dominating the

commercial market owing to their high operation potential window typically in the range of 2.5 to 2.8 V. The increased operation cell voltage can provide a significant improvement in both the energy and power densities. Furthermore, using organic electrolytes allows the use of cheaper materials (e.g., Al) for the current collectors and packages. Typical organic electrolytes for the commercial EDLCs consist of the conductive salts (e.g., tetraethylammonium tetrafluoroborate (TEABF<sub>4</sub>)) dissolved in the ACN or PC solvent. Table 3 lists the typical ES systems using different organic electrolytes and their associated performances.

Table 3 Organic electrolyte-based supercapacitors and their performance

Electrolyte	Electrode materials	Specific capacitance (F g <sup>-1</sup> )	Cell voltage (V)	Energy density (Wh kg <sup>-1</sup> )	Power density (W kg <sup>-1</sup> )	Temp. (°C)	Ref.
<b>Carbon-based symmetric ESs:</b>							
1 M TEABF <sub>4</sub> /ACN	highly porous interconnected carbon nanosheets	~120–150 at 1 mV s <sup>-1</sup>	2.7	25	25000–2 7000	–	142
1 M TEABF <sub>4</sub> /PC	graphene–CNT composites	110 at 1 A g <sup>-1</sup>	3	34.3	400	–	143
1 M TEABF <sub>4</sub> /HFIP	AC	110 at 1 mV s <sup>-1</sup>	–	–	–	–	144
0.7 M TEABF <sub>4</sub> /ADN	AC	25 at 20 mV s <sup>-1</sup>	3.75	~28	–	RT	145
1.6 M TEAODFB/PC	AC	21.4 at 1 A g <sup>-1</sup>	2.5	~28 (20 °C)	~1000	–40 to 60	146
1 M TEMABF <sub>4</sub> /(PC-PS 95:5)	microporous TiC-CDC	100 at 10 mV s <sup>-1</sup> (60 °C)	2.7	~25–27	~1000	–45 to 60	147
1 M SBPBF <sub>4</sub> /ACN	carbon (provided by Batscap)	109	2.3	–	–	–30 to 60	148
1.5 M SBPBF <sub>4</sub> /PC	AC	122 at 0.1 A g <sup>-1</sup>	3.5	52	–	RT	149
1 M LiPF <sub>6</sub> /(EC-DE C 1:1)	heteroatom doped porous carbon flakes	126 at 1 A g <sup>-1</sup>	3	29	2243	RT	150
1 M NaPF <sub>6</sub> /(EC-D MC-PC-EA 1:1:1:0.5)	microporous carbide derived carbon	120 at 1 mV s <sup>-1</sup>	3.4	~40	~90	–40 to 60	151
<b>Pseudocapacitive electrode material-based symmetric ESs:</b>							
1 M LiPF <sub>6</sub> /(EC-DE C 1:1)	nanoporous Co <sub>3</sub> O <sub>4</sub> –graphene composites	424.2 at 1 A g <sup>-1</sup>	–	–	–	RT	152
1 M LiClO <sub>4</sub> /PC	MoO <sub>3</sub> nanosheets	540 at 0.1 mV s <sup>-1</sup>	–	–	–	–	153

	heterostructured						
0.5 M	poly(3,6-dithien-2-yl-9- <i>H</i> -carbazol-9-yl acetic acid)/TiO <sub>2</sub> nanoparticles composite	462.88 at 2.5 mA cm <sup>-2</sup>	1.2	89.98	–	RT	154
Bu <sub>4</sub> NBF <sub>4</sub> /ACN							
0.5 M	PANI/graphite	~420 at 50 mV s <sup>-1</sup>	1	–	–	RT	155
LiClO <sub>4</sub> /PC							
<b>Asymmetric ESs:</b>							
1 M	non-porous activated mesophase carbon microbeads//AC	–	3.5	~47	~100	–	156
SBPBF <sub>4</sub> /PC							
1.5 M	non-porous activated mesophase carbon microbeads/ graphitized carbon commercial AC	–	4	~60	~30	RT	157
TEMABF <sub>4</sub> /PC							
1 M	(MSP-20)//mesoporous Nb <sub>2</sub> O <sub>5</sub> –carbon nanocomposite	–	3.5	74	~100	–	158
LiPF <sub>6</sub> /EC-DMC (1:1:1)							
1 M	Fe <sub>3</sub> O <sub>4</sub> –graphene nanocomposite//3D graphene	–	3	147	150	RT	159
LiPF <sub>6</sub> /EC-DMC (1:1:1)							
1 M	porous graphitic carbon//Li <sub>4</sub> Ti <sub>5</sub> O <sub>12</sub>	–	3	~55	~110	–	160
LiPF <sub>6</sub> /EC-DMC (1:1:1)							
1 M	MnO <sub>2</sub> nanorodes–rGO//V <sub>2</sub> O <sub>5</sub> NWs–rGO	36.9	2	15.4	436.5	RT	161
LiTFSI/ACN							

Note: A//B means A is the negative electrode and B is the positive electrode.

Abbreviations: Temp: temperature; RT, room temperature; CNT, carbon nanotube; HFIP, 1,1,1,3,3,3-Hexafluoropropan-2-ol; AC, activated carbon; ADN, adiponitrile; TEAODFB, Tetraethylammonium difluoro(oxalato)borate; TEMABF<sub>4</sub>: triethylmethylammonium tetrafluoroborate; PS, 1,3-propylene sulfite; TiC-CDC: titanium carbide derived carbon; SBPBF<sub>4</sub>, spiro-(1,1')-bipyrrrolidinium tetrafluoroborate; EC: ethylene carbonate; DEC: diethyl carbonate; DMC: dimethyl carbonate; EA, ethyl acetate; PANI, polyaniline; NWs, nanowires; rGO, reduced graphene oxide.

However, there are other issues that should be considered when using the organic electrolytes for ESs. Compared to ESs using aqueous electrolytes, ES with organic electrolytes usually have higher cost, smaller specific capacitance, lower conductivity, and safety concerns related to the flammability, volatility and toxicity. Furthermore, organic electrolyte requires complicated purification and assembling processes under strictly-controlled environment to remove any residual impurities (e.g., water)




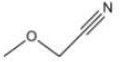
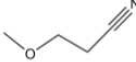
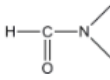
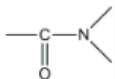
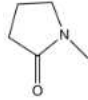
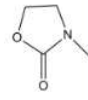
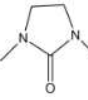
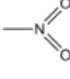
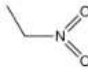
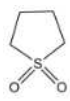

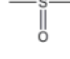
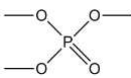
that can lead to large performance degradation and serious self-discharge issues.<sup>22</sup>

### 3.2.1. General composition, properties and ES performance of organic electrolytes

Organic electrolytes for ESs typically consist of conducting salts dissolved in organic solvents. Table 4 and 5 show some commonly used salts and solvents, respectively, for the organic electrolytes. For aiding in developing understanding in a convenient way, the corresponding abbreviations of these salts and solvents are also given in the tables. Similar to aqueous electrolyte-based ESs, the nature of salts and solvents, such as ion size, ion-solvent interaction, conductivity, viscosity and ESPW, has profound influences on the performance of organic electrolyte-based ESs, which will be discussed below in more detail. In the literature, most studies related to organic electrolytes have focused on EDLCs. With advances in the development of new electrode materials and electrolytes in recent years, research on organic electrolytes for pseudocapacitors and hybrid ESs has also received increasing attention.

Table 4 Summary of abbreviations, physical properties, limiting electrochemical reduction and oxidation potentials of commonly used organic solvents containing 0.65 M TEABF<sub>4</sub> at 25 °C.

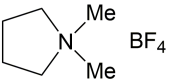
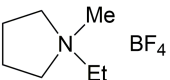
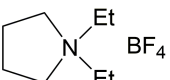
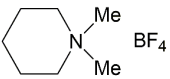
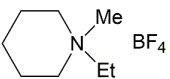
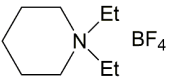
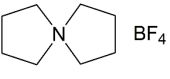
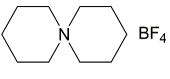
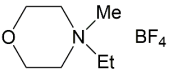
Solvent	$\epsilon_r$	$\eta$ (cp)	bp (°C)	mp (°C)	MW	$\sigma$ (mS cm <sup>-1</sup> )	$E_{red}$ (V vs.SCE)	$E_{ox}$
Propylene carbonate (PC)	65	2.5	242	-49	102	10.6	-3.0	3.6
Butylenes carbonate (BC)	53 <sup>a</sup>	3.2 <sup>a</sup>	240 <sup>a</sup>	-53 <sup>a</sup>	116	7.5	-3.0	4.2
$\gamma$ -butyrolactone (GBL)	42	1.7	204	44	86	14.3	-3.0	5.2
$\gamma$ -valerolactone (GVL)	34 <sup>a</sup>	2.0 <sup>a</sup>	208 <sup>b</sup>	-31 <sup>b</sup>	100	10.3	-3.0	5.2
Acetonitrile (ACN)	36	0.3	82	-49	41	49.6	-2.8	3.3
Propionitrile (PN)	26 <sup>a</sup>	0.5 <sup>a</sup>	97	-93	55	insoluble		
Glutaronitrile (GLN)	37 <sup>a</sup>	5.3 <sup>a</sup>	286 <sup>b</sup>	-29 <sup>b</sup>	94	5.7	-2.8	5.0

Adiponitrile (ADN)		30 <sup>a</sup>	6.0 <sup>a</sup>	295 <sup>b</sup>	2 <sup>b</sup>	108	4.3	-2.9	5.2
Methoxyacetonitrile (MAN)		21 <sup>a</sup>	0.7 <sup>a</sup>	120 <sup>b</sup>	-35 <sup>a</sup>	71	21.3	-2.7	3.0
3-methoxypropionitrile (MPN)		36 <sup>a</sup>	1.1 <sup>a</sup>	165 <sup>b</sup>	-57 <sup>a</sup>	85	15.8	-2.7	3.1
N,N-dimethylformamide (DMF)		37	0.8	153	-61	73	22.8	-3.0	1.6
N,N-dimethylacetamide (DMA)		38	0.9	166	-20	87	15.7		
N-methylpyrrolidinone (NMP)		32	1.7	202	-24	99	8.9		
N-methyloxazolidinone (NMO)		78 <sup>c</sup>	2.5 <sup>c</sup>	270 <sup>b</sup>	15 <sup>b</sup>	101	10.7	-3.0	1.7
N,N'-dimethylimidazolidinone (DMI)		38 <sup>d</sup>	1.9 <sup>d</sup>	226 <sup>d</sup>	8 <sup>d</sup>	114	7.0	-3.0	1.2
Nitromethane (NM)		38	0.6	101	-29	61	33.8	-1.2	2.7
Nitroethane (NE)		28 <sup>a</sup>	0.7 <sup>a</sup>	115 <sup>b</sup>	-90 <sup>b</sup>	75	22.1	-1.3	3.2
Sulfolane (TMS)		43	10.0 (30°C)	287	28	120	2.9	-3.1	3.3
3-methylsulfolane (3MS)		29 <sup>e</sup>	11.7 <sup>e</sup>	276 <sup>b</sup>	6 <sup>b</sup>	134	Insoluble		
Dimethylsulfoxide (DMSO)		47	2.0	189	19	78	13.9	-2.9	1.5
Trimethyl phosphate (TMP)		21 <sup>a</sup>	2.2 <sup>a</sup>	197 <sup>b</sup>	-46 <sup>b</sup>	140	8.1	-2.9	3.5

Physical properties are cited from Ref. 162 and 163 except <sup>a</sup> Ref. 26, <sup>b</sup> Ref. 164, <sup>c</sup> Ref. 165, <sup>d</sup> Ref. 166 and <sup>e</sup> Ref. 167. Abbreviations:  $\epsilon_r$ , relative permittivity;  $\eta$ , viscosity; bp, boiling point; mp, melting point; MW, molecular weight;  $\sigma$ , ionic conductivity;  $E_{red}$ , limiting reduction potential;  $E_{ox}$ , limiting oxidation potential (glassy carbon electrode

was used as a working electrode to measure the  $E_{\text{red}}$  and  $E_{\text{ox}}$ ).

Table 5 Summary of abbreviations, electrolyte conductivities, and limiting electrochemical reduction and oxidation potentials of some quaternary ammonium or phosphonium tetrafluoroborate conducting salts (0.65 M) in PC at 25 °C.<sup>26</sup>

Electrolyte	$\sigma$ (mS $\text{cm}^{-1}$ )	$E_{\text{red}}$ (V vs.SCE)	$E_{\text{ox}}$ (V vs.SCE)	Electrolyte	$\sigma$ (mS $\text{cm}^{-1}$ )	$E_{\text{red}}$ (V vs.SCE)	$E_{\text{ox}}$ (V vs.SCE)
Methyl ammonium tetrafluoroborate ( $\text{Me}_4\text{N BF}_4$ )	2.41*	-3.10*	3.50*		10.36	-3.00	3.65
Triethylmethylammonium Tetrafluoroborate ( $\text{Me}_3\text{EtN BF}_4$ )	10.16	-3.00	3.60		10.82	-3.00	3.70
Tetrafluoroboric acid dimethyl diethylammonium ( $\text{Me}_2\text{Et}_2\text{N BF}_4$ )	10.34	-3.00	3.65		10.40	-3.00	3.60
Triethylmethylammonium Tetrafluoroborate ( $\text{MeEt}_3\text{N BF}_4$ )	10.68	-3.00	3.65		10.20	-3.05	3.65
Tetraethylammonium tetrafluoroborate ( $\text{Et}_4\text{N BF}_4$ or TEA $\text{BF}_4$ )	10.55	-3.00	3.65		10.40	-3.05	3.70
Tetrapropyl ammonium tetrafluoroborate ( $\text{Pr}_4\text{N BF}_4$ )	8.72	-3.00	3.65		10.17	-3.05	3.60
$\text{MeBu}_3\text{N BF}_4$	7.80				10.94	-3.00	3.60
Tetraethylammonium tetrafluoroborate ( $\text{Bu}_4\text{N BF}_4$ )	7.23	-3.05	3.65		9.67	-3.00	3.60
$\text{Hex}_4\text{N BF}_4$	5.17	-3.10	3.85		8.78	-3.00	3.60
Tetramethylammonium	9.21	-3.05	3.60				

tetrafluoroborate (Me <sub>4</sub> P BF <sub>4</sub> )			
Tetraethyl	10.52	-3.00	3.60
phosphonium tetrafluoroborate (Et <sub>4</sub> P BF <sub>4</sub> )			
Pr <sub>4</sub> P BF <sub>4</sub>	8.63	-3.05	3.60
Tetrabutylphospho nium tetrafluoroborate (Bu <sub>4</sub> P BF <sub>4</sub> )	7.14	-3.05	3.80

Abbreviations:  $\sigma$ , ionic conductivity;  $E_{\text{red}}$ , limiting reduction potential;  $E_{\text{ox}}$ , limiting oxidation potential (glassy carbon electrode was used as a working electrode to measure the  $E_{\text{red}}$  and  $E_{\text{ox}}$ ).

### 3.2.1.1. Organic electrolytes for electrical double-layer capacitors

From Tables 2 and 3, it can be seen that for carbon-based ESs, the specific capacitances obtained in organic electrolytes are normally lower than those in aqueous electrolytes.<sup>168-170</sup> Generally, organic electrolytes have larger solvated ion sizes and lower dielectric constants, which can lead to lower EDL capacitance values. Furthermore, the pseudocapacitance contribution of carbon-based electrode materials is small or negligible in organic electrolytes such as the TEABF<sub>4</sub>/ACN.<sup>168, 171</sup> This can be understood by considering the nature of carbon surface functionalities. For example, the pseudocapacitive contribution of AQ-modified carbons requires the proton participation, but this is not favoured in the aprotic organic electrolytes, resulting in lower specific capacitance.

As mentioned before, the specific capacitance of an EDLC depends not only on the specific surface area but also on the pore size/size distribution of the carbon materials.<sup>7</sup> The accessibility of pores is closely related to the properties of organic electrolyte, such as the sizes of cation and anion species, and the ion-solvent interaction. The presence of pores in a carbon material with very small particle size may increase the specific surface area, but it can also limit the accessibility of electrolyte ions. Especially the larger organic ions can not easily get access with the small pores, resulting in a negative effect on specific capacitance. Therefore, it is important to match the pore size of carbon materials with the size of electrolyte ions to maximize the specific capacitance. With respect to this, considerable efforts have been devoted to understand the relationship between ion size and the capacitive behaviour of carbons with different pore size distributions, and then optimize the matching between pore size and electrolyte ion size.<sup>7, 169, 170</sup> In addition, both the sizes of solvated ions and bare (desolvated) ions should also be considered. As observed, the desolvation or distortion of ion solvation shell when the ion entered into the pores with a size close to the size of desolvated ion could lead to an anomalous increase in the specific capacitance of EDLCs.<sup>7</sup> Besides the specific capacitance, other properties such as the ESR, charging/discharging rate and power density should also be

considered when optimizing the pore structures and designing the electrolytes.

Recently, as discussed by Jiang et al.,<sup>172</sup> theoretical modeling and simulations of the EDL in organic electrolytes have received increasing attention, which may provide useful guidance for EDLC design from a microscopic point of view. These theoretical approaches using molecular dynamics (MD) simulation, density functional theory (DFT) calculations and Monte Carlo (MC) simulation, gave some insight into the solvation of ions in organic solvents,<sup>173</sup> the EDL structure and capacitance,<sup>173</sup> the effect of carbon pore size<sup>174</sup> and their morphologies.<sup>175</sup> In parallel, a number of experimental approaches on the electrolyte/electrode interactions have also been carried out in order to give a deeper understanding of the electrolyte behaviour under working condition.<sup>173, 176-181</sup> In this regard, various instrumental analysis methods, including nuclear magnetic resonance (NMR),<sup>176-179</sup> quartz-crystal microbalance (QCM),<sup>180</sup> *in-situ* Raman microspectrometry,<sup>182</sup> and *in-situ* small angle neutron scattering (SANS),<sup>181</sup> were also employed for the performance analysis. With the help of these analysis methods, fundamental understanding of ion dynamics during charging/discharging process,<sup>177-180</sup> local ion structures at the electrolyte/electrode interface,<sup>173, 177</sup> ion electroadsorption,<sup>181</sup> and pore size effect<sup>183</sup> have been greatly advanced.

The ESPW of the organic electrolyte is a rather important property that determines the ES operation cell voltage, then the energy and power densities. In fact, the ESPW of an organic electrolyte depends on several factors, including the type of conducting salts (i.e., cation and anion),<sup>26</sup> solvent,<sup>26</sup> and impurities especially the trace amount of water.<sup>184</sup> The ESPW could be obtained through both experimental methods<sup>26</sup> and theoretical methods.<sup>185, 186</sup> It should be noted that for fundamental research, the experimental measurements for determining the ESPW are normally carried out on the Pt or glassy carbon electrode, which are quite different from the actual electrodes (e.g., porous carbons) in EDLCs. The obtained EDLC voltage windows are usually much lower than those obtained on the Pt or glassy carbon electrode.

Aging and the related failure of organic electrolyte-based EDLCs are also important issues needing to be addressed. The degradation is mainly due to the following reasons: (1) Wide operation cell voltage could accelerate the oxidation of electrode materials. In order to increase the energy density, the higher the operation cell voltage, the higher the energy density. However, when the cell voltage is higher than the typical values of 2.5–2.8 V such as above 3 V, the electrode material oxidation may happen. This could lead to gas evolution due to the electrolyte decomposition and carbon electrochemical oxidation;<sup>3, 187</sup> (2) the electrolyte ion intercalation<sup>188</sup> or the electrochemical reaction of the organic electrolytes<sup>187</sup> could also cause the degradation of the ES performance; and (3) harsh working conditions (e.g., high peak temperature and working voltage) may cause the degradation of ES performance. Therefore, understanding the aging and failure mechanisms will be beneficial to the development of ESs with wider voltage windows. In addition, from the point of view of safety and reliability, it is also important to have a better understanding of the ES aging behavior. In the effort to understand the failure mode, Ishimoto et al.<sup>3, 187</sup> separately analyzed the gases evolved from the positive and negative compartments in an H-type cell after float-tests (Fig. 9). Two main gaseous products (CO<sub>2</sub> and CO) were found in the positive compartment while H<sub>2</sub>, propylene, CO<sub>2</sub> and CO were detected in the negative compartment at higher cell voltages above 3 V.

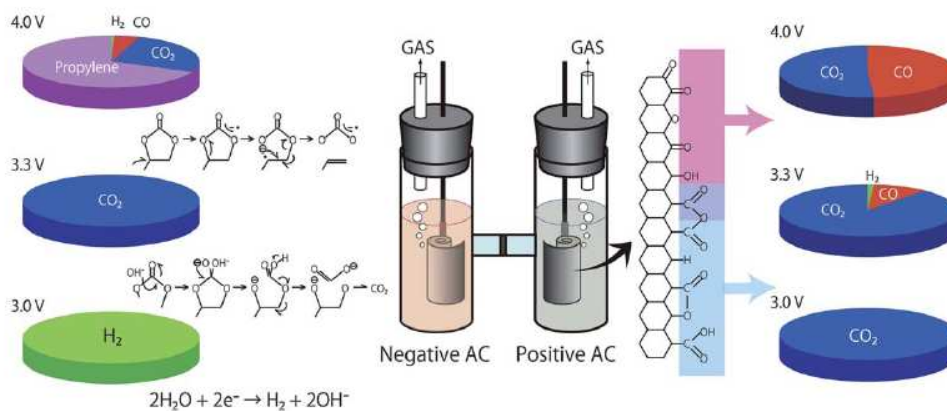


Fig. 9 Gas evolution from an EDLC cell upon over-voltage application. Reproduced from Ref. 3 with permission of The Royal Society of Chemistry.

Another drawback of organic electrolytes is their much lower ionic conductivity when compared to the aqueous electrolyte. For example, the ionic conductivity of the commonly used 1 M TEABF<sub>4</sub>/ACN electrolyte is 0.06 S cm<sup>-1</sup>, which is significantly lower than that of the 30 wt.% H<sub>2</sub>SO<sub>4</sub> electrolyte (0.8 S cm<sup>-1</sup> at 25°C).<sup>29</sup> The low conductivity of the organic electrolyte can result in ES a much higher ESR compared to the aqueous electrolyte-based ESs,<sup>171</sup> which then limits the maximum power density.

Since the ESs can work under a wide temperature range, the effect of electrolyte on their performance at different temperatures should be considered. Kötz et al.<sup>189</sup> reported that the specific capacitance of an EDLC with 1 M TEABF<sub>4</sub>/ACN did not change obviously while that of EDLC with TEABF<sub>4</sub>/PC as electrolyte did change significantly with decreasing temperature from 60 to -40°C. Normally, the lower temperature limit of typical ESs with organic electrolytes is -40°C.<sup>4, 22</sup> To widen the temperature range for some even lower temperature operation (e.g., space-rated electronics), a number of studies have been devoted to the development of organic electrolytes with the temperature limits lower than -40°C.<sup>4, 190</sup> This could be achieved through the careful design of the salts, solvents and/or additives, which will be further discussed in the following sections.

Regarding the self-discharge of the ESs, the presence of trace water in the organic electrolyte was identified to be majorly responsible for the self-discharge process.<sup>191</sup> The self-discharge mechanism was also found to be dependent on the type of organic electrolytes, as reported by Zhang et al.<sup>192</sup>

### 3.2.1.2. Organic electrolytes for pseudocapacitors

Besides the EDLCs, organic electrolytes are also used for pseudocapacitors with pseudocapacitive materials such as metal oxides,<sup>153</sup> ECPs,<sup>155</sup> and composite materials,<sup>154</sup> as seen from Table 3. To facilitate the ion intercalation/deintercalation, most of the organic electrolytes used for pseudocapacitors contain Li ions due to its smaller bare ion size. As reported, LiClO<sub>4</sub><sup>153</sup> and LiPF<sub>6</sub>,<sup>158, 193, 194</sup> were typically salts used in these organic electrolytes. The typically organic solvents used in literature were PC,<sup>153</sup> ACN, or a mixture of different solvents such as EC-DEC,<sup>152</sup> EC-DMC,<sup>158</sup> EC-EMC,<sup>193</sup> EC-DMC-EMC,<sup>195</sup> and EC-DMC-DEC.<sup>194</sup> Actually, the most of these

organic electrolytes are widely used in the Li-ion batteries. Regarding ECPs, although they have been considered to be promising pseudocapacitive electrode materials due to their low cost, light weight, and easily processed, mechanical flexibility and relatively fast ion insertion/extraction (doping/dedoping) process, their cycling stabilities are normally poor, probably caused by trace impurity of water in the electrolytes.<sup>155</sup> In this regard, the choice of appropriate organic electrolytes may be able to minimize the degradation of the ECP materials, then improve the cycling stability.<sup>155</sup>

### 3.2.1.3. Organic electrolytes for hybrid capacitors

In order to further increase the energy density, asymmetric ESs with organic electrolytes have also drawn considerable attention. Since the early studies on the asymmetric ESs with the organic electrolytes by Amatucci et al.,<sup>196</sup> a number of organic electrolyte-based asymmetric ESs, such as graphite//AC (electrolyte: 1.5 M TEMABF<sub>4</sub>/PC),<sup>157</sup> carbon//TiO<sub>2</sub> (1 M LiPF<sub>6</sub>/EC-DMC),<sup>197</sup> carbon//V<sub>2</sub>O<sub>5</sub> (1 M LiTFSI/ACN),<sup>198</sup> carbon//Li<sub>4</sub>Ti<sub>5</sub>O<sub>12</sub> (1 M LiPF<sub>6</sub>/EC-EMC),<sup>193</sup> and carbon//ECP (1 M TEABF<sub>4</sub>/PC),<sup>199</sup> have been developed. Due to the much wider operative cell voltages (generally 3–4 V) obtained in the organic electrolyte, these asymmetric ESs can deliver energy densities (usually above 30 Wh kg<sup>-1</sup>) much higher than those reported for aqueous-based asymmetric ESs, although the formers have lower specific capacitances compared to the latters.

Among these asymmetric ESs, Li-ion capacitors (LICs) have attracted particular attention.<sup>193, 197, 200</sup> Typical LICs combine a Li-ion battery-type negative electrode and an EDLC-type positive electrode (e.g., AC) with an Li-containing organic electrolyte such as LiPF<sub>6</sub>, LiClO<sub>4</sub>, and mixtures of two or more solvents (e.g., EC-DMC). There are two types of the negative electrodes, i.e., carbon-based (mostly graphite) and lithium titanate (Li<sub>4</sub>Ti<sub>5</sub>O<sub>12</sub>) electrodes. LICs using a single solvent are very rare. In some cases, additives are used in the electrolytes.<sup>201</sup> Actually, the compositions of the reported electrolytes for LICs are almost the same as those for LIBs, which have already been reviewed elsewhere.<sup>202</sup> Even extensive studies have been focused on the development of electrode materials, the effect of electrolytes on LIC performance has received relatively limited attention.<sup>77, 200</sup> Unlike the ACN-based EDLCs whose performance was reported to be relatively insensitive to temperatures between –30 and 40 °C, the LIC performance (e.g., energy and power densities) with carbonate-based electrolytes was found to degrade severely at low temperature especially below 0 °C.<sup>200</sup> Besides the poor low-temperature performance, the LICs also suffer from a relatively low rate capability arising from the battery-type negative electrode. Further effort on both LIC electrode materials and electrolytes is necessary to solve this temperature limitation.

### 3.2.2. Organic solvents

The solvent is part of the ES electrolyte, playing a critical role in achieving high performance. For an ideal organic solvent, it should fulfill several criteria including good solvation ability for a certain conducting salt, high ESPW, low viscosity within

the operating temperature range as well as high safety (e.g., non-flammability and non-toxic). As mentioned previously, the most commonly used organic solvents for EDLCs so far are acetonitrile (ACN), and propylene carbonate (PC). As shown in Table 4, compared to the PC, ACN has a higher low viscosity, lower melting point and higher dielectric constant. Normally, ACN-based electrolytes have higher conductivity when compared to those of PC-based electrolytes, which can make a lower ESR and a higher power performance of the resultant EDLCs even at low temperatures. However, the low flash point and toxicity of the ACN are two major drawbacks. Due to its high toxicity, the use of ACN in ESs is prohibited in Japan.<sup>203-205</sup> Since PC has a higher flash point and is less toxic than the ACN solvents, there has been a growing interest in the PC-based electrolyte as an alternative to the ACN-based electrolytes. Due to the lower conductivity of PC-based electrolyte than ACN-based electrolyte, both a lower power density and energy efficiency of the PC-based EDLCs could be expected. This problem is more serious at low temperature due to the high viscosity of the PC (Fig. 10).<sup>206</sup> Furthermore, as previously discussed, the operating cell voltages of both the ACN- and PC-based EDLCs are limited to 2.5–2.8 V, and further increasing of the working voltages and thereby increasing the energy densities would be highly desirable. With respect to this, extensive efforts have been devoted to the development of other organic electrolytes for high-performing EDLCs in the last decade.



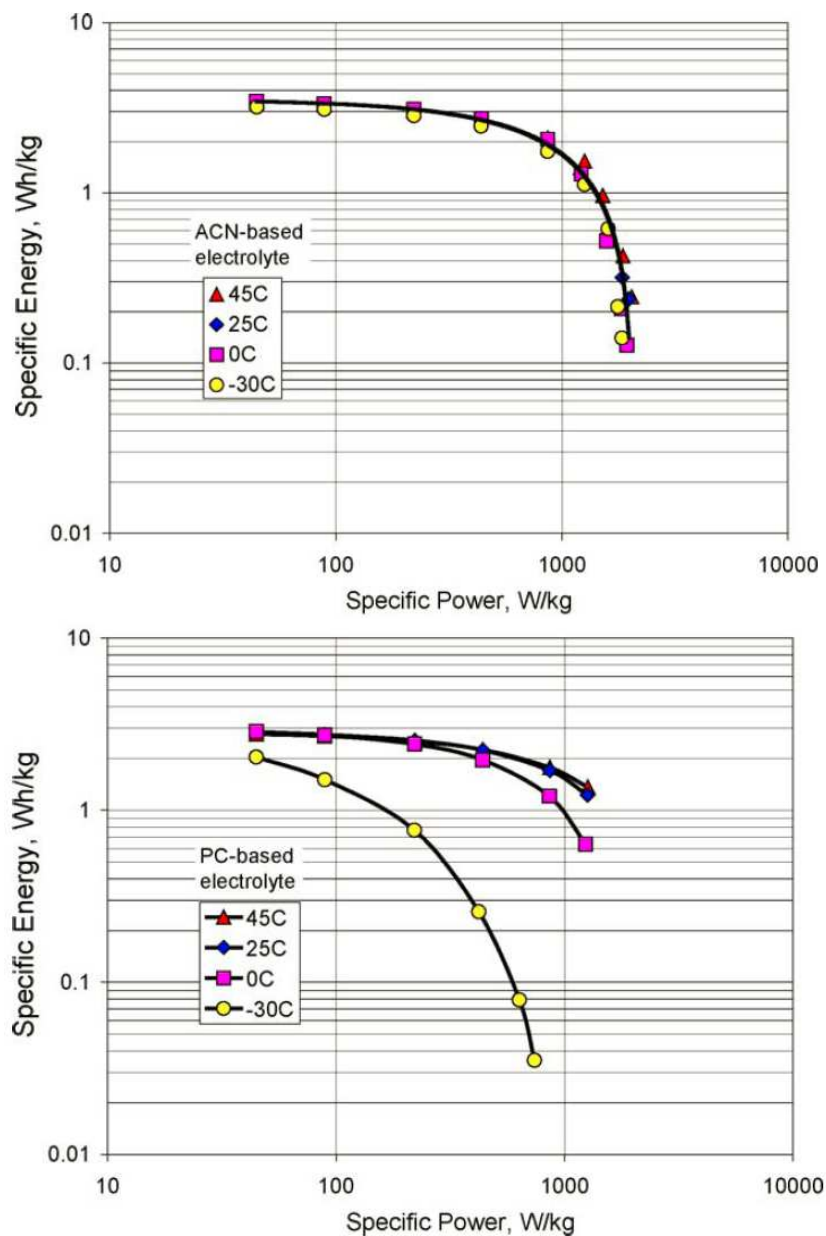


Fig. 10 Ragone plots for ACN- and PC-based electrochemical supercapacitors at different temperatures. Reprinted from Ref. 206, with permission from Elsevier.

### 3.2.2.1. Single organic solvents for electrolytes

Regarding the single organic solvent, several studies focused on the  $\gamma$ -butyrolactone (GBL) and its associated electrolyte performance in ESs. Some comparisons between GBL-based electrolyte and both ACN- and PC-based electrolytes were made when they were used for EDLCs.<sup>207-209</sup> For example, Ue et al.<sup>26</sup> reported GBL-based electrolyte had a higher oxidative stability than the PC-based electrolyte (both with 0.65 M TEABF<sub>4</sub>). It was also observed that the lower

viscosity and ionic conductivity of the GBL-based electrolyte could result in a lower power performance when compared to ACN-based electrolyte.<sup>207</sup>

Based on the observation made by Ue et al.<sup>26</sup>, that butylene carbonate (BC) exhibited a better oxidative stability than the PC, Chiba et al.<sup>210</sup> postulated that the alkyl substituent at the 4<sup>th</sup> and/or 5<sup>th</sup> position on the five-membered rings of carbonates (Fig. 11(a)) might be able to increase the oxidation resistance. It was found that when the 2,3-BC whose 4<sup>th</sup> and 5<sup>th</sup> positions were substituted by methyl groups, a much higher withstand voltage up to 3.5 V (containing SBPBF<sub>4</sub> salt) could be observed, which was much higher than those of PC solvent-based EDLCs (2.5–2.7 V).

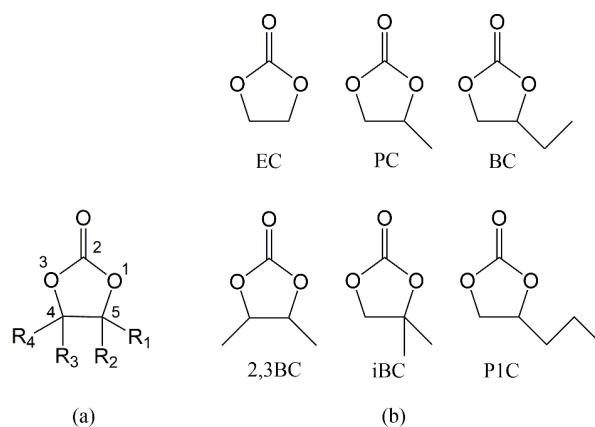


Fig. 11 Structure of (a) fluorinated carbonates, (b) cyclic carbonates studied in Ref. 210 Reproduced by permission of The Electrochemical Society from Ref. 210.

It was also reported that the substitution of C–H bonds by C–F in the solvent molecule could result in a remarkably higher chemical and electrochemical stability.<sup>144</sup> For example, a highly fluorinated solvent, i.e., a non-flammable 1,1,1,3,3,3-Hexafluoropropan-2-ol (HFIP), was investigated by Francke et al.<sup>144</sup> Due to the higher electrochemical stability, the HFIP-based electrolyte for active carbon (AC) electrodes could be stable up to almost 2 V, while ACN-based electrolyte had been degraded already at a lower voltage of 1.4 V. However, the HFIP has a small liquid-state range of –3 to 59 °C, which is narrower than those of the ACN and PC, limiting its application in a wide temperature range. Suzuki et al.<sup>211</sup> explored fluoroacetonitrile (FAN) as an alternative solvent for EDLCs. The ionic conductivity of a 1 M TEABF<sub>4</sub>/FAN electrolyte was found to be slightly lower than that of 1 M TEABF<sub>4</sub>/ACN solution, but much higher than of a 1 M TEABF<sub>4</sub>/PC solution.

The requirements for further increasing the operation voltage of organic electrolyte-based EDLCs have driven the development of other novel solvent systems such as sulfolanated solvents. For example, sulfolane (SL)- and dimethyl sulfide (DMS)-based electrolytes were reported to have a higher operation voltage than the carbonates-based electrolytes.<sup>205</sup> However, due to the higher melting point and viscosity of SL solvents (28.5 °C) than both those of PC (–49 °C) and ACN (–45 °C), their practical usage could be limited.<sup>212</sup> In an effort to decrease the melting point and viscosity of SL-based electrolytes, Chiba et al.<sup>212</sup> explored eight different types of linear sulfones with relatively low molecular weights (Fig. 12). It was found that by

changing the molecular structure of cyclic SL to a linear structure, the melting point and viscosity can be significantly decreased. EDLCs with SBPBF<sub>4</sub>/Ethyl isopropyl sulfone (EiPS) showed a higher operating voltage (3.3–3.7 V), leading to an approximately double-increase in energy density when compared to that with PC-based electrolytes. However, this electrolyte system's high viscosity (for example, EiPS has a value as high as 5.6 mPa s at 25°C) still needs to be reduced because it is much higher than those of both PC (2.5 mPa s at 25°C) and ACN (0.3 mPa s at 25°C).

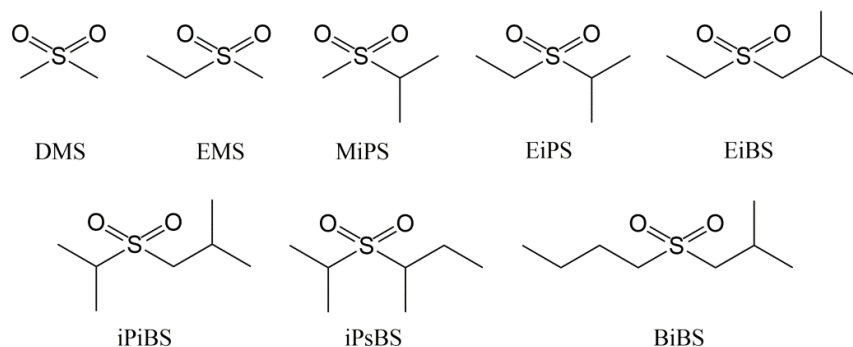


Fig. 12 Structures of sulfones investigated in Ref. 212. Reproduced by permission of The Electrochemical Society from Ref. 212.

To address the shortcoming of ACN-based electrolytes such as the low flash point and relatively low electrochemical stability, adiponitrile (ADN) was also explored as a possible solvent for EDLCs.<sup>145</sup> Brandt et al.<sup>145</sup> reported the use of 0.7 M TEABF<sub>4</sub>/ADN as the electrolyte for EDLCs. An operative voltage as high as 3.75 V was achieved for the ADN-based EDLCs, due to the high ESPW of the ADN. Unfortunately, this ADN solvent has a low solubility for the commonly conducting salts such as TEABF<sub>4</sub>, leading to a much lower ionic conductivity than that of the ACN-based electrolytes.

Based on the above discussion, it can be seen that so far there has been no ideal single solvent that can replace the commercially used solvents (e.g., ACN) in terms of the viscosity, conductivity and thermal stability, as well as overall ES performance. Although some promising solvents have been proposed to have higher ESPW, they generally cannot compete with ACN-based electrolytes in ES application.

### 3.2.2.2. Mixtures of solvents for electrolytes

In the effort to address the issues related to the single solvent systems, solvents based on a combination of different organic solvents or additives have been proposed in the literature. As mentioned previously, although PC has been regarded as a promising alternative for the ACN solvent, it suffers from lower conductivity and viscosity, and poorer thermal stability when compared to the ACN-based electrolytes. To make improvements in viscosity and ionic conductivity, a number of studies have recently focused on the development of PC-based solvent mixtures, such as PC-TMC (TMC: trimethylene carbonate), PC-EC (EC: ethylene carbonate), and PC-FEC (FEC: fluoroethylene carbonate).<sup>213, 214</sup>

In the literature, carbonates (EC, DEC, and DMC<sup>147,148, 215</sup>) and sulfites (diethyl sulfite (DES) and 1,3-propylene sulfite (PS)<sup>147</sup>) were studied as the additives or co-solvents for the binary PC-based solvents. The addition of DES or PS into PC solvent could noticeably change both the viscosity and the conductivity of electrolytes, positively affecting the capacitance, time constant, energy/power densities of the obtained ESs.<sup>147</sup>

Actually, the solvent mixtures have already been widely studied as the battery solvents for LIBs and currently have received growing interest in the field of EDLCs. In this regard, binary, ternary and quaternary solvent mixtures based on the organic carbonates (e.g., PC, EC, DMC, EMC and DEC) and organic esters (e.g., methyl formate (MF), methyl acetate (MA) and ethyl acetate (EA)) have also been investigated.<sup>216</sup> Depending on the composition, these solvent mixtures had different properties. These properties include the relative macroscopic dielectrical permittivity, viscosity, melting temperatures and dipole moment. Variation in any of these properties can produce solvents with different solubilities of salts and ionic conductivities. It is noted that the use of some organic esters such as EA and MA may introduce a safety issue due to their low flash point and high volatility. To address this concern, Perricone et al.<sup>217</sup> proposed the addition of organic ester co-solvents with methoxy or fluorinated groups to improve safety when compared to EA.

Despite the toxicity of the ACN solvent, the ACN-based mixed solvents are still very attractive and have been developed with the aims of increasing the operating cell voltage and/or to extend the lower temperature limit of the ACN-based EDLCs. Ding et al.<sup>208</sup> found the addition of GBL into ACN could significantly expand the liquid-state range of ACN (with 1 M TEMABF<sub>4</sub>) on both sides of the temperature range. The oxidative stabilities of the solvents was increased by increasing the GBL content. In an effort to extend the low temperature operating limit of the ACN-based EDLCs to below -40 °C, Brandon et al.<sup>190</sup> produced some mixed solvents by integrating low melting co-solvents (such as formates, esters or cyclic ether) into the ACN solvent. Electrolytes based on these solvents containing 0.75 M TEABF<sub>4</sub> were found to enable the EDLCs to charge and discharge at a temperature as low as -75°C.

Regarding LICs, Lee et al.<sup>201</sup> found the addition of 1,3,5-trifluorobenzene (TFB) (3.0 wt.%) into 1 M LiBF<sub>4</sub>/EC-DEC could increase the high rate performance of AC-based Li batteries.

### 3.2.3. Conducting salts for electrolytes

#### 3.2.3.1. Effect of conducting salt on ES performance

A conducting salt dissolved in an organic solvent to form an organic electrolyte can provide charge carriers (i.e., cations and anions) for ES operation. In this regard, the ion concentration and mobility should play an important role in electrolyte ionic conductivity. The conducting salts also have a profound influence on the ESPW, the thermal stability of the organic electrolytes, as well as the ES capacitance. When choosing or developing appropriate salts for certain solvents, several factors such as solubility, conductivity, stability, safety, and cost should be considered. Due to the good overall properties, TEABF<sub>4</sub> is currently the most commonly used salt and has been widely applied in commercial ESs. Besides TEABF<sub>4</sub>, many other salts have also

been studied or developed with the aim of further improving one or several of the following properties of the electrolytes: (1) solubility, (2) conductivity, (3) stability and (4) temperature performance.

Regarding the solubility, ion concentration (salt concentration) in the electrolyte cannot only affect the ionic conductivity but also the maximum energy density of its associated ESs.<sup>218</sup> Fig. 13 shows an example demonstrating there are optimum ion concentration values for achieving the maximum ionic conductivity of the electrolytes.<sup>204, 219</sup> It can also be seen that TEABF<sub>4</sub> has a limited solubility (up to 1 M) in PC whereas other salts show a higher solubility above 2 M.

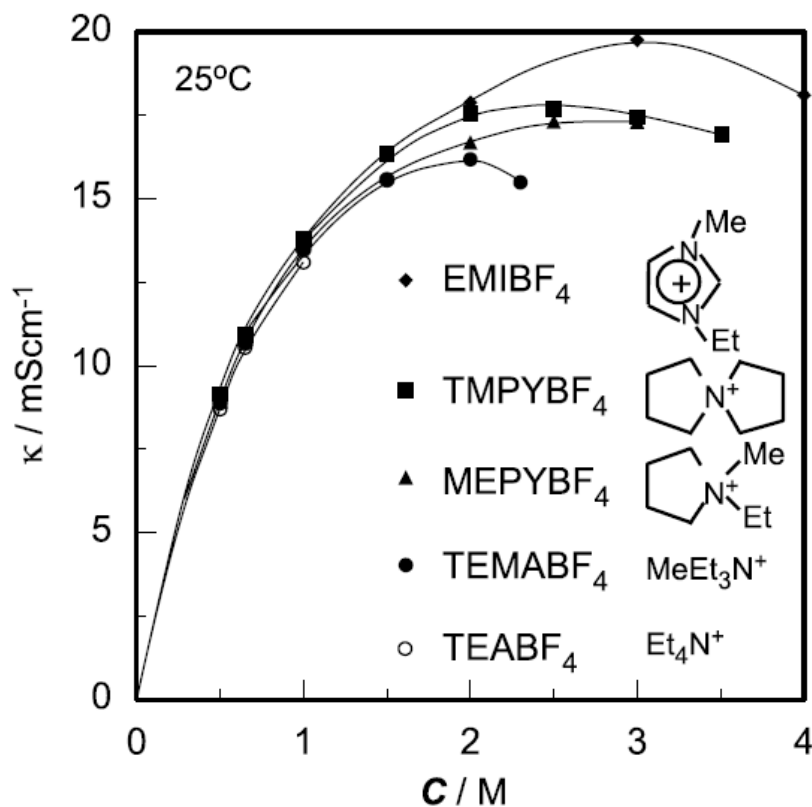


Fig. 13 Ionic conductivity as a function of quaternary ammonium tetrafluoroborate concentration in PC. Reproduced by permission of The Electrochemical Society of Japan from Ref. 204.

Since ESs generally work in a wide temperature range (e.g., from  $-30$  to  $70$  °C) for many applications, the salt solubility at lower temperatures is an important issue. The conductivity of the electrolyte is strongly dependent on a number of factors such as salt concentration, dissociation degree of the dissolved salt to provide free charge carriers (cations and anions), mobility of these dissociated ions, type of solvents (as mentioned previously), and the temperature. Normally, many aqueous electrolytes for ESs have high dissociation degree values (close to 1) while common organic electrolytes have much lower dissociation degree values. Therefore the salt solubilities in organic solvents are normally low, leading to low ionic conductivity of the organic electrolytes and then high ESR when compare to aqueous electrolytes. Actually, the structure of organic salts (e.g., symmetrical ones or asymmetric ones, and the ionic size of cation and anion) can also affect the dissociation degree and ion

mobility, thus playing a critical role in conductivity of the electrolytes. Ue et al.<sup>26</sup> investigated the conductivities of some common salts in different solvents including PC, GBL, N,N-dimethylformamide (DMF), and ACN.<sup>26</sup> Regarding the cations, the conductivity generally decreases in the following order:  $\text{TEA}^+ > \text{Pr}_4\text{N}^+ > \text{Bu}_4\text{N}^+ > \text{Li}^+ > \text{Me}_4\text{N}^+$ , while for the anions, the conductivity decreases in the following order:  $\text{BF}_4^- > \text{PF}_4^- > \text{ClO}_4^- > \text{CF}_3\text{SO}_3^-$ , respectively.

The conducting salt also plays an important role in the ESPW of organic electrolytes.<sup>204, 220</sup> For example, Xu et al.<sup>220</sup> found the ESPWs of different cations at an AC electrode were followed in the order of:  $\text{Pr}_3\text{MeN}^+ > \text{Et}_4\text{N}^+ > \text{Bu}_3\text{MeN}^+ > \text{Et}_3\text{MeN}^+ > \text{iPr}^2\text{MeEtN}^+ > \text{Me}_3\text{EtN}^+ > \text{Bu}_3\text{MeP}^+ > \text{Et}_3\text{MeP}^+$  while that of the anions at a glassy carbon electrode followed the order of:  $\text{AsF}_6^- \sim \text{BF}_4^- > \text{PF}_6^- > \text{Tf}^- \sim \text{Im}^-$  (solvent: EC-DMC).

Since various salts contain different types of cations and anions with different bare and solvated ion sizes, the matching between the pore size of carbon-based electrode materials and the electrolyte ions is fairly important to achieving high ES performance. To make a good match, the partial removal or distortion of the ion solvation shell should be considered when the pore size is close to the bare ion size. Research has identified, this matching has a large effect on the capacitance and power performance of EDLCs. Koh et al.<sup>221</sup> employed several salts including TEABF<sub>4</sub>, TEMABF<sub>4</sub>, trimethylpropylammonium BF<sub>4</sub> (TMPABF<sub>4</sub>), and diethyldimethylammonium BF<sub>4</sub> (DEDMABF<sub>4</sub>) to investigate the effect of ionic size of different salts on the EDLC specific capacitance. These salts have different lengths of hydrocarbon chains and thus different cation sizes. It was observed the EDLC specific capacitance could be increased by decreasing the cation size of quaternary ammonium salts. In addition, the charged state (valent) of ions was also found to have an effect on the capacitance or energy density of EDLCs.<sup>222</sup>

Using asymmetric ESs, Yokoyama et al.<sup>223</sup> observed the capacitance could be strongly affected by the type of anions, and the decreasing order was found to be:  $\text{PF}_6^- > \text{BF}_4^- > \text{ClO}_4^-$  (all with TEA cations and the solvent is PC-EMC). It was established that  $\text{PF}_6^-$  was the most stable anion among the investigated anions, contributing to the largest capacitance.

### 3.2.3.2. Exploration of new conducting salts

To increase the salt solubility in organic solvents (especially PC), some asymmetric tetraalkylammonium salts and cyclic quaternary ammonium salts, such as TEMABF<sub>4</sub>, 1-ethyl-1-methylpyrrolidinium, (MEPYBF<sub>4</sub>), and tetramethylenepyrrolidinium (TMPYBF<sub>4</sub>), have been explored for use in ESs. These salts were found to have much higher solubilities in PC when compared to TEABF<sub>4</sub>, as shown in Fig. 13.<sup>204</sup> However, since salts contribute a large part of the cost to the total electrolyte cost, a balance between performance and cost (i.e., salt concentration) should be considered. For example, recently, a spiro-type quaternary ammonium salt called spiro-(1,1')-bipyrrrolidinium tetrafluoroborate (SBPBF<sub>4</sub>) received considerable attention due to its smaller cation size, higher mobility, and higher solubility compared to the common TEABF<sub>4</sub>.<sup>149, 156, 212, 224, 225</sup> However, SBPBF<sub>4</sub> is expensive compared to TEABF<sub>4</sub>, which may limit its widespread applications.

In addition, Kurig et al.<sup>226</sup> tested a series of substituted phosphonium cation based

electrolytes for EDLCs with titanium carbide derived carbon (C(TiC)) as the electrodes. The C(TiC) electrodes were found to be ideally polarizable in 1 M tetrakis(diethylamino)-phosphonium hexafluorophosphate (TDENPPF<sub>6</sub>)/ACN electrolyte up to 3.2 V. The EDLC with 1 M TDENPPF<sub>6</sub>/ACN electrolyte showed a gravimetric capacitance of 85 F g<sup>-1</sup>, characteristic relaxation time of 0.9 s, and gravimetric energy density of 27 Wh kg<sup>-1</sup> when the cell voltage was 3.2 V. No visible loss in the discharging capacitance could be observed after 10,000 charging/discharging cycles. However, the conductivities of these substituted phosphonium cation based electrolytes was much lower than those of TEABF<sub>4</sub>/ACN and TEMABF<sub>4</sub>/ACN, which might have some negative effects on an ES's ESR, rate performance or thermal stability.

Regarding the anion, as can be seen from the above discussion, the commonly used anions (e.g., BF<sub>4</sub>) contain halogen. Several authors pointed out that these fluoro-complex salts might be hydrolyzed to generate highly toxic hydrogen fluoride (HF).<sup>227, 228</sup> To address this issue, they explored bis(oxalato)borates (BOB anion)-based salts, such as TMABOB, ETMABOB, TEMABOB, and TEABOB.<sup>228</sup> Changing bis(oxalato)borate anion to asymmetric difluoro(oxalato)borate anion was found to increase the solubility of the salts.<sup>146, 229</sup>

In addition to the organic cations, organic salts based on the inorganic cations, such as Li<sup>+</sup>,<sup>215, 230, 231</sup> Na<sup>+</sup>,<sup>151</sup> and Mg<sup>2+</sup>,<sup>232</sup> have also attracted attention. As mentioned previously, organic electrolytes based on the lithium salts have been widely used in the pseudocapacitors and hybrid ESs such as LICs due to the small ionic size of Li<sup>+</sup>. There are also some studies on the application of lithium salt-based organic electrolytes for EDLCs.<sup>215, 231</sup> The use of lithium salts for the ESs are largely inspired by the development of LIBs.

### 3.3. Ionic liquid based ES electrolytes

#### 3.3.1. General composition, properties and ES performance of ionic liquid electrolytes

Ionic liquids (ILs, also known as low temperature or room temperature molten salts) are generally defined as those salts composed solely of ions (cations and anions) with melting points below 100 °C.<sup>233</sup> An IL usually consists of a large asymmetric organic cation and an inorganic or organic anion, and this special combination of certain cation and anion contributes to a low melting point.<sup>234</sup> Owing to the unique structures and properties, ILs have recently received a significant interest as alternative electrolytes for ESs. In normal, ILs have several potential advantages including high thermal, chemical and electrochemical stability, negligible volatility, and non-flammability (depending on the combination of cations and anions).<sup>10, 234</sup> Furthermore, ILs' physical and chemical properties can be highly tunable due to their large variety (virtually unlimited) of combinations of cations and anions.<sup>235</sup> In this sense, ILs are also regarded as “designer solvents”.<sup>236</sup> This property tenability of ILs is very attractive for ES electrolytes because the electrolyte compositions can be

optimized or customized to meet certain requirements of ES performance such as operative cell voltage, working temperature range, ESR (related with the ionic conductivity), and so on.

Based on their composition, ILs can be basically classified as aprotic, protic and zwitterionic types (Fig. 14).<sup>234</sup> The cited ILs used in ESs so far represents only a very small part of the large family of ILs. In the published literature, the employed ILs for ESs are commonly based on imidazolium, pyrrolidinium, ammonium, sulfonium, phosphonium cations, and so on (Fig. 15). Typical anions of ILs are tetrafluoroborate ( $\text{BF}_4^-$ ), hexafluorophosphate ( $\text{PF}_6^-$ ), bis(trifluoromethanesulfonyl)imide ( $\text{TFSI}^-$ ), bis(fluorosulfonyl)imide ( $\text{FSI}^-$ ), and dicyanamide ( $\text{DCA}^-$ ) (Fig. 15).

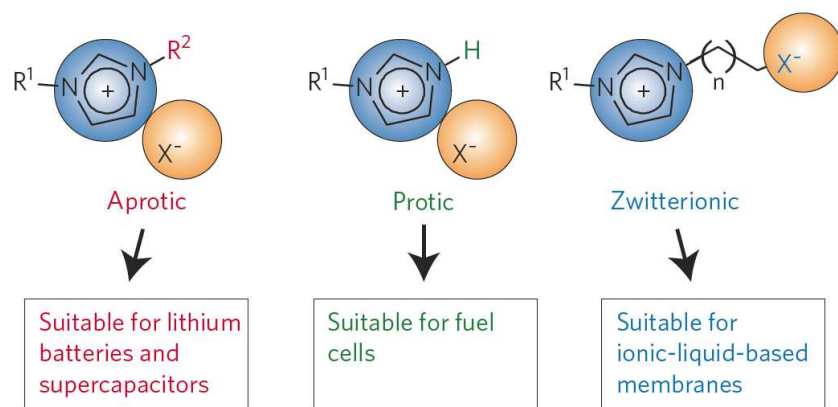
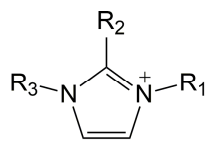


Fig. 14 Basic types of ionic liquids: aprotic, protic and zwitterionic types. Reprinted by permission from Macmillan Publishers Ltd: Nature (Ref. 234), copyright 2009.

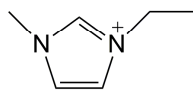
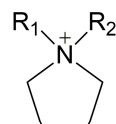


## Commonly used cations

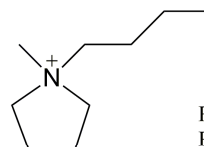
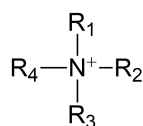
## Typical examples



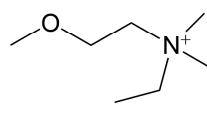
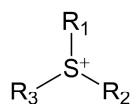
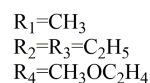
Imidazolium

[EMIM]<sup>+</sup>

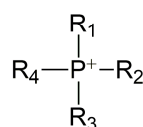
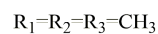
Pyrrolidinium

PYR<sub>14</sub>

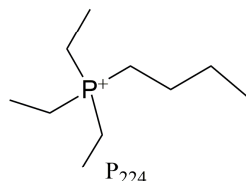
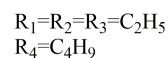
Ammonium

[DEME]<sup>+</sup>

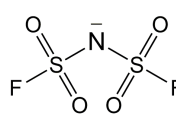
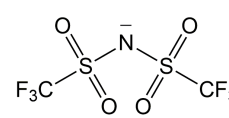
Sulfonium

[Me<sub>3</sub>S]<sup>+</sup>

Phosphonium

P<sub>224</sub>

## Commonly used anions

Tetrafluoroborate  
[BF<sub>4</sub>]<sup>-</sup>Hexafluorophosphate  
[PF<sub>6</sub>]<sup>-</sup>bis(Fluorosulfonyl)imide  
[FSI]<sup>-</sup>bis(Trifluoromethanesulfonyl)imide  
[TFSI]<sup>-</sup>

## Commonly used cations for protic ionic liquids

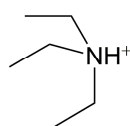
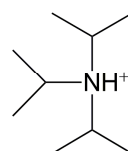
[Et<sub>3</sub>NH]<sup>+</sup>[DIPEA]<sup>+</sup>

Fig. 15 Commonly used cations, anions of ILs for ESs, and some typical examples of ILs.

In general, the imidazolium-based ILs can provide higher ionic conductivity while the pyrrolidinium-based ILs have larger ESPWs.<sup>29, 237</sup> Actually, there exists a trade-off between the IL ionic conductivity and ESPW. As mentioned previously, the operative cell voltages of commercial organic electrolytes (e.g., ACN and PC) based EDLCs are generally limited to 2.5–2.8 V, and increasing the cell voltage beyond this limit would cause serious electrochemical decomposition of organic solvents. However, many studies using IL- electrolyte-based ESs could give operative cell voltages above 3 V.<sup>10, 237, 238</sup> Besides, commercially used organic solvents (e.g., ACN) also face safety issues due to their volatile and flammable nature especially when used at high temperatures. In this regard, the solvent-free ILs may have an advantage in solving the safety problems associated with those organic solvents, making IL-based ESs favorable for high-temperature applications.

Unfortunately, there are several main drawbacks with most ILs, such as high viscosity, low ionic conductivity and high cost, which can limit their practical use in ESs. Even for [EMIM][BF<sub>4</sub>] electrolyte, which has a relatively high ionic conductivity among the common ILs, its conductivity (14 mS cm<sup>-1</sup> at 25 °C) is still much lower than that of the TEABF<sub>4</sub>/ACN (59.9 mS cm<sup>-1</sup> at 25 °C). Furthermore, the viscosities of ILs such as [EMIM][BF<sub>4</sub>] and [BMIM][BF<sub>4</sub>] are 41 cp and 219 cp,<sup>239, 240</sup> respectively, which are much higher than that of the organic electrolyte (e.g., 0.3 cp for ACN organic electrolyte<sup>162</sup>). Both low conductivity and high viscosity of IL-based electrolytes can significantly increase the ESR values of the ILs-based ESs, limiting both the rate and power performance if the loss of the power density due to the increased ESR cannot be buffered by the increase of cell voltage. This issue seemed more serious at room temperature and low temperature, as demonstrated by some comparative studies between organic and IL electrolytes.<sup>10, 237, 238</sup> In addition, the specific capacitance values of IL electrolyte-based EDLCs are often lower than those of both aqueous and organic electrolyte-based ones especially at high scan rates or high charging/discharging rates, probably due to the high viscosity of ILs.<sup>241, 242</sup>

To improve the performance of IL-based ESs, optimizing the selection of IL composition and cell design have been carried out through both experimental and theoretical understanding,<sup>243-245</sup> to provide fundamental insights into the electrochemical behaviour, structure and corresponding capacitive behavior of the electric double-layer (EDL) at the IL/electrode interface. With respect to this, some achievements have recently been made, as documented by several excellent reviews.<sup>172, 245-248</sup> These reviews discussed the EDL structure and capacitance, influencing factors on the EDL, effects of carbon electrode morphology and pore size on EDL structure, capacitance and dynamics of IL ions. In addition, some cations of the investigated ILs for ESs have a structure similar to that of surfactants.<sup>249, 250</sup> Whether these cations tend to aggregate in ILs like surfactants is an important issue since this would be able to affect both the ion mobility and ionic conductivity.<sup>249, 250</sup>

In order to understand the aging or failure mechanisms of IL electrolyte-based

EDLCs, the electrochemical decomposition of ILs beyond the ESPW have been investigated by using instrumental analysis methods such as *in-situ* infrared and electrochemical spectroscopy methods,<sup>251</sup> and *in-situ* XPS.<sup>252</sup>

The research activities in this field can be briefly summarized as follows: (1) fundamentally understanding the EDL structure and capacitance in ILs, (2) developing ILs for pseudocapacitive electrode material-based ESs with improved charge storage ability, (3) improving ILs' properties (e.g., ionic conductivity, viscosity and ESPW) by modifying the cations or anions or both, and (4) using mixture of ILs or utilizing organic solvents to improve the overall performance of IL-based electrolytes.

### 3.3.2. Solvent-free ionic liquids

#### 3.3.2.1. Solvent-free ionic liquids for EDLCs

As previously mentioned, the major challenge in developing ILs for EDLCs is to design or choose ILs with high ionic conductivity, large ESPW and wide temperature range. Although [EMIM][BF<sub>4</sub>] electrolyte has been extensively studied for EDLCs due to its relatively high conductivity, its narrower ESPW compared to other ILs and relatively high melting point (15 °C) seem to be the drawbacks. To overcome these drawbacks, considerable work has been devoted to the development of other alternative ILs based on the tunable properties of ILs to change the structure of either the anion, or the cation, or both as well as the IL composition itself.<sup>235</sup>

##### 3.3.2.1.1. Aprotic ionic liquids

Regarding 1-ethyl-3-methylimidazolium ([EMIM])-based ILs, Sun et al.<sup>253</sup> investigated the performance of AC-based EDLCs with [EMIM][SCN] IL electrolytes (SCN: thiocyanate), which had both lower viscosity and higher ionic conductivity compared to those of [EMIM][BF<sub>4</sub>] IL. Handa et al.<sup>254</sup> found the ionic conductivity of [EMIM][FSI] IL (FSI: bis(fluorosulfonyl)imide) was comparable to TEMABF<sub>4</sub>/PC organic electrolyte, and the EDLCs with this [EMIM][FSI] IL electrolyte showed a good rate capability similar to that with TEMABF<sub>4</sub>/PC organic electrolyte. Pandey et al.<sup>255</sup> demonstrated that 1-ethyl-3-methylimidazolium tetracyanoborate ([EMIM][TCB]) IL (TCB: tetracyanoborate) could be an electrolyte for AC-based EDLCs since it had a high ionic conductivity ( $\sim 1.3 \times 10^{-2}$  S cm<sup>-1</sup> at 20 °C) and low viscosity ( $\sim 22$  cP). Matsumoto et al.<sup>256</sup> found that the [EMIM][PO<sub>2</sub>F<sub>2</sub>] IL (PO<sub>2</sub>F<sub>2</sub>: difluorophosphate) electrolyte could provide a higher specific capacitance when compared to the [EMIM][BF<sub>4</sub>] IL at a charging voltage of 2.5 V. Unfortunately, the operative cell voltage of the EDLC with [EMIM][PO<sub>2</sub>F<sub>2</sub>] IL electrolyte was below 3 V, lower than that with [EMIM][BF<sub>4</sub>] IL electrolyte. Kurig et al.<sup>257</sup> systematically

investigated various IL electrolytes with  $[\text{EMIM}]^+$  cation and different anions for EDLCs using carbon cloth electrodes. The structure and chemical composition of the IL anion were found to have a profound influence on both the ESPW and operative cell voltage (Fig. 16). It was concluded that the  $[\text{EMIM}][\text{BF}_4]$  and  $[\text{EMIM}][\text{B}(\text{CN})_4]$  ILs could give the best overall performance among the investigated ILs.

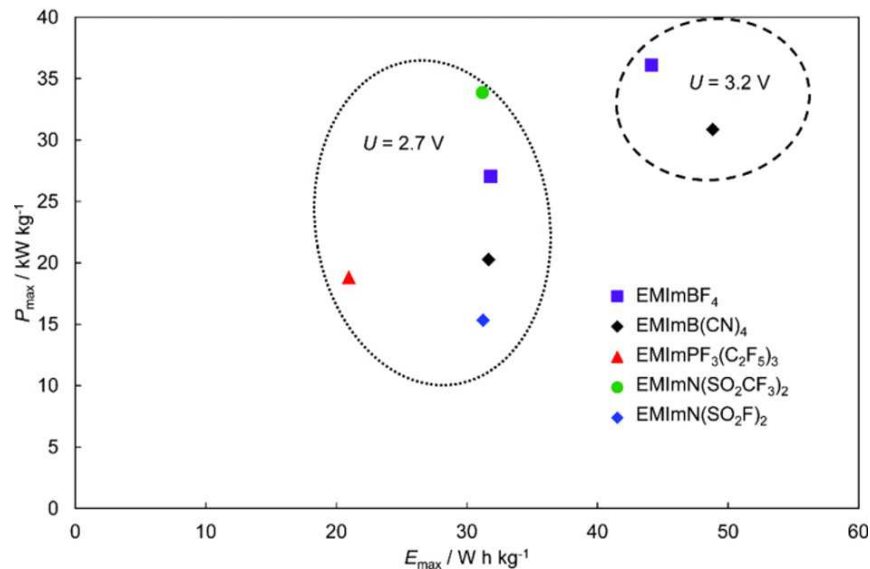


Fig. 16 Power density vs. energy density plots at 2.7 V and at 3.2 V for electrochemical supercapacitors with ILs studied. Reproduced by permission of The Electrochemical Society from Ref. 257.

Shi et al.<sup>258</sup> investigated the performance of graphene-based EDLCs with a series of ILs composed of  $[\text{EMIM}]^+$  cation and different anions including  $\text{BF}_4^-$ ,  $\text{NTF}_2^-$ ,  $\text{DCA}^-$ ,  $\text{EtSO}_4^-$  and  $\text{OAc}^-$ . It was found the hydrogen-bond-accepting ability of these anions was closely related to the viscosity of the ILs. EDLCs with the  $[\text{EMIM}][\text{DCA}]$  IL electrolyte showed the highest specific capacitance and rate capability as well as the smallest resistance due to the lowest viscosity, ion size and molecular weight among the investigated ILs. However,  $[\text{EMIM}][\text{DCA}]$  IL-based EDLCs had a much smaller ESPW (2.3 V) which was much narrower than that of the  $[\text{EMIM}][\text{BF}_4]$  IL-based EDLC (~4 V) (Fig. 17). As a result, the latter delivered the highest specific energy density ( $67 \text{ Wh kg}^{-1}$  at  $1 \text{ A g}^{-1}$ ), which was much higher than the former ( $20 \text{ Wh kg}^{-1}$ ).

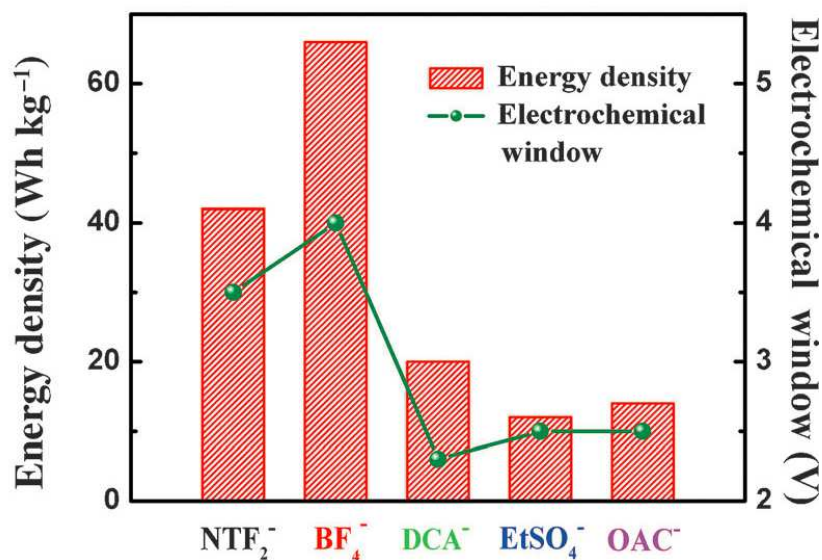


Fig. 17 Relationship between the electrochemical window and the energy density of graphene electrodes measured in different IL electrolytes. Reprinted from Ref. 258, with permission from John Wiley and Sons.

In addition to changing the anion of [EMIM]-based IL electrolytes, other methods have also been proposed to improve the properties (e.g., ESPW and ionic conductivity).<sup>259-261</sup> For example, Kong et al.<sup>259</sup> reported that the addition of small amounts of single walled CNTs (e.g., 0.1 and 0.5 wt.%) into [EMIM][BF<sub>4</sub>] IL electrolyte could increase the ionic conductivity of the electrolyte. As a result, the specific capacitance, energy density and cycling stability of EDLCs with this CNT-added IL electrolyte were all improved. Some studies showed that the addition of Li salt into IL electrolyte could negatively shift the cathodic potential limit for increasing the cathodic stability.<sup>260, 261</sup>

Other imidazolium-based cations besides [EMIM]<sup>+</sup>, such as 1-butyl-2,3-dimethylimidazolium bis(trifluoromethylsulfonyl)imide ([BDMIM]), 1-butyl-3-methylimidazolium bis(trifluoromethylsulfonyl)imide ([BMIM]), and 1-dodecyl-3-methylimidazolium bis(trifluoromethylsulfonyl)imide ([C<sub>12</sub>MIM]), have also been studied.<sup>262, 263</sup> For instance, Bettini et al.<sup>263</sup> found that among the four investigated ILs ([BMIM][NTf<sub>2</sub>], [C<sub>12</sub>MIM][NTf<sub>2</sub>], [EMIM][NTf<sub>2</sub>] and 1-butyl-1-methylpyrrolidinium bis(trifluoromethylsulfonyl)imide ([BPyrr][NTf<sub>2</sub>])), [BMIM][NTf<sub>2</sub>]-based ES could exhibit the highest specific capacitance of 75 F g<sup>-1</sup>. This high specific capacitance was thought to be related to the IL's shortest alkyl chain.

ILs with other cations (e.g., pyrrolidinium-based,<sup>264-266</sup> ammonium-based,<sup>267-269</sup> sulfonium-based,<sup>270</sup> and fluorohydrogenate ILs<sup>269</sup>) have also been extensively studied as potential electrolytes for EDLCs. Regarding the ILs with pyrrolidinium cations, Lazzari et al.<sup>264</sup> employed N-butyl-N-methylpyrrolidinium bis(trifluoromethanesulfonyl)imide ([PYR<sub>14</sub>][TFSI]) as the electrolyte for EDLCs

with mesoporous carbon xerogel electrodes. In order to fully take advantage of the high ESPW of [PYR<sub>14</sub>][TFSI] IL, the EDLCs had the asymmetric configuration with a higher carbon loading at the positive electrode than that at the negative one. A maximum cell voltage of 3.7 V was achieved only for that asymmetric EDLC using [PYR<sub>14</sub>][TFSI] IL as the electrolyte, which was higher than that using [EMIM][TFSI] IL (3.4 V). Both EDLCs delivered a maximum specific energy of ~30 Wh kg<sup>-1</sup> at their maximum cell voltage at 60 °C. Lazzari et al.<sup>265</sup> tested [PYR<sub>12</sub>O<sub>1</sub>][TFSI] IL as the electrolyte for asymmetric EDLCs (AEDLCs) with different carbon loadings on the positive and negative electrodes. It was observed that the [PYR<sub>12</sub>O<sub>1</sub>][TFSI]-based AEDLC could operate within a wide temperature range from -30 to 60 °C at a high operative cell voltage of 3.7 V. A high cycling stability was also observed for this IL-based AEDLCs with a capacitance loss of 2% over 27,000 deep cycles at 60 °C.<sup>266</sup> Such AEDLC could reach a maximum cell voltage of 4 V and could deliver a maximum energy density of 40 Wh kg<sup>-1</sup> (only electrode materials included).<sup>266</sup>

Considering that azepanium-based ILs were much cheaper than pyrrolidinium-based ILs, Pohlmann et al.<sup>271</sup> tested two azepanium-based ILs, (N-methyl, N-butyl-azepanium bis(trifluoromethanesulfonyl)imide ([AZP<sub>14</sub>][TFSI]) and N-methyl, N-hexyl-azepanium bis(trifluoromethanesulfonyl)imide ([AZP<sub>16</sub>][TFSI])), as electrolytes for EDLCs, and compared them with [PYR<sub>14</sub>][TFSI]. Both of these two IL electrolytes showed operative working voltages up to 3.5 V, which was similar to [PYR<sub>14</sub>][TFSI]. However, EDLCs utilizing these two IL electrolytes were found to deliver less energy densities especially at higher current density when compared to that with [PYR<sub>14</sub>][TFSI] IL as the electrolyte, which was attributed to the larger cation sizes and thus lower accessibilities to the electrode material surfaces.

Regarding the ILs with ammonium-based cations, Sato et al.<sup>267</sup> employed N,N-diethyl-N-methyl-N-(2-methoxyethyl)ammonium tetrafluoroborate ([DEME][BF<sub>4</sub>]) and [DEME][TFSI] ILs as electrolytes for the EDLCs, and compared them with both [EMIM][BF<sub>4</sub>] IL and 1 M TEABF<sub>4</sub>/PC organic electrolytes. The ESPW of [DEME][BF<sub>4</sub>] IL (6 V) was obtained on a Pt electrode, which was wider than that of [EMIM][BF<sub>4</sub>] (4.5 V). The EDLC using [DEME][BF<sub>4</sub>] IL as electrolyte showed a much better high-temperature performance up to 150 °C. Kim et al.<sup>268</sup> found that [DEME][BF<sub>4</sub>] and [DEME][TFSI] ILs showed wider ESPW than both those of TEABF<sub>4</sub>/PC organic electrolyte and conventional [EMIM][BF<sub>4</sub>] IL. The specific capacitance of AC-based electrodes in both ionic liquids could be increased with increasing applied voltage from 2.5 to 3.5 V.

Senda et al.<sup>269</sup> studied AC-based EDLCs with fluorohydrogenate ILs (FHILs) as electrolytes. Five such FHILs contained different cations such as 1,3-dimethylimidazolium (DMIM), 1-ethyl-3-methylimidazolium (EMIM), 1-butyl-3-methylimidazolium (BMIM), 1-ethyl-1-methylpyrrolidinium (EMPy), and 1-methoxymethyl-1-methylpyrrolidinium (MOMMPyr), respectively. The specific capacitances obtained using these fluorohydrogenate ILs were all higher than those obtained in [EMIM][BF<sub>4</sub>] IL or 1 M TEABF<sub>4</sub>/PC organic electrolyte at the investigated cell voltage from 1 to 3.2 V. For three imidazolium-based FHILs, the

maximum specific capacitances were decreased in the following order: [DMIM][(FH)<sub>2,3</sub>F] (178 F g<sup>-1</sup>) > [EMIM][(FH)<sub>2,3</sub>F] (162 F g<sup>-1</sup>) > [BMIM][(FH)<sub>2,3</sub>F] (135 F g<sup>-1</sup>). This was in accordance with order of cation size increasing. AC-based EDLCs using some FHILs with low melting points had sufficient specific capacitance even at -40°C (e.g., 64 F g<sup>-1</sup> for [EMIM][(FH)<sub>2,3</sub>F]), which was much higher than that of TEABF<sub>4</sub>/PC ((20 F g<sup>-1</sup>).

Regarding the sulfonium-based cations, Anouti et al.<sup>270</sup> studied trimethylsulfonium bis(trifluorosulfonimide) [Me<sub>3</sub>S][TFSI] IL electrolyte for AC-based EDLCs. [Me<sub>3</sub>S][TFSI] IL had an ESPW of about 5 V on a Pt electrode and could operate up to 3 V on AC electrodes-based EDLCs. It was also observed the EDLC using this IL as electrolyte was suitable for high temperature operation, delivering a maximum energy density of 44.1 Wh kg<sup>-1</sup> at 80°C.

Comparative studies on ILs with different type of cations were also carried out.<sup>272, 273</sup> Sillars et al.<sup>272</sup> studied a series of ILs including [EMIM][BF<sub>4</sub>], 1-ethyl-3-methylimidazolium dicyanamide ([EMIM][N(CN)<sub>2</sub>]), 1,2-dimethyl-3-propylimidazolium bis(trifluoromethylsulfonyl) imide ([DMPIM][TFSI]), and 1-butyl-3-methylpyrrolidinium tris(pentafluoroethyl) trifluorophosphate ([BMPy][FAP]) as electrolytes for AC-based EDLCs, and compared them with 1 M TEABF<sub>4</sub>/PC organic electrolyte. EDLC using [BMPy][FAP] IL showed the highest operating voltage of 3.5 V (Fig. 18). The capacitive performances of EDLCs using these ILs were decreased in the following order: [EMIM][BF<sub>4</sub>] > [DMPIM][TFSI] > [BMPy][FAP] > [EMIM][N(CN)<sub>2</sub>], which was thought to be related to the electrolyte viscosity and ion size. The ESR values were increased in the following order: [EMIM][N(CN)<sub>2</sub>] < [EMIM][BF<sub>4</sub>] < [DMPIM][TFSI] < [BMPy][FAP], which was in accordance with the increasing order of viscosity. EDLC using [EMIM][BF<sub>4</sub>] IL could deliver much higher energy and power densities when compared to an EDLC using 1 M TEABF<sub>4</sub>/PC as organic electrolyte.

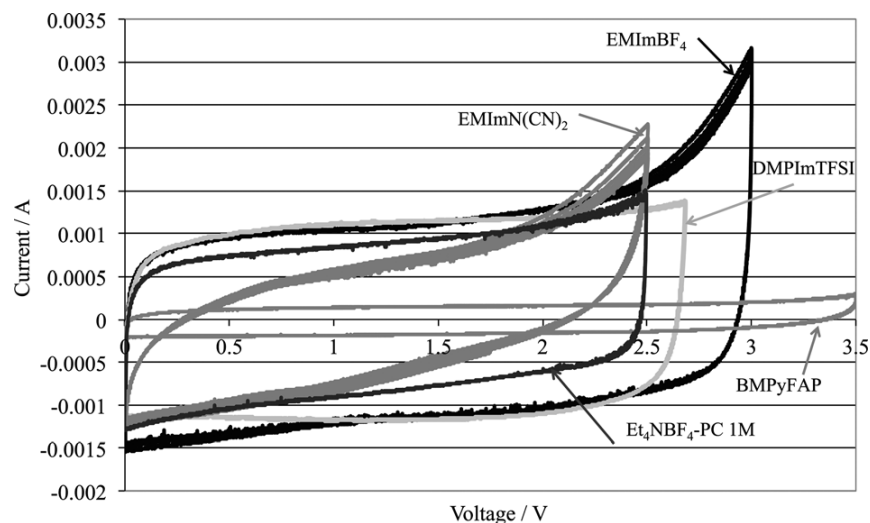


Fig. 18 Cyclic voltammograms for different ILs at 5 mV s<sup>-1</sup>. Reproduced from Ref. 272 with permission of The Royal Society of Chemistry.

Rennie et al.<sup>273</sup> investigated ILs with different types of cation (Fig. 19). It was found that the introduction of ether bond into the cation alkyl side chain could effectively increase the specific capacitance and reduce the ESR of EDLCs (Fig. 20). The authors attributed this to the introduction of small electronegative region to the cation structure through ether bond, facilitating a denser packing of ions at the electrolyte-electrode interface, resulting in an increased charge amount.

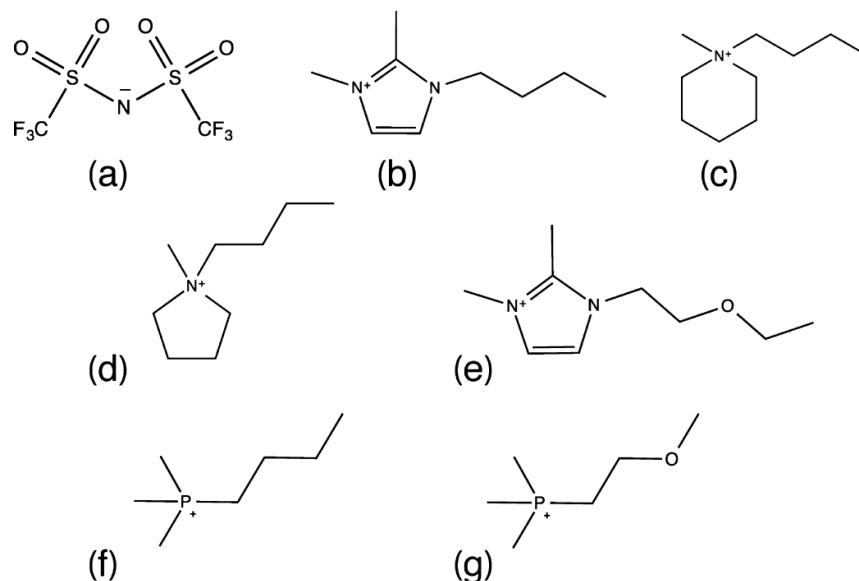


Fig. 19 Schematic structure of the constituent ions in ILs studied in Ref. 273: (a)  $\text{Tf}_2\text{N}^-$ , (b) 1-n-butyl-2,3-dimethylimidazolium (BMIM)<sup>+</sup>, (c) N-n-butyl-N-methylpiperidinium (BMPi)<sup>+</sup>, (d) N-n-butyl-N-methylpyrrolidinium (BMPy)<sup>+</sup>, (e) 1-(2-ethoxyethyl)-2,3-dimethyl-1H-imidazol-3-ium (EtO(CH<sub>2</sub>)<sub>2</sub>MMIM)<sup>+</sup>, (f) butyltrimethylphosphonium (P<sub>2225</sub>)<sup>+</sup>, and (g) (2-methoxyethyl)trimethylphosphonium (P<sub>222(201)</sub>)<sup>+</sup>. Reprinted with permission from Ref. 273 (open access).



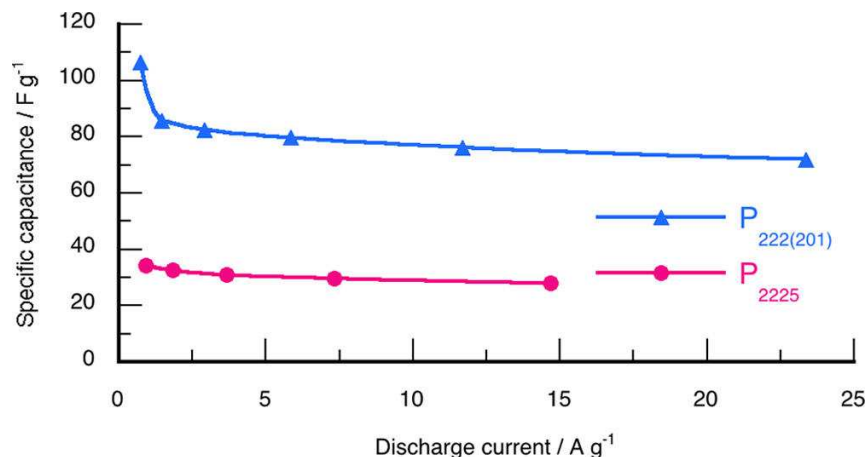


Fig. 20 Specific capacitance determined at different rates of constant current discharge between 0 and 2.5 V for cells using phosphoniumbased ILs as electrolytes. Reprinted with permission from Ref. 273 (open access).

Anions of ILs also play an important role in their hydrophilic–hydrophobic properties. The hydrophobicity was found to increase in the following order:  $\text{CH}_3\text{CO}_2^-$  (Acetate),  $\text{NO}_3^-$  (Nitrate) <  $\text{Tf}^-$ ,  $\text{BF}_4^-$  <  $\text{PF}_6^-$ ,  $\text{TFSI}^-$  (hydrophobic).<sup>274</sup> In addition, a small amount of water in ILs is often deleterious to their ESPW.<sup>275</sup> Therefore, hydrophobic anions such as  $\text{TFSI}^-$  and  $\text{FSI}^-$  have received increasing attention for their usage in ESs.<sup>254, 276</sup>

### 3.3.2.1.2. Protic ionic liquids

Protic ILs, normally attract limited interest as electrolytes for EDLCs.<sup>277–280</sup> This may be because a much lower operative cell voltage (1.2–2.5 V) can be seen for EDLCs with protic ILs when compared with aprotic ILs. The protic ILs include protic pyrrolidinium nitrate ( $\text{PyNO}_3$ ),<sup>277</sup> triethylammonium bis(trifluoromethylsulfonyl)imide ( $[\text{Et}_3\text{NH}][\text{TFSI}]$ ),<sup>278, 280</sup> pyrrolidinium bis(trifluoromethanesulfonyl)imide ( $[\text{Pyr}][\text{TFSI}]$ ),<sup>279</sup> and diisopropyl-ethyl-ammonium bis(trifluoromethanesulfonyl)imide ( $[\text{DIPEA}][\text{TFSI}]$ ).<sup>279</sup> Protic ILs, however, have some advantages such as being generally easier to synthesize and cheaper compared to aprotic ILs.<sup>280, 281</sup>

### 3.3.2.1.3. Mixture of ionic liquids

As previously mentioned, the most commonly studied ILs have higher melting points above 0 °C, which prevent their use as ES electrolytes for low-temperature applications. In order to extend the operative temperature range to lower temperatures significantly below 0 °C, the strategy of a mixture of IL mixtures has been explored.<sup>276, 282, 283</sup> For example, Lin et al.<sup>282</sup> developed some eutectic IL mixtures of propylpiperidinium bis[fluorosulfonyl]imide ( $[\text{PIP}_{13}][\text{FSI}]$ ) and  $[\text{PYR}_{14}][\text{FSI}]$  (1:1 by

weight or molar ratio). This IL mixture had a liquid-state range lowered to  $-80\text{ }^{\circ}\text{C}$ . Using exohedral nanostructured carbon (nanotubes and onions) as electrodes, the EDLCs using this  $[\text{PIP}_{13}][\text{FSI}] + [\text{PYR}_{14}][\text{FSI}]$  IL mixture electrolyte could be operable within a significantly expanded temperature range from  $-50$  to  $100\text{ }^{\circ}\text{C}$  (Fig. 21).

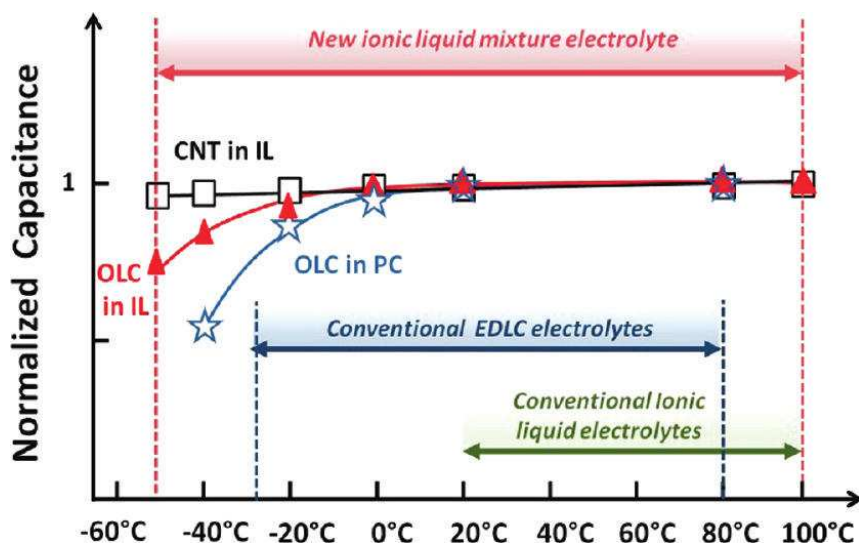


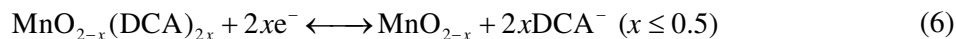
Fig. 21 Normalized capacitance ( $C/C_{20\text{ }^{\circ}\text{C}}$ ) for the OLC and VA-CNT electrodes in  $([\text{PIP}_{13}][\text{FSI}]_{0.5}([\text{PYR}_{14}][\text{FSI}]_{0.5})$  IL mixture and PC + 1 M TEABF<sub>4</sub> electrolytes. Capacitances were calculated at  $100\text{ mV s}^{-1}$ , except for the  $-50\text{ }^{\circ}\text{C}$  ( $1\text{ mV s}^{-1}$ ) and  $-40\text{ }^{\circ}\text{C}$  ( $5\text{ mV s}^{-1}$ ) experiments. Reprinted with permission from Ref. 282. Copyright 2011 American Chemical Society.

### 3.3.2.2. Solvent-free ionic liquids for pseudocapacitors

Ionic liquids have also been explored as the electrolytes for pseudocapacitors. Normally, for ES electrode materials, the pseudocapacitance contribution is closely related to surface functionalities, IL's hydrophobicity (the anions) and free water in ILs.<sup>277</sup> In an earlier work, Rochefort et al.<sup>284</sup> provided experimental evidence pseudocapacitance could be achieved on thermally prepared RuO<sub>2</sub> electrodes in a protic IL composed of 2-methylpyridine ( $\alpha$ -picoline) and trifluoroacetic acid (TFA) while no obvious pseudocapacitance could be observed in  $[\text{EMIM}][\text{BF}_4]$  IL. It was reported the shape of cyclic voltammograms and the specific capacitance ( $83\text{ F g}^{-1}$ ) of the RuO<sub>2</sub> electrode in a protic IL were similar to those obtained in  $0.1\text{ M H}_2\text{SO}_4$  aqueous electrolyte. However, the high viscosity and slow proton transfer in the IL electrolyte could limit the charging rate. Mayrand-Provencher et al.<sup>285</sup> tested a series of pyridinium-based protic ILs as ES electrolytes, and found the alkyl chain length of a cation's substituent and the substituent position had an effect on the electrolyte conductivity and viscosity, ESPW, specific capacitance and cycling stability of the

RuO<sub>2</sub> electrodes. Using *in-situ* infrared spectroscopy technique, Richey et al.<sup>286</sup> tried to obtain a fundamental understanding of individual cation and anion dynamics of [EMIM][Tf] IL in a working RuO<sub>2</sub>-based pseudocapacitor.

Other less expensive metal oxides than RuO<sub>2</sub>, such as Mn oxides, have also been investigated as electrode materials for IL electrolytes-based ESs.<sup>287-290</sup> For example, Chang et al.<sup>291</sup> obtained pseudocapacitive performance from a Mn oxide in an aprotic 1-ethyl-3-methylimidazolium-dicyanamide aprotic IL electrolyte (i.e., without involving protons and alkali cations in the electrolyte). Mn oxide showed a specific capacitance of 72 F g<sup>-1</sup> with a potential window of ~2 V in [EMIM][DCA] electrolyte. Using XPS and *in-situ* X-ray absorption spectroscopy (XAS), Chang et al.<sup>292</sup> found that smaller [DCA]<sup>-</sup> anions, instead of [BMP]<sup>+</sup> cations, could reversibly insert/desert into the tunnels between MnO<sub>6</sub> octahedral units, compensating the Mn<sup>3+</sup>/Mn<sup>4+</sup> valent state variation during the charging/discharging process in the [BMP][DCA] IL electrolyte, as expressed as Equation (6):



When using protic ILs rather than aprotic ones, Ruiz et al.<sup>293</sup> found MnO<sub>2</sub> electrodes could exhibit a pseudocapacitive behaviour in protic ILs composed of 2-methoxyppyridinium and trifluoroacetate, as observed by *in-situ* UV-visible spectroscopy. In addition to the extensively studied MnO<sub>2</sub> materials, other pseudocapacitive material-IL electrolyte systems have also been studied, such as Ru-doped Cu oxide in 3-carboxymethyl-1-methylimidazolium bisulfate [CMIM][HSO<sub>4</sub>],<sup>294</sup> TiO<sub>2</sub> in [EMIM][TFSI],<sup>295</sup> Fe<sub>2</sub>O<sub>3</sub> in [EMIM][BF<sub>4</sub>],<sup>296</sup> porous Ni in [EMIM][BF<sub>4</sub>],<sup>297</sup> nanocomposites composed of VN and N-doped carbon in [PYR<sub>14</sub>][TFSI] and [PYR<sub>14</sub>][FSI],<sup>298</sup> poly(3-methylthiophene) in [EMIM][TFSI],<sup>299</sup> as well as PAN in [EMIM][BF<sub>4</sub>]<sup>300</sup> and [EMIM][TFSI].<sup>301</sup>

### 3.3.2.3. Solvent-free ionic liquids for hybrid electrochemical capacitors

ILs have also been explored as electrolytes for hybrid ESs with asymmetric electrode configurations (e.g., AC//poly(3-methylthiophene),<sup>302, 303</sup> AC//MnO<sub>2</sub>,<sup>304</sup> and AC//graphene-supported Fe<sub>2</sub>O<sub>3</sub><sup>296</sup>). For example, Balducci et al.<sup>302</sup> used both [BMIM][PF<sub>6</sub>] and [PYR<sub>14</sub>][TFSI] ILs as electrolytes for AC//poly(3-methyl-thiophene) (PMeT) hybrid ESs, and observed some enhanced cell voltage, cycling life at high temperatures when compared to that of ESs using organic electrolyte (e.g., TEABF<sub>4</sub>/PC). The AC//pMeT hybrid ES using [PYR<sub>14</sub>][TFSI] IL could deliver maximum energy and power densities of 24 Wh kg<sup>-1</sup> and 14 kW kg<sup>-1</sup>, respectively, after the first thousand cycles at 10 mA cm<sup>-2</sup> and 60 °C. Sun et al.<sup>296</sup> used [EMIM][BF<sub>4</sub>] IL as an electrolyte for asymmetric ESs with activated PANI-derived carbon nanorods as negative electrode and graphene sheets-supported Fe<sub>2</sub>O<sub>3</sub> nanoparticles as positive electrode. This hybrid ES was able to operate within a wide voltage range of 0–4 V, and could deliver a very high maximum energy density of 177 W h kg<sup>-1</sup> and showed a relatively large energy density of 62.4 W h kg<sup>-1</sup> at a high

power density of  $8 \text{ kW kg}^{-1}$ . As discussed previously, the cycling stability of a hybrid ES is always an important concern when compared to that of EDLC. In this regard, Arbizzani et al.<sup>266</sup> reported although AC//pMeT hybrid ES using [PYR<sub>14</sub>][TFSI] IL as electrolyte could deliver a 30% of higher energy than the carbon-based AEDLC, its cycling stability was much lower than the latter. The specific capacitance of this hybrid ES was decreased by 50% after 5000 cycles due to the deterioration of the pMeT electrode.

### 3.3.3. Mixtures of ionic liquids and organic solvents

In order to reduce the viscosity and increase the conductivity of ILs, particularly at low temperatures, mixture solutions containing ILs and organic solvents have been explored as electrolytes for ESs. Similar to the research for solvent-free ILs-based ESs, imidazolium-based ILs have been seen to be the most extensively studied ones in organic solvents due to their relatively high conductivity among commonly used ILs. In this aspect, McEwen et al.<sup>305</sup> found the conductivities of IL-based carbonate electrolytes (ILs: ([EMIM][PF<sub>6</sub>]) and [EMIM][BF<sub>4</sub>], both of which contain EMI cation) were roughly 25% greater than that based on the TEABF<sub>4</sub> organic electrolyte. A conductivity as high as  $27 \text{ mS cm}^{-1}$  was observed in 2 M [EMIM][PF<sub>6</sub>] plus EC-DMC solvent. In addition, a 2 M [EMIM][PF<sub>6</sub>]/PC electrolyte could give both a higher specific capacitance and more thermal stability than 1 M TEABF<sub>4</sub>/PC. Orita et al.<sup>306</sup> studied a series of alkyl-functionalized ILs mixed with organic solvents (typically PC) as electrolytes for EDLCs. Two ILs, one composed of imidazolium cations with allyl groups (diallylimidazolium (DAIM)) and TFSI<sup>-</sup> anion, and the other composed of imidazolium with saturated alkyl groups (EMIM) and TFSI<sup>-</sup> anion, were used in the preparation of solvent-based IL electrolytes. EDLC measurements in 1.4 M IL electrolytes showed the former electrolyte could give higher capacitance and lower resistance within a wider temperature range than the latter. However, the stability of the EDLC using 1.4 M [DAIM][BF<sub>4</sub>]/PC was lower than the one using [EMIM][BF<sub>4</sub>]/PC. It was also demonstrated the stability could be improved though the addition of DMC to PC.

Lin et al.<sup>307</sup> found although the bare molecular sizes of [EMIM]<sup>+</sup> and [TFSI]<sup>-</sup> were similar, they had different solvated ion sizes in ACN solvent and increased in size in the order of: [TFSI]<sup>-</sup> in ACN > [EMI]<sup>+</sup> in ACN > [EMI]<sup>+</sup>@ [TFSI]<sup>-</sup>. Therefore, the optimization of pore structure and size distribution of porous carbon with respect to IL size in an organic solvent should consider the solvated ion size, which might be different from that in pure IL electrolyte.

As mentioned in Section 3.2.2., the use of ADN as an organic solvent has advantages of a larger EDLC operative cell voltage and higher flash point than the ACN solvent.<sup>145</sup> However, the solubility of commonly used conducting salt such as TEABF<sub>4</sub> in ADN is much lower than in ACN, thus limiting its application.<sup>145</sup> The use of IL such as 1-ethyl-3-methylimidazolium bis[(trifluoromethyl)sulfonyl]imide ([C<sub>2</sub>mIM][TFSI]) as the salt in ADN was tested to address this issue, and the results

showed higher salt solubility.<sup>308</sup>

It should be pointed out that not all the mixtures of IL and organic solvents provide a benefit to ES performance. For example, Palm et al.<sup>309</sup> reported the addition of an organic solvent (ACN, PC or GBL) to pure [EMIM][BF<sub>4</sub>] to compose an electrolyte for EDLCs, and the results showed some negative effects although this mixing strategy could lead to a decreased viscosity and melting point, and increased conductivity when compared to those of pure [EMIM][BF<sub>4</sub>]. Therefore, attention should be paid to not compromising the important advantages of pure IL when adding solvent into the IL for ES electrolyte.

In addition, imidazolium-based ILs mixed with organic solvents have also been explored as electrolytes for both pseudocapacitors and hybrid ESs.<sup>304</sup> For example, Zhang et al.<sup>304</sup> found the introduction of DMF to [BMIM][PF<sub>6</sub>] IL increased the capacitance and at the same time decreased the internal resistance of the asymmetric AC/MnO<sub>2</sub> ES. This improvement was attributed to the improved electrolyte penetration and ion mobility when compared to pure IL.

Due to the relatively high ESPWs, pyrrolidinium-based ILs have also been mixed with organic solvents to form mixture electrolytes for ESs.<sup>310-312</sup> As observed, the addition of organic solvents to the pyrrolidinium-based ILs significantly increased the conductivity and decreased the viscosity of the electrolytes due to the solvation effect provided by the organic solvents.<sup>310</sup> Compared to conventional TEABF<sub>4</sub>/PC organic electrolyte, the use of pyrrolidinium-based ILs mixed with PC effectively increased the operative EDLC cell voltage to 3.2–3.5 V.<sup>311, 312</sup>

Regarding ammonium-based ILs, Abdallah et al.<sup>313</sup> found the addition of [TMPA][TFSI] IL could reduce both the flammability and volatility of ACN solvent-based electrolytes. With respect to sulfonium-based ILs, Brandt et al.<sup>314</sup> reported the EDLC using an electrolyte containing 3.8 M [Me<sub>3</sub>S][TFSI] in PC could show an operative cell voltage up to 2.9 V. This EDLC also showed a stable performance at both 20 and 60 °C while an EDLC using [Me<sub>3</sub>S][TFSI]/PC with a lower concentration of 1.9 M did not show a stable performance. This result was thought to be the different abilities to inhibit the anodic oxidation of the Al current collector in these two different electrolytes. Regarding the phosphonium-based ILs, Frackowiak et al.<sup>315</sup> found the amount of ACN in trihexyl(tetradecyl)phosphonium bis(trifluoromethylsulfonyl)imide ( $[(C_6H_{13})_3(P(C_{14}H_{29}))](Tf_2N)]$ ) or trihexyl(tetradecyl) phosphonium dicyanamide ( $[(C_6H_{13})_3(P(C_{14}H_{29}))](CN)_2N]$ ) could play an important role in both specific energy and power densities of EDLCs.<sup>315</sup> An AC-based EDLC using  $[(C_6H_{13})_3(P(C_{14}H_{29}))](Tf_2N)]$  IL with 25 wt.% ACN could achieve an operative cell voltage of 3.4 V and had a higher energy density of about 40 Wh kg<sup>-1</sup> and better cycling stability when compared to that using conventional ILs and containing a different amount of ACN. Regarding piperidinium-base ILs, Lewandowski et al.<sup>316</sup> reported the ionic conductivity (1.5 mS cm<sup>-1</sup> at 25 °C) of pure N-Methyl-N-propylpiperidinium bis(trifluoromethanesulphonyl)imide ([MePrPip][NTf<sub>2</sub>]) IL could be significantly increased to about 40 mS cm<sup>-1</sup> after the addition of 52 wt.% ACN. This mixture electrolyte showed an ESPW of about 3.7 V on AC electrodes.

Some comparative studies between different types of ILs mixed with organic solvents solvents have also been reported.<sup>311, 317, 318</sup> For example, Orita et al.<sup>318</sup> investigated various sulfonium- and thiophenium-based ILs (Fig. 22

Fig. 22) in PC solvent as EDLC electrolytes. They found [DEMS][TFSA]/PC had the highest ionic conductivity among the investigated ILs with TFSA anion. The ionic conductivity of [DEMS][BF<sub>4</sub>]/PC was higher than those of [DEMS][PF<sub>6</sub>]/PC and [DEMS][TFSA]/PC. The EDLC using [DEMS][BF<sub>4</sub>]/PC electrolyte showed a higher specific capacitance than the one using conventional [EMIM][BF<sub>4</sub>]/PC or [TEMA][BF<sub>4</sub>]/PC electrolyte. However, [DEMS][BF<sub>4</sub>]/PC electrolyte resulted in EDLC having a shorter lifetime when compared to that in an [EMIM][BF<sub>4</sub>] electrolyte.

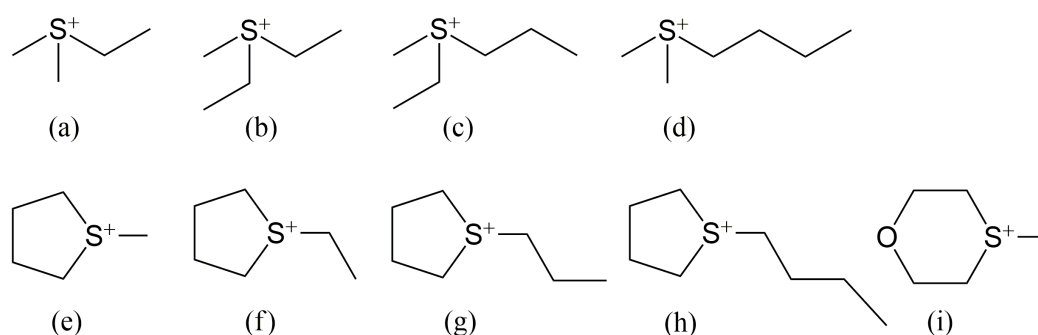


Fig. 22 Chemical structures of cations used in Ref. 318: (a) DMES (dimethylethylsulfonium), (b) DEMS (diethylethylsulfonium), (c) EMPS (ethylmethylpropylsulfonium), (d) BDMS (butyldimethylsulfonium), (e) MTT (1-methyltetrahydrothiophenium), (f) ETT (1-ethyltetrahydrothiophenium), (g) PTT (1-propyltetrahydrothiophenium), (h) BTT (1-butyltetrahydrothiophenium), (i) MOT (1-methyl-1,4-thioxonium). Reprinted from Ref. 318, with permission from Elsevier.

Brandt et al.<sup>319</sup> found EDLCs with a 1.9 M [PYR<sub>14</sub>][BF<sub>4</sub>]/PC electrolyte could show both higher energy and power densities than EDLCs with 1.5 M [PYR<sub>14</sub>][TFSI]/PC, 3.8 M [Me<sub>3</sub>S][TFSI]/PC or conventional 1 M TEABF<sub>4</sub>/PC at all investigated current densities. This was attributed to the larger operative cell voltage (Fig. 23).

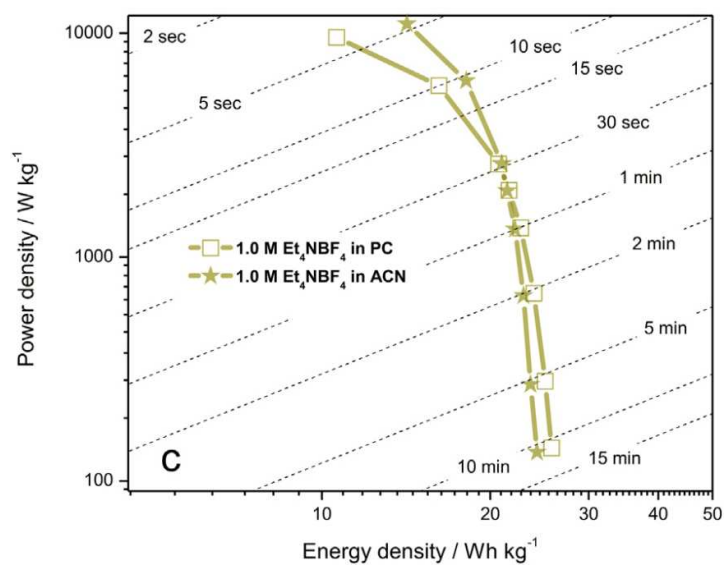
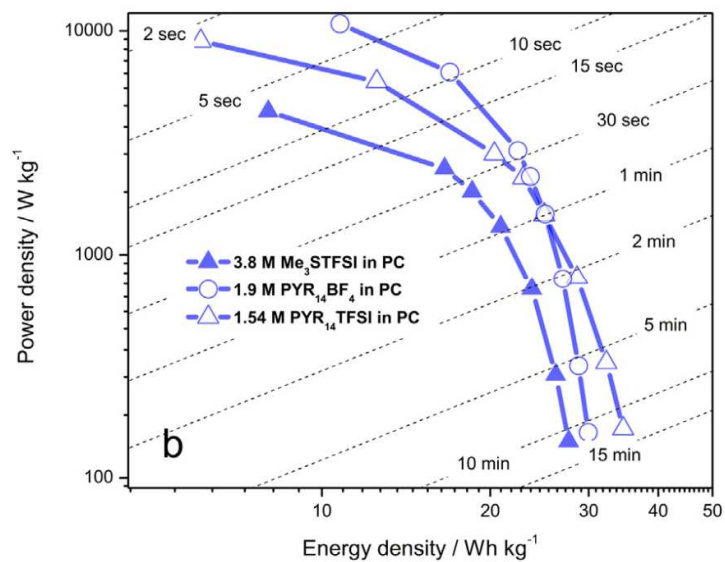
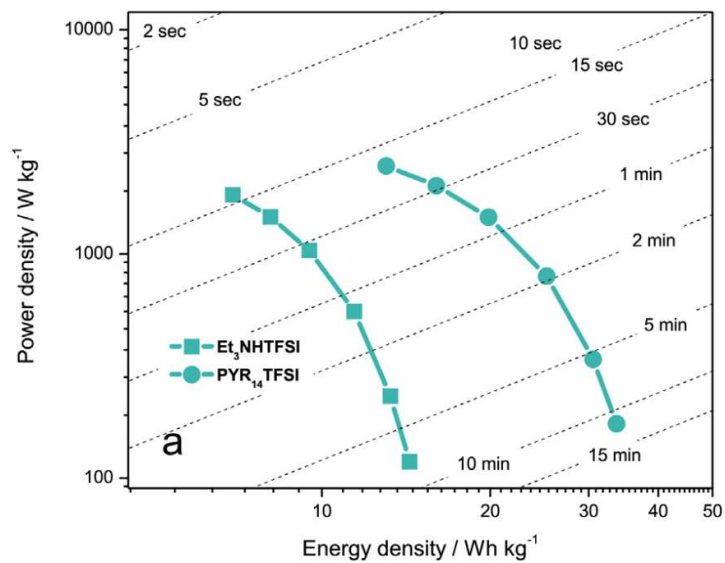


Fig. 23 Ragone-like plots of EDLCs containing different electrolytes. The average values of energy and power densities refer to the total AC loading in the cell. Reprinted from Ref. 319, with permission from Elsevier.

It should be noted that besides aprotic ILs, protic ILs mixed with organic solvents have also been studied although it received much less attention when compared to aprotic ILs due to their lower cell operative cell voltage (1.5–2.5 V).<sup>278, 280, 320-322</sup> Several studies reported EDLCs using mixture electrolytes containing protic ILs and organic solvents (e.g., [Bu<sub>3</sub>PH][BF<sub>4</sub>] in GBL<sup>320</sup> and [Pyrr][NO<sub>3</sub>] in GBL<sup>321</sup>) could operate within a wide temperature range from –40 °C to 80 °C.

In addition, theoretical modeling and simulation work has also been carried out to study the EDL structure and capacitance in the mixtures of ILs and organic solvents by using MD simulations.<sup>244, 323</sup>

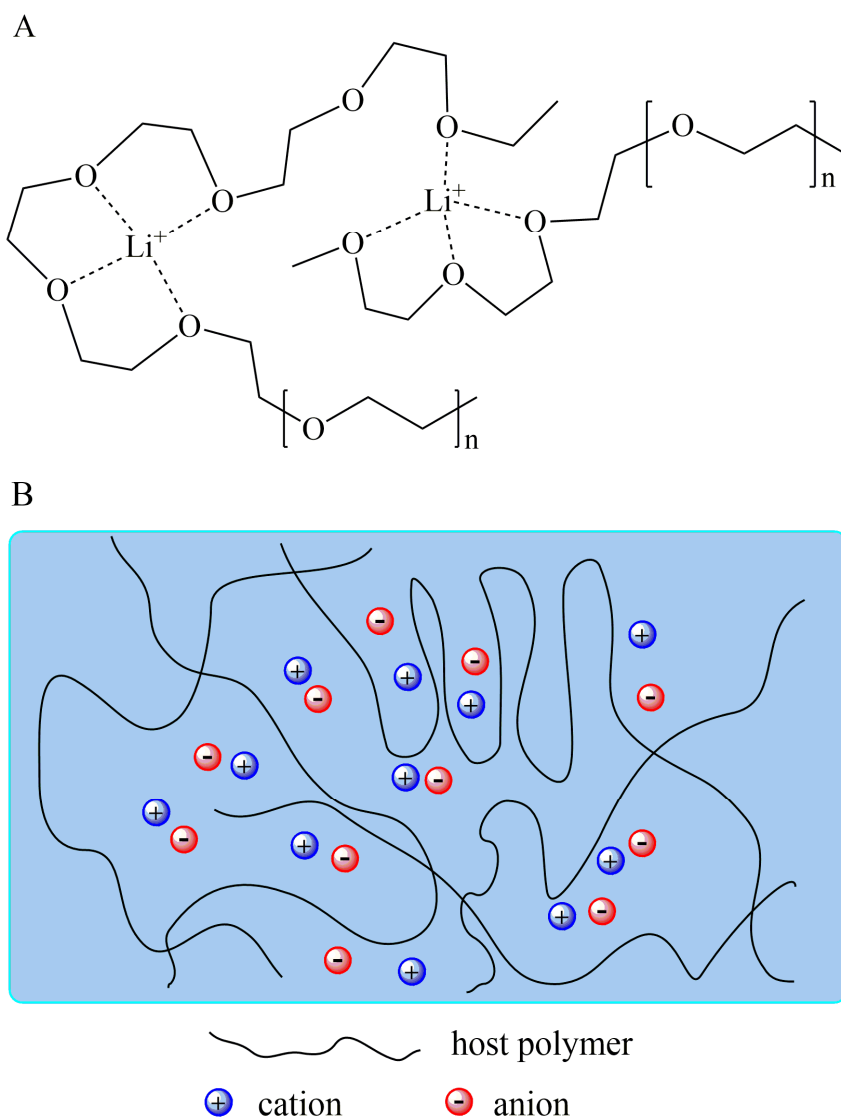
### 3.4. Solid- or quasi-solid-state electrolytes for ESs

With the rapid growing demand of powers for portable electronics, wearable electronics, micro-electronics, printable electronics and especially flexible electronic devices, solid-state electrolyte-based electrochemical energy devices have attracted great interest in recent years. The solid-state electrolytes can not only serve as the ionic conducting media but also as the electrode separators. The major advantages when using solid-state electrolytes are the simplification of packaging and fabrication processes of ESs and liquid-leakage free. To date, major types of the solid-state electrolytes developed for ESs are based on polymer electrolytes, and only very limited work has been focused on inorganic solid materials (e.g., ceramic electrolyte<sup>324, 325</sup>).

The polymer-based solid electrolytes for ESs can be further grouped into three types: the solid polymer electrolyte (SPEs, also known as dry polymer electrolytes), the gel polymer electrolyte (GPE) and the polyelectrolyte. Due to the presence of liquid phase in GPEs, some studies called them as quasi-solid-state electrolytes.<sup>326, 327</sup> As shown in Fig. 24, the SPE is composed of a polymer (e.g., PEO) and a salt (e.g., LiCl), without any solvents (e.g. water). The ionic conductivity of SPE is provided by the transportation of salt ions through the polymer. On the contrary, the GPE consists of a polymer host (e.g., PVA) and an aqueous electrolyte (e.g., H<sub>2</sub>SO<sub>4</sub>) or a conducting salt dissolved in solvent. In this case, the polymer serves as a matrix, which can be swollen by the solvent, and the ions transport in the solvent instead of in the polymer phase, which is different from that of SPE. In the polyelectrolyte, the ionic conductivity is contributed by the charged polymer chains. As identified, each type of these solid-state electrolytes has their own advantages and disadvantages. In normal, GPEs have the highest ionic conductivity among these three types of solid-state electrolytes. Due to the presence of liquid phase in a GPE, its ionic conductivity is significantly higher than that of the dry SPE. Due to this reason, GPE-based ESs currently dominate the solid electrolyte-based ES



products, and studies on ESs using dry SPEs are very limited.<sup>328</sup> However, depending on their composition, GPEs may suffer from relative poor mechanical strength and narrow operative temperature range particularly when water is used as the solvent. Furthermore, the weak mechanical strength of some GPEs is the main concern, as it may lead to internal short circuits, causing safety issues.<sup>21</sup> Although dry SPEs normally have low ionic conductivities, they have relatively high mechanical strength when compared to GPEs. It should be noted these solid-state electrolytes for ESs normally have some common disadvantages including the limited contact surface area between solid-state electrolytes and electrode materials especially for the nanoporous materials. This issue could increase the ESR value, reduce the rate performance, and limit the utilization of active electrode materials, resulting in a low specific capacitance of ESs.



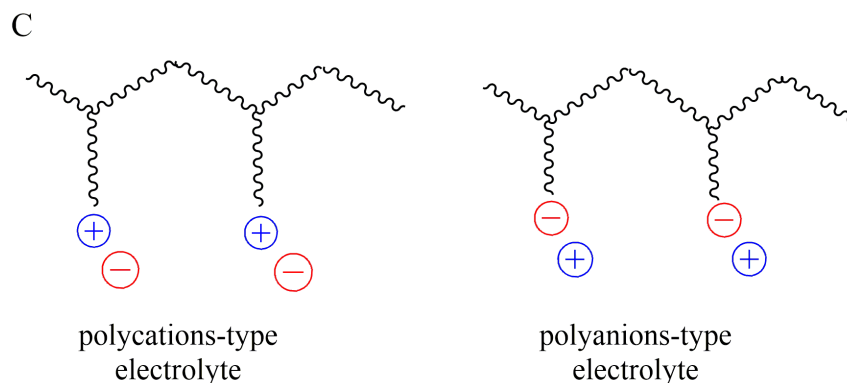


Fig. 24 Schematic diagrams of (a) dry solid-state polymer electrolyte (e.g., PEO/Li<sup>+</sup>), (b) gel polymer electrolyte, and (c) polyelectrolyte.

As reported in the literature, solid electrolytes have been used for various types of ESs such as EDLCs, pseudocapacitors and hybrid ESs with different kinds of electrode materials. When developing solid-state electrolytes for ESs, the following critical requirements should be considered: (1) high ionic conductivity, (2) high chemical, electrochemical and thermal stability, and (3) sufficient mechanical strength and dimensional stability. In practice, it is difficult for a solid-state electrolyte to meet all of these requirements. There are often some trade-off between ionic conductivity and mechanical strength. In this aspect, several reviews have been published recently (i.e., focusing on the solid-stated electrolytes for ESs).<sup>11, 12, 20, 21, 329</sup> Therefore, this present review mainly focuses on the latest new developments.

### 3.4.1 Gel polymer electrolytes

As mentioned previously, GPEs are currently the most extensively studied electrolytes for solid-state ESs due to their high ionic conductivity. A GPE is typically composed of a polymer matrix (host polymer) and a liquid electrolyte (e.g., aqueous electrolyte, organic solvent containing conducting salt and IL). Regarding the host polymer, various polymer matrices have been explored for preparing GPEs, including poly(vinyl alcohol) (PVA), poly(-acrylic acid) (PAA), potassium polyacrylate (PAAK), poly(ethyl oxide) (PEO), poly(methylmethacrylate) (PMMA), poly(ether ether ketone) (PEEK), poly(acrylonitrile)-block-poly(ethylene glycol)-block-poly(acrylonitrile) (PAN-*b*-PEG-*b*-PAN), and poly(vinylidene fluoride-co-hexafluoropropylene) (PVDF-HFP). When water is used as a plasticizer, the resulting GPE is also called a hydrogel polymer electrolyte, which has some three-dimensional polymeric networks which can trap water in the polymer matrices mainly through surface tension.<sup>11</sup> Besides water, organic solvents such as PC,<sup>330</sup> EC and DMF<sup>331</sup> or their mixtures (e.g., PC-EC<sup>332</sup>, PC-EC-DMC,<sup>333</sup> and PC-EC<sup>331</sup>) have also been commonly used as the plasticizers in GPEs. The composition ratio between polymer and plasticizer normally plays an important role in the degree of plasticization, thus affecting the glass-transition temperature of GPEs.<sup>11</sup>

One of the most significant advantages of using solid-state electrolytes including GPEs in ESs is it allows the development of diverse and bendable structures and tunable shapes for various desired applications. For example, based on the PVA-based hydrogels, various solid-state ESs have been developed, including flexible ESs,<sup>334</sup> stretchable ESs,<sup>335</sup> flexible micro-ESs,<sup>336</sup> printable micro-ESs,<sup>337</sup> on chip micro-ESs,<sup>338</sup> 3D micro-ESs,<sup>339</sup> yarn ESs,<sup>340</sup> wire or fiber-shaped ESs,<sup>341</sup> transparent ESs,<sup>342</sup> ultrathin ESs,<sup>343</sup> weaveable ESs,<sup>344</sup> paper-like ESs,<sup>345</sup> and integrated ESs with other devices.<sup>346</sup>

#### 3.4.1.1. Hydrogel polymer electrolyte

Poly(vinyl alcohol) (PVA), as a linear polymer, has so far been the most extensively studied polymer matrix among the various kinds of host polymers for hydrogel electrolytes. This results from its ease of preparation, high hydrophilicity, good film forming properties, non-toxic characteristic and low cost.<sup>347</sup> PVA is generally mixed with various aqueous solutions such as strong acid (e.g., H<sub>2</sub>SO<sub>4</sub> and H<sub>3</sub>PO<sub>3</sub>), strong alkaline (e.g., KOH) and neutral (e.g., LiCl) electrolyte to prepare hydrogels.

##### *Hydrogel polymer electrolytes for carbon-based electrodes*

When GPEs are used as ES electrolytes, the design of the electrode/electrolyte interface for high performance is very important. Some studies showed GPE-based ESs could suffer from poor rate capabilities due to the limited ion diffusion rate or large interfacial resistance at the electrode/electrolyte interface.<sup>348</sup> Kaempgen et al.<sup>348</sup> also found the thickness of the electrode layer played an important role in achieving high capacitance of PVA/H<sub>3</sub>PO<sub>3</sub>-based ESs. As shown in Fig. 25, in a 1 M H<sub>2</sub>SO<sub>4</sub> aqueous electrolyte, the capacitance increases linearly with increasing thickness of the electrode layer, while a saturation of the capacitance value can be observed when using PVA/H<sub>3</sub>PO<sub>3</sub> hydrogel as the electrolyte. This was thought to be caused by the limited ion penetration into the porous electrodes. In this case, the hydrogel electrolyte may not be the suitable electrolyte for applications requiring high charge storage capability.

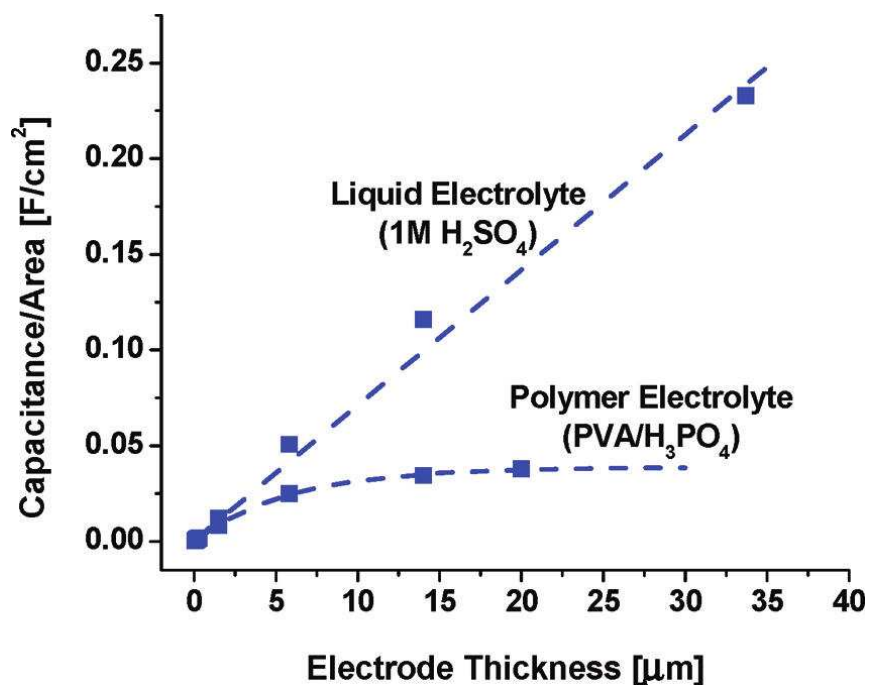


Fig. 25 Capacitance per area as a function of electrode layer thickness (CNT film) in two different ES electrolytes (1 M  $\text{H}_2\text{SO}_4$  aqueous electrolyte and PVA/ $\text{H}_3\text{PO}_4$  gel electrolyte). Reprinted with permission from Ref. 348. Copyright 2009 American Chemical Society.

Normally, the matching among the electrode/hydrogel electrolyte interface, the electrode material, and hydrogel electrolyte is very critical in achieving high ES performance. With respect to this, electrode materials with various structures, such as CNTs grown on carbon cloth,<sup>349</sup> activated carbon cloth,<sup>350</sup> 3D graphene network,<sup>351</sup> porous graphene ribbons,<sup>352</sup> and graphene/porous carbon aerogels,<sup>353</sup> have been studied using PVA-based hydrogel electrolytes. It was observed these advanced carbon structures can facilitate the infiltration of hydrogel electrolyte into the porous electrode, leading to a large ES performance improvement and a high utilization of the active electrode materials.

The type of aqueous solutions in a hydrogel electrolyte also has a significant effect on the ES performance due to their different ionic conductivities, thermal and environmental stabilities. Optimization is generally needed through careful selection of the electrolyte solution for the PVA, modifying the PVA and incorporating additives into the hydrogel. Chen et al.<sup>354</sup> prepared six different PVA-based hydrogels using different electrolytes such as  $\text{H}_3\text{PO}_4$ ,  $\text{H}_2\text{SO}_4$ , KOH, NaOH, KCl and NaCl for graphene-based ESs. Based on electrochemical measurements, they found the PVA/ $\text{H}_3\text{PO}_4$  hydrogel electrolyte exhibited the best capacitive performance among all the investigated PVA-based hydrogels.

Regarding the effect of temperature, PVA-based electrolytes generally suffer fluidity problems at high temperatures.<sup>347</sup> To improve this temperature related

performance, Fei et al.<sup>347</sup> prepared a cross-linked PVA/H<sub>2</sub>SO<sub>4</sub> hydrogel as an ES electrolyte, and the fabricated ES showed good cycling stability with 78.3% retention of the initial specific capacitance after 1000 cycles at a high temperature of 70 °C. Similarly, various additives (fillers), such as SiO<sub>2</sub>,<sup>355</sup> TiO<sub>2</sub>,<sup>356</sup> Sb<sub>2</sub>O<sub>3</sub>,<sup>357</sup> graphene oxide (GO)<sup>358</sup> and hydroxyethylcellulose,<sup>359</sup> have also been used for PVA-based hydrogels to improve performance. For example, Huang et al.<sup>358</sup> used electrically insulating GO as an ionic conducting promoter in a boron cross-linked PVA/KOH hydrogel for an EDLC electrolyte. It was observed that the ionic conductivity increased with an increasing amount of GO during the low GO content range. However, the ionic conductivity decreased with further increases in the GO content, probably due to the ion channel blocking effect caused by the aggregation of GO sheets (Fig. 26). The specific capacitance of EDLC using boron cross-linked PVA/KOH hydrogel containing 20 wt.% GO was found to be 141.8 F g<sup>-1</sup> at 0.1 A g<sup>-1</sup>, which was 29% higher than the specific capacitance using a bare KOH aqueous electrolyte.

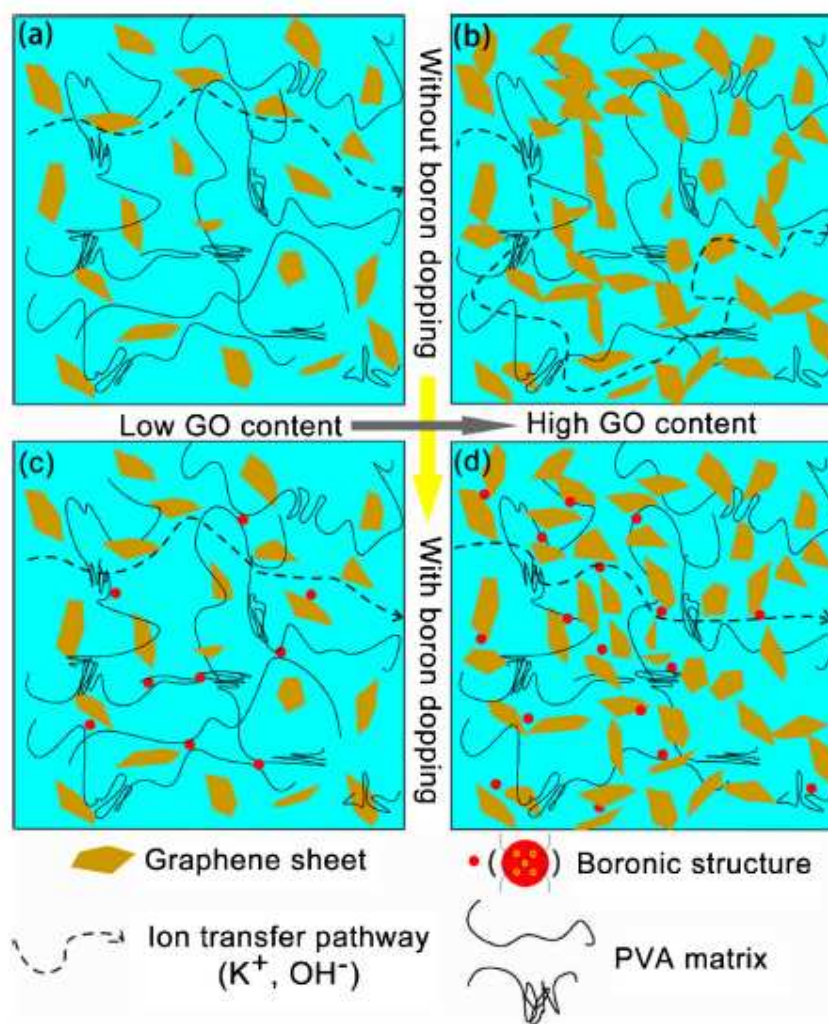


Fig. 26 Illustration of ion transport mechanism in GO-PVA and GO-B-PVA alkaline

gel electrolytes with low and high GO contents. Reprinted from Ref. 358, with permission from Elsevier.

The environmental stability of hydrogel electrolyte-based ESs is also one of the important factors used in evaluating the ES performance. It was found the performance of a PVA/KOH hydrogel electrolyte-based ES could suffer a significant loss over time (e.g., after 40–67 days of shelf storage) due to the dehydration of the KOH/PVA electrolyte.<sup>360</sup> In order to improve the environmental stability of ESs using alkaline PVA hydrogel electrolytes, Gao et al.<sup>360</sup> explored using a tetraethylammonium hydroxide (TEAOH) replacement for the KOH in the PVA-based hydrogel electrolyte. It was thought this TEAOH would have a higher water retention capability than KOH. The addition of SiO<sub>2</sub> into a PVA/silicotungstic acid (SiWA)-H<sub>3</sub>PO<sub>4</sub> hydrogel was also found to stabilize the water content in the hydrogel at relative low humidity, leading to an ES with improved environmental stability. This was attributed to the strong bond interaction between SiO<sub>2</sub> and water molecules.<sup>355</sup>

### *Hydrogel polymer electrolytes for pseudocapacitors and hybrid capacitors*

Beside EDCLs, considerable efforts have also been focused on the development of both hydrogel electrolyte-based pseudocapacitors and hybrid ESs. As mentioned previously, the electrochemical behaviour of pseudocapacitive electrode materials is strongly dependent on the nature of electrolytes. For ESs using acid PVA-based hydrogels (e.g., PVA/H<sub>2</sub>SO<sub>4</sub> and PVA/H<sub>3</sub>PO<sub>4</sub>), typical pseudocapacitive electrode materials explored include transition metal oxides (e.g., RuO<sub>2</sub>,<sup>361</sup> TiO<sub>2</sub>,<sup>362</sup> and manganese oxide<sup>343</sup>), metal nitrides (e.g., molybdenum nitride<sup>363</sup>), sulfides (e.g., MoS<sub>2</sub>,<sup>341</sup> TiS<sub>2</sub>,<sup>341</sup> and TaS<sub>2</sub><sup>341</sup>), selenides (e.g., GeSe<sub>2</sub><sup>334</sup> and NbSe<sub>2</sub><sup>341</sup>) and ECPs (e.g., PANI<sup>364</sup>, PPy,<sup>365</sup> and PEDOT<sup>366</sup>). In the case of alkaline PVA-based (mostly PVA/KOH) ESs, the most extensively studied pseudocapacitive electrode material is Ni(OH)<sub>2</sub>,<sup>88</sup> other electrode materials such as NiCo<sub>2</sub>O<sub>4</sub>,<sup>367</sup> CoMn-layered double hydroxide,<sup>368</sup> and MnO<sub>2</sub>,<sup>369</sup> have also been investigated. For neutral PVA-based hydrogel electrolytes (e.g., PVA/LiCl,<sup>370</sup> PVA/Na<sub>2</sub>SO<sub>4</sub>,<sup>371</sup> and PVA/NaNO<sub>3</sub><sup>372</sup>), pseudocapacitive materials such as MnO<sub>2</sub>,<sup>372</sup> V<sub>2</sub>O<sub>5</sub>,<sup>373</sup> ZnO,<sup>374</sup> VOPO<sub>4</sub>,<sup>375</sup> VN,<sup>376</sup> and KCu<sub>4</sub>Se<sub>8</sub><sup>373</sup> were frequently studied as electrode materials. To improve the intercalation/deintercalation performance, Li-containing PVA-based hydrogels (e.g., PVA/LiCl,<sup>370, 375</sup> PVA/LiOH,<sup>368</sup> PVA/LiNO<sub>3</sub><sup>377</sup>) have also been studied with pseudocapacitive electrode materials. It should be noted that compared to aqueous electrolytes, hydrogels provided greatly improved electrochemical stability for some pseudocapacitive electrode materials in particular (e.g., vanadium oxide<sup>370</sup> and VN<sup>376</sup>).

Once again, the matching between the electrode surface and the PVA-based hydrogel electrolyte needs to be optimized.<sup>375, 378</sup> To improve the conductivity and the utilization degree of the pseudocapacitive electrode materials in the hydrogel electrolyte, they could be dispersed on high-surface-area carbonaceous supports<sup>343</sup> or

combined with carbonaceous materials to make hybrid composites.<sup>341, 378</sup>

Hydrogel electrolytes generally have the similar shortcomings as aqueous electrolytes. For instance, symmetric ESs using hydrogel electrolytes can suffer from limited operative cell voltages and thus low energy density due to the narrow ESPW of the aqueous component in the hydrogel. To increase the operative cell voltage, hydrogel electrolyte-based asymmetric ESs using two different electrodes with complementary potential windows have recently been explored.<sup>346, 376</sup> It was determined that compared to the symmetric PVA hydrogel-based ESs, the operating cell voltage of asymmetric ESs can be greatly improved up to a high value such as 1.8 V.<sup>376</sup>

Besides PVA, other polymers have also been studied for use in hydrogels in ESs. For example, poly(acrylate)- and poly(acrylic acid)-based hydrogels were tested as promising ES electrolytes. These polymers can promote proton conduction since the protons in their side chains can be easily subtracted in an aqueous medium.<sup>379-381</sup> These alternative hydrogel electrolytes have been tested for AC-based EDLCs,<sup>382</sup> pseudocapacitors with electrode materials such as RuO<sub>2</sub><sup>379</sup>, MnO<sub>2</sub><sup>381</sup> and ECPs,<sup>380</sup> as well as asymmetric ESs.<sup>383</sup> Because the performance of pseudocapacitive electrode material depends on the properties of the electrolyte, the nature of the polymer host in a hydrogel electrolyte should have an influence on the performance of their associated pseudocapacitors. In this regard, Kim et al.<sup>379</sup> investigated the performance of RuO<sub>2</sub>-based ESs using various acrylic hydrogel electrolytes, such as poly(-acrylic acid) (PAA), potassium polyacrylate (PAAK), and poly(2-acrylamido-2-methyl-1-propanesulfonic acid) (PAMPS). The specific capacitance of a RuO<sub>2</sub> electrode in different electrolytes was found to decrease in the following order: PAMPS/H<sub>2</sub>O > 1 M H<sub>2</sub>SO<sub>4</sub> (aqueous electrolyte) > PAA/H<sub>2</sub>SO<sub>4</sub> > PAAK/H<sub>2</sub>SO<sub>4</sub> > PAMPS/H<sub>2</sub>SO<sub>4</sub>. They attributed the highest capacitance of RuO<sub>2</sub> electrode obtained in PAMPS electrolyte to the most favorable proton accommodation in the side chain groups of PAMPS.

In general, hydrogel electrolytes have limited thermal stability. To improve the thermal stability, Shimamoto et al.<sup>384</sup> explored a phosphosilicate gel as the electrolyte for asymmetric ES with MnO<sub>2</sub>/CNT composite positive electrode and AC negative electrode. The resulting ESs could be operated within a wide temperature range from -30 to 100 °C.

In addition, Nafion® (a perfluorosulfonic acid polymer), a famous proton-conducting polymer, has also been employed as an electrolyte for various kinds of solid-state ESs due to its high ionic conductivity.<sup>385, 386</sup> Several studies showed ESs using Nafion® as an electrolyte could support high potential scan rates.<sup>385</sup>

### 3.4.1.2. Organogel electrolytes

To increase the working cell voltage, GPEs based on organic solvents

(plasticizers), known as organogel electrolytes, have been studied as electrolytes for ESs. In these organogel electrolytes, various polymer hosts, such as PEO,<sup>333, 387</sup> PMMA,<sup>388, 389</sup> polyvinylpyrrolidone (PVP), PEEK,<sup>390</sup> and copolymers,<sup>331, 391-393</sup> were reported in the literature as having been tested. Copolymers with different constituent units, such as poly(acrylonitrile)-block-poly(ethylene glycol)-block-poly(acrylonitrile) (PAN-*b*-PEG-*b*-PAN) have shown to be the most promising polymeric hosts in organogel electrolyte-based ESs.<sup>331, 391</sup> For example, Hsueh et al.<sup>391</sup> reported a synergistic effect between PAN and PEG when they were used as the GPE host. The ionic conductivity of copolymer-based organogels could be optimized by tuning the AN/EG chain length ratio. A maximal ionic conductivity of  $1.1 \times 10^{-2} \text{ S cm}^{-1}$  was obtained, which was much higher than that of LiClO<sub>4</sub>/DMF organic liquid electrolyte ( $1.6 \times 10^{-3} \text{ S cm}^{-1}$ ). Carbon-based EDLCs using this copolymer-based organogel electrolyte could deliver both higher energy and power densities ( $20 \text{ Wh kg}^{-1}$  at  $10 \text{ kW kg}^{-1}$ ) than those of EDLCs using organic liquid electrolytes, suggesting a positive synergistic effect between PAN and PEG blocks.

Regarding the organic solvent (plasticizer) in the organogel electrolyte, typically investigated systems include PC, EC, DMC or their mixtures,<sup>333, 387</sup> ACN,<sup>388, 389</sup> DMSO,<sup>392</sup> and DMF.<sup>331, 391</sup> Using these organogel electrolytes, the ES cell voltages were increased up to 2.5–3 V,<sup>331, 391-394</sup> which was much higher than those of hydrogel electrolyte-based ESs including asymmetric ones. These high cell voltages indicate one of the most significant advantages of organogel electrolyte-based ESs. As a direct result of the high cell voltages, most of the reported maximum energy density of organogel electrolyte-based ESs had relatively high values from approximately 18 to  $25 \text{ Wh kg}^{-1}$ .<sup>333, 387, 388, 391</sup> Interestingly, as reported by Schroeder et al. in Fig. 27,<sup>394</sup> a LIC using the methacrylate-based organogel electrolyte, can be operated at a cell voltage of 4 V, resulting in a further increase in energy density.



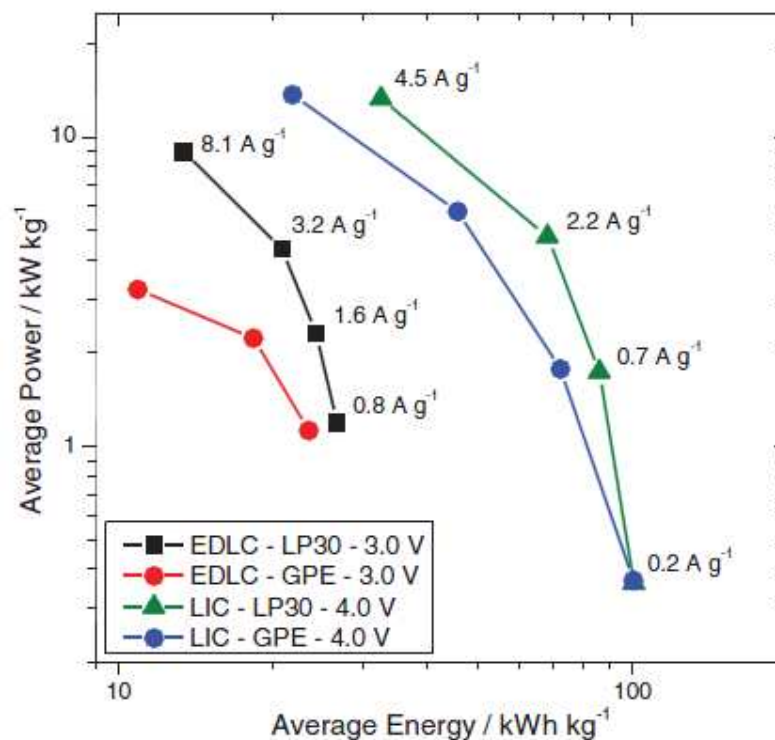


Fig. 27 Ragone-like plot for two ESs and two LICs each containing either the liquid electrolyte LP30 or the methacrylate-based GPE. The average energy and power indicated in the figure is referred to the total active mass of the LIC. Reproduced by permission of The Electrochemical Society from Ref. 394.

Regarding the salts used in organogel electrolytes, the ones typical investigated include  $\text{LiClO}_4$ ,<sup>331, 391</sup>  $\text{LiPF}_6$ ,<sup>393</sup>  $\text{TBAPF}_6$ ,<sup>388, 389</sup>  $\text{NaTFSI}$ ,<sup>333</sup> and so on. Research has determined, the selection of the salt and the ratio between salt and the host polymer has a great influence on the electrolyte's ionic conductivity.<sup>395</sup> As Mg is much more abundant than Li, several studies tested Mg salt in organogel electrolytes.<sup>387, 392</sup> Normally, the organogel electrolytes would suffer from low ionic conductivities. In an effort to overcome this issue, Jain et al.<sup>396</sup> added  $\text{SiO}_2$  particles into the PVDF-HFP/Mg( $\text{ClO}_4$ )<sub>2</sub>-PC electrolytes for EDLCs. The resulting organogel electrolyte with the optimized composition showed a relatively high ionic conductivity of  $5.4 \times 10^{-3} \text{ S cm}^{-1}$  at room temperature, and also had good mechanical and dimensional stability.<sup>396</sup> In addition, organogel electrolytes were found to have high cycling stability especially at higher ES cell voltages.<sup>393</sup>

### 3.4.1.3. IL-based solid-state electrolytes

Recognizing the large ESPW and high thermal stability of ILs, considerable research efforts have been put into learning about the IL-based GPEs (also known as

ionogels), which are made by incorporation of ILs into polymer hosts. Recently, the majority of the studies were focused on the ionogel electrolyte-based EDLCs with electrode materials such as AC,<sup>397</sup> porous carbon,<sup>398</sup> and CNT.<sup>399</sup> There were also some studies devoted to ionogel electrolyte-based pseudocapacitors with electrode materials such as MnO<sub>2</sub>,<sup>400</sup> PEDOT<sup>401</sup> and composite materials (e.g., PMeT with hydrous RuO<sub>2</sub><sup>402</sup>). With ionogel electrolytes, ESs such as flexible ESs,<sup>400</sup> stretchable ESs,<sup>403</sup> micro-ESs,<sup>398</sup> and stretchable micro-ESs<sup>404</sup> were developed.

The properties (e.g., conductivity and ESPW) of an ionogel depend on the nature of the IL and the host polymer, as well as their interaction. Liew et al.<sup>405</sup> found that with the incorporation of [BMIM][Cl] IL, the glass transition temperature ( $T_g$ ) of PVA-based polymer electrolytes could be decreased down to the sub-ambient temperature range. Regarding the IL as the solvent, the selection or design of an appropriate host polymer should be crucial for achieving high ES performance of the IL-based GPE. Currently, the variety of host polymers studied for ionogel electrolytes include PVA,<sup>405</sup> PEO,<sup>406</sup> PMMA,<sup>403</sup> poly(ethylene glycol) diacrylate,<sup>404</sup> and PVDF-HFP.<sup>399, 400, 407</sup> Using PMMA as a polymeric host, Tamilarasan et al.<sup>403</sup> prepared a highly transparent and stretchable PMMA/[BMIM][TFSI] ionogel with at least four-fold stretchability. The assembled PMMA/[BMIM][TFSI]-based EDLC with graphene electrodes showed a specific capacitance of 83 F g<sup>-1</sup>, and energy density of 26.1 Wh kg<sup>-1</sup> at a power density of 5 kW kg<sup>-1</sup> (in terms of mass of total electrode material). In addition, a positive effect of the Chitosan host on the performance of ionogel-based EDLCs was reported by Yamagata et al.<sup>408</sup>

Due to the high chemical and thermal stabilities as well as high flexibility of PVDF, it was used as the host for the [BMIM][BF<sub>4</sub>] IL solvent to form an ionogel for flexible ESs by Yang et al.<sup>409</sup> They blended amorphous polyvinyl acetate (PVAc) with PVDF as polymeric matrix, and the resulting ionogel containing PVDF-PVAc host and 50 wt.% of [BMIM][BF<sub>4</sub>] exhibited good flexibility, high thermal stability (~300 °C), and also had an ionic conductivity of  $2.42 \times 10^{-3}$  S cm<sup>-1</sup> at room temperature. AC-based EDLCs using this ionogel electrolyte could be operated at a cell voltage of 3 V, with a specific capacitance of 93.3 F g<sup>-1</sup> (in terms of the mass of AC) at 200 mA g<sup>-1</sup>, and the capacitance retained was more than 90% after 5000 charge/discharge cycles.

Since the properties of ILs have a great influence on ES performance, it is important to properly select and design the IL component in an IL-based polymer electrolyte. To overcome the high viscosity issue with common ILs, some low viscosity ILs such as [EMIM][SCN]<sup>410</sup> and [EMIM][TCB]<sup>399</sup> were explored. However, EDLCs using these ionogel electrolytes could only give some low specific energy densities such as ~3.5–4.7 Wh kg<sup>-1</sup> due to the limited cell voltage.<sup>399, 410</sup> Pandey et al.<sup>411</sup> demonstrated the addition of Li-salt into the PVDF-HFP/[EMIM][FAP] GPE could markedly improve the specific capacitance of CNT-based EDLCs from about 76 F g<sup>-1</sup> (without Li-salt) to about 127 F g<sup>-1</sup>. Ketabi et al.<sup>406</sup> found the addition of 10wt.% SiO<sub>2</sub> into PEO/EMIHSO<sub>4</sub> could increase the ionic conductivity of the electrolyte from 0.85 (without SiO<sub>2</sub>) to 2.15 mS cm<sup>-1</sup> at room temperature. The obtained EDLC showed a good capacitive behaviour after 5000 cycles at a relatively

high scan rate of  $1 \text{ V s}^{-1}$ . In addition, incorporating plastic crystalline materials (e.g., succinonitrile (SN)) into IL-based GPEs were also studied by Suleman et al.<sup>407</sup> in the effort to increase the mechanical stability of the electrolyte.

Preparation methods seem to play an important role in ES performance of IL-based GPEs.<sup>412</sup> For example, Liu et al.<sup>412</sup> described a self-triggered UV photopolymerization method to prepare ionogel electrolytes made from [BMIM][Cl], chitosan and HEMA, during which, initiators and crosslinkers were not needed. AC-based EDLCs with this ionogel electrolyte could be operated well at a high temperature of  $100 \text{ }^\circ\text{C}$ , with a good performance stability for 2000 cycles at  $0.5 \text{ A g}^{-1}$  under normal and bent conditions. Interestingly, such ionogel electrolytes not only exhibited a high mechanical strength but also possessed a self-recovering ability, induced by the crosslinking interaction via hydrogen bonds.<sup>412</sup>

Some IL-based solid-state electrolytes composed of new polymeric ILs were also explored for ESs.<sup>397, 413</sup> For example, Ayalneh Tiruye et al.<sup>397</sup> studied a binary blend of polymeric IL, i.e., poly(diallyldimethylammonium) bis(trifluoromethanesulfonyl)imide ([pDADMA][TFSI]) and [PYR<sub>14</sub>][TFSI] (4:6 by mass ratio) and used as the solvent. This pyrrolidinium-based IL had a wide ESPW when compared with imidazolium-based IL. The AC-based EDLC with this ionogel electrolyte could be operated at a large cell voltage up to  $3.5 \text{ V}$ , and consequently delivering high specific capacitance of  $32 \text{ Wh kg}^{-1}$ .

#### 3.4.1.4. Environmentally friendly gel polymer electrolytes

Considering the environmental impact, the use of environmentally friendly materials from renewable nature sources (e.g., corn starch<sup>414</sup> and chitosan<sup>332, 415</sup>) or biodegradable materials (e.g., poly(epsilon-caprolactone)<sup>416</sup>) as polymer hosts for solid-state electrolytes has also been received increasing attention. However, natural polymers such as starch film generally suffer from low mechanical properties. To improve the mechanical property of natural polymers, blended materials such as a blend of chitosan and starch,<sup>415</sup> and a blend of chitosan and PEG<sup>332</sup>, were developed.

#### 3.4.1.5. Structural electrolytes

For application of solid-state ESs in some vibration devices such as electric vehicles), developing load-bearing solid-state electrolytes (also called structural electrolytes) has attracted attention.<sup>417, 418</sup> For example, Shirshova et al.<sup>417</sup> prepared some IL-epoxy resin composites as structural electrolytes for ESs. The morphology, ionic conductivity and mechanical properties of these kinds of electrolytes were found to be dependent on the weight ratio between the IL and the epoxy resin. The optimized electrolyte (30 wt.% of resin and 70 wt.% of IL) can provide a room temperature ionic conductivity of  $0.8 \text{ mS cm}^{-1}$  and a Young's modulus of  $0.2 \text{ GPa}$ .

### 3.4.2. Inorganic solid-state electrolytes

Some studies have been devoted to the development of inorganic solid-state electrolytes for ESs,<sup>324, 325, 419</sup> although they receive much less attention when compared to the polymer-based solid-state electrolytes. In general, this kind of inorganic solid-state electrolyte is not bendable and has almost no flexibility. However, they are generally mechanically robust and thermally stable. Francisco et al.<sup>324</sup> reported the use of a  $\text{Li}_2\text{S}-\text{P}_2\text{S}_5$  glass-ceramic electrolyte as both the ion conductor and separator for all-solid-state ESs. This electrolyte was found to have a relatively high Li-ion conductivity. CNTs were also incorporated into the electrode to improve the interfacial contact between the solid-state electrolyte and the electrode material. As a result, the assembled ES exhibited a specific capacitance of nearly  $10 \text{ F g}^{-1}$ . Ulihin et al.<sup>325</sup> presented a composite  $\text{LiClO}_4\text{-Al}_2\text{O}_3$  solid electrolyte (4:6 ratio of  $\text{LiClO}_4\text{-Al}_2\text{O}_3$ ) for both symmetric and asymmetric ESs. The active electrode materials were based on the mixtures of manganese oxides and lithium–manganese–nickel spinel. It should be noted that the fabricated ESs could be operated at high temperatures in a range of  $150\text{--}200 \text{ }^\circ\text{C}$ . However, the specific capacitance was low ( $29 \text{ F g}^{-1}$  at  $0.05 \text{ A g}^{-1}$  under  $150 \text{ }^\circ\text{C}$ ). GO have also been reported as a solid electrolyte for ESs.<sup>419, 420</sup> Interestingly, Zhang et al.<sup>419</sup> studied an all-solid-state sandwiched RGO//GO//RGO supercapacitor with a layering structure. This ES exhibited a fairly high specific capacitance (up to  $\sim 0.86 \text{ mF cm}^{-2}$ ).

### 3.5. Redox-active electrolytes

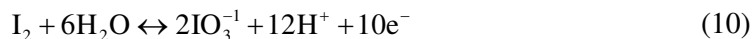
Recently, a new strategy has been explored to increase the capacitance of ES by inducing the pseudocapacitive contribution from the redox-active electrolytes. The Faradaic reactions occur in the electrolyte, which can contribute extra capacitance to the ESs.<sup>13, 421</sup> In this case, the pseudocapacitance is not only contributed by the pseudocapacitive electrode materials but can also be contributed from the electrolyte (i.e., from the reduction/oxidation of the redox mediator in the electrolyte).

#### 3.5.1 Redox-active aqueous electrolytes

##### 3.5.1.1. Redox-active aqueous electrolytes for carbon-based ESs

One typical example is an iodide/iodine redox pair, which is used for the redox-active aqueous electrolyte for carbon-based ESs by Lota et al.<sup>13</sup> The maximum capacitance of the carbon positive electrode in  $1 \text{ M KI}$  electrolyte could reach to an extremely high value of  $1840 \text{ F g}^{-1}$ , due to the pseudocapacitive capacitance

contribution from the electrolyte based on the following reactions:<sup>13</sup>



However, such a high capacitance value was observed only at the positive electrode within a very narrow potential range (Fig. 28). Two-electrode cell using KI electrolyte showed a specific capacitance of 125 F g<sup>-1</sup> at 50 A g<sup>-1</sup>.

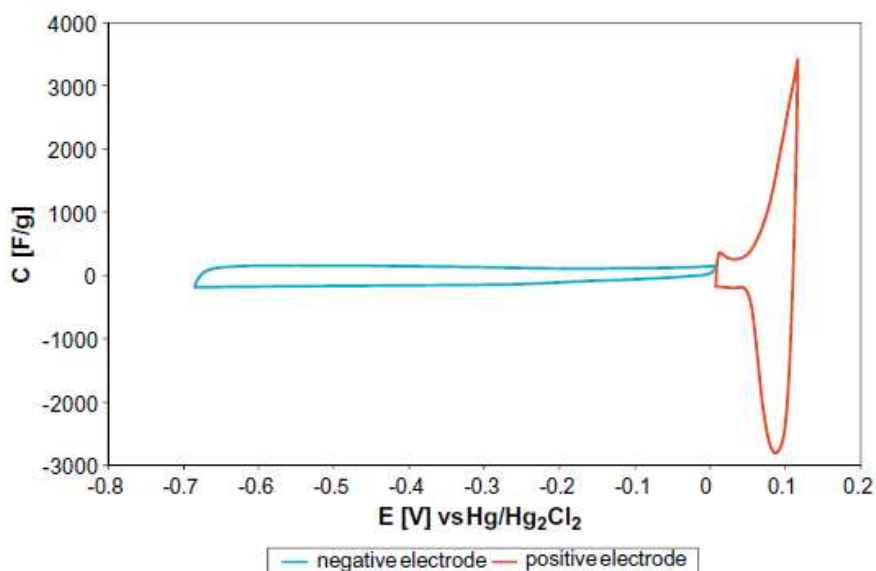
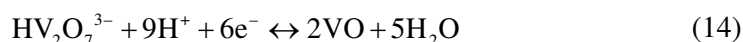
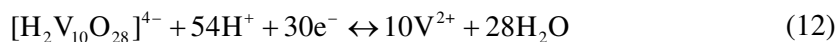


Fig. 28 Voltammetry curve at 5 mV s<sup>-1</sup> scan rate for AC-carbon electrode in 1 mol L<sup>-1</sup> KI solution. Potentials of both electrodes are measured separately vs. a saturated calomel electrode. Reprinted from Ref. 13, with permission from Elsevier.

In these reactions (Reactions (7)–(10)), the type of the alkali metal counter-ion of the iodides was found to play a significant role in the capacitive behaviour of the electrode.<sup>422</sup> The capacitance of the positive electrode was decreased with a decreasing van der Waals radius of alkali metal, following in the order of: RbI (2272 F g<sup>-1</sup>) > KI (1078 F g<sup>-1</sup>) > NaI (492 F g<sup>-1</sup>) > LiI (300 F g<sup>-1</sup>) (all with 1 M concentration).<sup>422</sup>

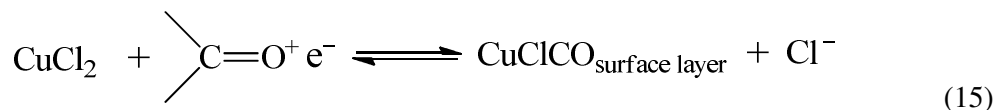
Since the total capacitance of an ES is largely dominated by the electrode with low capacitance, the low capacitance of the negative electrode in the iodides-based electrolyte should be the limitation. In order to increase the total capacitance, Frackowiak et al.<sup>423</sup> used 1 M KI aqueous electrolyte for the positive electrode and 1 M VOSO<sub>4</sub> for the negative electrode. The Faradaic reactions (Equations (11)–(14))

can occur at the negative electrode in  $\text{VOSO}_4$  electrolyte, making a high pseudocapacitance contribution to the negative electrode.<sup>423</sup>



To avoid the mixing of electroactive species in the cell, the assembled AC-based ES used a glassy paper and a Nafion<sup>®</sup> 117 membrane to separate two different electrolytes. This EDLC could deliver a high capacitance of  $500 \text{ F g}^{-1}$  at  $0.5 \text{ A g}^{-1}$  with a cell voltage of  $1 \text{ V}$ , and also exhibited an energy density of  $20 \text{ Wh kg}^{-1}$  with a maximum power density of  $2 \text{ kW kg}^{-1}$ .

Heteropoly acids, such as phosphotungstic acid (PWA) and silicotungstic acid (SiWA), were explored as the redox mediators for redox-active electrolytes. These acids could give high proton conductivities and also multiple rapid electron transfer redox processes.<sup>424-426</sup> Suarez-Guevara et al.<sup>424</sup> found the use of phosphotungstic acid ( $\text{H}_3\text{PW}_{12}\text{O}_{40}$ ,  $\text{PW}_{12}$ ) as the electrolyte for AC-based ESs could not only provide pseudocapacitance from the electrolyte but also increase the operative cell voltage to  $1.6 \text{ V}$  due to  $\text{PW}_{12}$ 's high overpotential towards  $\text{H}_2$  evolution. Redox-active electrolytes based on redox pair of metal ions were also investigated for ESs.<sup>427, 428</sup> For example, Mai et al.<sup>427</sup> used  $\text{Cu}^{2+}$  reduction by the surface oxygen group on the carbon electrode to enhance the specific capacitance. Electrochemical measurements showed the electrode capacitance could be increased by about 10 times more in  $0.09 \text{ M CuCl}_2 + 1 \text{ M HNO}_3$  electrolyte than the conventional  $1 \text{ M H}_2\text{SO}_4$  electrolyte. This was attributed to the pseudocapacitive contribution from the following reaction:<sup>427</sup>



It should be noted that when using such electrolytes (i.e., containing metal ions), the ES self-discharge may be an issue, as mentioned in section 3.1.1.

In addition, there have been considerable studies focused on the organic redox mediators as pseudocapacitive sources, including hydroquinone (HQ),<sup>429, 430</sup> methylene blue (MB),<sup>431</sup> indigo carmine (IC),<sup>432</sup> *p*-phenylenediamine (PPD),<sup>433</sup> *m*-phenylenediamine (MPD),<sup>434</sup> lignosulfonates,<sup>435</sup> sulfonated polyaniline (SPANi)<sup>436</sup> as well as humic acids.<sup>437</sup> **Error! Reference source not found.** shows some typical redox-active aqueous electrolytes containing organic redox-active molecules, the corresponding redox processes, and their corresponding ES performance. In general, the addition of these organic redox additives can greatly increase the specific capacitance value of the carbon-based ESs by about 2–4 times.

Table 6 Some typical redox couples from selected literature related to the redox active electrolyte-based ESs

Redox mediator	Redox reactions	Supporting electrolyte	Capacitance without redox mediator (F g <sup>-1</sup> )	Capacitance with redox mediator (F g <sup>-1</sup> )	Cycling stability	Ref.
HQ		1 M H <sub>2</sub> SO <sub>4</sub>	72 (at 2.65 mA cm <sup>-2</sup> )	220 (at 2.65 mA cm <sup>-2</sup> )	–	429
IC		1 M H <sub>2</sub> SO <sub>4</sub>	17 (at 41 mA g <sup>-1</sup> )	50 (at 41 mA g <sup>-1</sup> )	70% capacitance retention after 10,000 cycles	432
MB		1 M H <sub>2</sub> SO <sub>4</sub>	5	23	88% capacitance retention after 6000 cycles	431
SPAni		4 M H <sub>2</sub> SO <sub>4</sub>	47.5 (at 5.22 A g <sup>-1</sup> )	57 (at 5.22 A g <sup>-1</sup> )	99% capacitance retention after 1000 cycles	436
PPD		2 M KOH	144.037 (at 1 A g <sup>-1</sup> ) (electrode capacitance)	605.225 (at 1 A g <sup>-1</sup> ) (electrode capacitance)	94.53% capacitance retention after 4000 cycles	433
MPD		2 M KOH	36.43 (at 0.5 A g <sup>-1</sup> )	78.01 (at 0.5 A g <sup>-1</sup> )	90.68% capacitance retention after 10,000 cycles	434

It should be noted that ESs using a HQ-based redox-active electrolyte showed a much faster self-discharge process.<sup>430</sup> Chen et al.<sup>430</sup> revealed the main reason for this faster self-discharge was the migration of redox-active electrolyte between two electrodes. To inhibit the migration of redox-active electrolyte and thus to decrease the self-discharge, two strategies were tested, one was to use an ion-exchange

membrane (e.g., Nafion<sup>®</sup>) as the separator, and the other was to choose a redox-active electrolyte that could be reversibly converted into insoluble species during the charging/discharging process.

### 3.5.1.2. Redox-active aqueous electrolytes for pseudocapacitive electrodes

Redox-active electrolytes have also been used for pseudocapacitors, asymmetric ESs and hybrid ESs. The pseudocapacitive electrode materials were RuO<sub>2</sub>,<sup>425, 426</sup> MnO<sub>2</sub>,<sup>97, 438</sup> Co(OH)<sub>2</sub>,<sup>439</sup> Bi<sub>2</sub>O<sub>3</sub>,<sup>440</sup> ECPs,<sup>441</sup> and so on. A wide variety of redox-active electrolytes, such as KI,<sup>440</sup> heteropoly acids,<sup>426</sup> HQ,<sup>441</sup> PPD,<sup>97</sup> and K<sub>3</sub>Fe(CN)<sub>6</sub>,<sup>438, 439</sup> were used to make the redox-active electrolytes. Similar to the results reported for carbon-based ESs, the addition of a redox mediator to the electrolyte could significantly increase the specific capacitance and thereby the energy and power densities of the pseudocapacitive ESs. Regarding the cycling stability, several studies found the redox-active electrolytes could lead to similar or poorer cycling stabilities especially during the initial cycles<sup>441, 442</sup> when compared to the conventional aqueous electrolytes without redox mediators. It is interesting to note that besides the increase in specific capacitance directly contributed to the pseudocapacitance of a redox-active electrolyte, the presence of the redox mediators could also speed up the relatively slow process of faradic reactions of pseudocapacitive electrode materials by providing the electron buffer source.<sup>438, 439</sup>

### 3.5.3. Redox-active non-aqueous electrolytes

To achieve higher cell voltage and thus a higher energy density, a number of non-aqueous electrolytes including organic and IL-based electrolytes<sup>443-446</sup> have been studied and reported in the literature. For example, Ionica-Bousquet et al.<sup>443</sup> found the introduction of a redox-active polyfluorododecaborate cluster ions (i.e., [B<sub>12</sub>F<sub>x</sub>H<sub>12-x</sub>]<sup>2-</sup>) into an organic PC-DMC mixture solvent could effectively contribute the additional pseudocapacitance to the total capacitance of the carbon-based ESs. Compared to the TEABF<sub>4</sub>/PC-DMC organic electrolyte, tetraethylammonium undecafluorododecaborate, (Et<sub>4</sub>N)<sub>2</sub>B<sub>12</sub>F<sub>11</sub>H/PC-DMC electrolyte was also able to provide overcharge protection of ESs due to the presence of redox-active anions. Regarding IL-based electrolytes, Tooming et al.<sup>445</sup> demonstrated the addition of 5 wt.% 1-ethyl-3-methylimidazolium iodide ([EMIM][I]) into [EMIM][BF<sub>4</sub>] IL could result in a nearly 50% increase in ES' specific capacitance when compared to a bare [EMIM][BF<sub>4</sub>] IL electrolyte. A very large increased specific energy density of 36.7 Wh kg<sup>-1</sup> was achieved for the ES using 5 wt.% [EMIM][I] + [EMIM][BF<sub>4</sub>] electrolyte. Taniki et al.<sup>444</sup> reported the N-ethyl-N-methylpyrrolidinium fluorohydrogenate (EMPy<sub>r</sub>(FH)<sub>2.3</sub>F) IL electrolyte could significantly contribute extra specific capacitance to the ES through the redox reaction of the electrolyte.



### 3.5.4. Redox-active solid electrolytes

The strategy of using a redox-mediator has also been tested in solid- or quasi-solid-state electrolytes-based ESs, and some enhanced performances were observed. In this regard, typically investigated redox additives in the solid-state electrolytes were iodides (e.g., NaI<sup>447, 448</sup> and KI<sup>327</sup>), K<sub>3</sub>Fe(CN)<sub>6</sub>,<sup>449</sup> Na<sub>2</sub>MoO<sub>4</sub>,<sup>450</sup> organic redox mediators (e.g., hydroquinone,<sup>451</sup> PPD,<sup>452</sup> p-benzenediol<sup>453</sup> and MB<sup>454</sup>), mixture of redox additives (e.g., KI-VOSO<sub>4</sub><sup>327</sup>), and so on. Actually, these redox mediators are almost the same as those used in the liquid electrolytes. Regarding the polymer hosts, the majority of the solid-state electrolytes studied were focused on the GPEs with polymer hosts such as PVA,<sup>327, 450-454</sup> PEO,<sup>448, 449, 455</sup> and Nafion<sup>®</sup>.<sup>447, 456</sup> Since these redox mediators are normally dissolved in the liquid phase of the GPE, their effect and the working principle are generally quite similar to those in aqueous or organic electrolytes. For example, these redox-active GPEs showed a much higher ES specific capacitance than those GPEs without redox mediators. Fan et al.<sup>327</sup> reported an AC-based ES using KI-VOSO<sub>4</sub>-containing PVA/H<sub>2</sub>SO<sub>4</sub> GPE could exhibit a high specific capacitance of 1232.8 F g<sup>-1</sup> and an energy density of 25.4 W h kg<sup>-1</sup>, which were nearly eight times higher than that of the ES without KI-VOSO<sub>4</sub>. The GPE using mixtures of redox mediators were also found to have higher energy densities than the GPE using a single redox additive (Fig. 29).

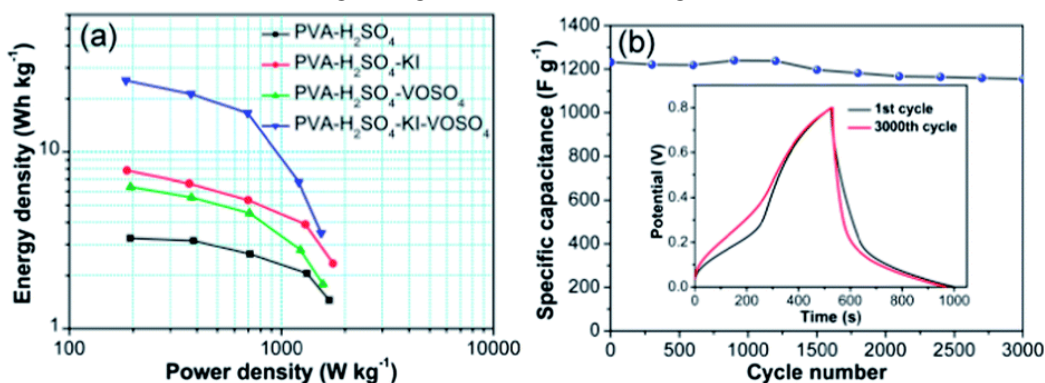


Fig. 29 (a) Ragone plots of EDLCs with PVA-H<sub>2</sub>SO<sub>4</sub>, PVA-H<sub>2</sub>SO<sub>4</sub>-KI, PVA-H<sub>2</sub>SO<sub>4</sub>-VOSO<sub>4</sub> and PVA-H<sub>2</sub>SO<sub>4</sub>-KI-VOSO<sub>4</sub> GPEs. (b) Cyclic performance of EDLC with PVA-H<sub>2</sub>SO<sub>4</sub>-KI-VOSO<sub>4</sub> GPE at a current density of 0.5 A g<sup>-1</sup>; the inset shows the GCD curves of the EDLC at the 1<sup>st</sup> and 3000<sup>th</sup> cycles. Reproduced from Ref. 327 with permission of The Royal Society of Chemistry.

To increase the operation cell voltage, Zhou et al.<sup>456</sup> used PEO/LiClO<sub>4</sub>-ACN organogel as the electrolyte for the ESs and investigated two types of redox mediators --NaI/I<sub>2</sub> and K<sub>3</sub>Fe(CN)<sub>6</sub>/K<sub>4</sub>Fe(CN)<sub>6</sub>. ESs containing NaI/I<sub>2</sub> and K<sub>3</sub>Fe(CN)<sub>6</sub>/K<sub>4</sub>Fe(CN)<sub>6</sub> could deliver specific energy densities of 49.1 Wh kg<sup>-1</sup> at 1.6 kW kg<sup>-1</sup> and 33.6 Wh kg<sup>-1</sup> at 1.3 kW kg<sup>-1</sup>, respectively. This indicated the enhancement effect of the NaI/I<sub>2</sub> mediator was more pronounced than the K<sub>3</sub>Fe(CN)<sub>6</sub>/K<sub>4</sub>Fe(CN)<sub>6</sub> mediator in this study. Furthermore, the introduction of a redox mediator into the GPE can also significantly

increase the ionic conductivity, especially for the GPE with a conducting salt dissolved in an organic solvent (e.g., ACN).<sup>447-449, 454</sup>

#### **4. Compatibility (interaction) of the electrolyte with inactive components of electrochemical supercapacitors**

In addition to considering the interaction between the electrolyte and the active electrode materials in ESs, it is also necessary to consider the compatibility or the possible interaction between the electrolyte and the inactive components including current collectors, binder and separator in the development of high-performing ESs. Depending on the type and nature of the electrolyte, inactive components may have a profound influence on both the performance and reliability of the ESs.

##### **4.1. Compatibility with current collectors**

In general, chemical and electrochemical stabilities of the current collector in a certain electrolyte can strongly affect ESs' lifetime and performance (e.g., operating cell voltage). Furthermore, the morphology or structure of the current collector plays an important role in the degree of utilization of the active electrode materials.

When a strong acid electrolyte (e.g., 1 M H<sub>2</sub>SO<sub>4</sub>) is used in ESs, due to its high corrosive nature, some corrosion-resistant metallic materials (e.g., Au) are traditionally used. To reduce the cost of the current collectors, other types of materials, such as indium tin oxide (ITO),<sup>457</sup> carbon-based materials<sup>458</sup> and ECPs,<sup>459</sup> have been investigated for ES current collectors using strong acid electrolyte. Free-standing electrodes (e.g., carbon-based composite paper) have also been developed for ESs, which have the advantage of avoiding the use of additional current collectors.<sup>460</sup> These newly developed current collectors (above) may have other benefits as well. For example, due to its high transparency, the ITO-based current collector is beneficial to the development of transparent ESs.<sup>457</sup> The use of carbon-based or ECP-based current collectors is particularly favorable for use in the flexible ESs.<sup>459</sup>

For alkaline electrolyte-based ESs, Ni current collectors are commonly used due to its relatively low cost, and good chemical and electrochemical stability in alkaline electrolytes.<sup>461</sup> To increase the surface area and the utilization of the active electrode materials, the Ni current collectors are often in the form of Ni foam.<sup>461</sup> Furthermore, the use of Ni foam as a current collector may have an additional pseudocapacitive contribution to the total capacitance due to the presence of Ni hydroxide/oxide on the Ni foam--especially when the amount of electrode material is small.<sup>462</sup> Other metallic materials, such as stainless steel<sup>463</sup> and Inconel 600 (a Ni-based alloy)<sup>464</sup> were also investigated as current collectors for alkaline electrolyte-based ESs. Carbonaceous materials, due to their light weight, good conductivity, high flexibility and good

mechanical strength, have attracted growing attention recently. These carbonaceous materials include carbon fabric,<sup>465</sup> CNT,<sup>466</sup> carbon cloth,<sup>467</sup> carbon fiber paper,<sup>468</sup> ultrathin-graphite foam,<sup>469</sup> and so on.

Due to their much less corrosive nature, neutral aqueous electrolytes can give more choice of ES current collectors. As a result, a wide variety of materials have been used for current collectors. These materials include Ni,<sup>470</sup> Ti,<sup>471</sup> stainless steel,<sup>110, 111</sup> titanium oxynitride,<sup>472</sup> ITO,<sup>473</sup> modified TiO<sub>2</sub>,<sup>474</sup> CNT,<sup>475</sup> and so on. Wang et al.<sup>126</sup> demonstrated the current-collection property of Ni foam was better than that of a Ti mesh in a 1 M LiAc–1 M MgSO<sub>4</sub> mixed electrolyte.

In the case of organic electrolyte-based ESs, the majority of the studies use Al as the current collector.<sup>151, 476</sup> Previous study found the aging of organic electrolyte-based ES also involved the degradation of Al current collectors.<sup>476</sup> Vali et al.<sup>151</sup> reported the type of conducting salt could greatly affect the electrochemical stability of Al current collectors in an organic solvent. The oxidation of an Al current collector in a NaFSI-based electrolyte was observed. This condition could lead, in turn, to a much lower electrochemical stability when compared to both NaPF<sub>6</sub>- and NaClO<sub>4</sub>-based electrolytes. This condition was indicated by an associated lower cell voltage of 2.5 V compared to those of 3.4 V and 3.2 V for NaPF<sub>6</sub> and NaClO<sub>4</sub> electrolytes, respectively.

With the development of new electrolytes such as IL and redox-active electrolytes, their compatibility with the ES current collectors should be given more attention. Regarding the IL electrolytes, Kühnel et al.<sup>477, 478</sup> investigated the anodic stability of some Al current collectors in [PYR<sub>14</sub>][FSI], [PYR<sub>14</sub>][TFSI] and [PYR<sub>14</sub>][FTFSI] IL electrolytes. It was found Al could be slowly corroded in [FSI]-based [PYR<sub>14</sub>][FSI] IL while it was much better passivated in [TFSI]-based [PYR<sub>14</sub>][TFSI] IL.<sup>478</sup> The same group<sup>477</sup> also found Al current collectors showed excellent anodic corrosion stability in [PYR<sub>14</sub>][TFSI] IL. Brandt et al.<sup>314</sup> reported the possible anodic oxidation of Al current collectors could strongly affect the operation cell voltage of EDLCs when IL-organic electrolyte mixtures (i.e., [Me<sub>3</sub>S][TFSI]-PC) were used.

Regarding the redox-active electrolytes, Meller et al.<sup>479</sup> reported an Au current collector was not suitable for iodide electrolytes due to its reactivity with iodides while stainless steel was a suitable material showing good long-term stability. When solid- or quasi solid-state electrolytes are used for ESs, the matching between the electrolyte and the current collector should be optimized with respect to the ES performance. Additional factors needing to be considered in connection with current collectors, include: flexibility, stretchability and transparency.

In order to avoid potential issues related to current collectors and to simplify the fabrication process, some studies have also focused on the development of free-standing electrodes (commonly carbon-based materials) without the use of current collectors.<sup>480</sup>

## 4.2. Binders

Binders are used for the fabrication of electrode layers composed of active material particles or powders such as AC powders, which hold up the structural integrity of the layer and also provide good adhesion between active particles and the current collector. Currently, the commonly used ES binder materials are fluorinated polymeric ones such as poly(vinylidene fluoride) (PVDF) and polytetrafluoroethylene (PTFE). As generally observed, the performance of electrodes and their associated ESs can be strongly affected by the property and content of the binders.<sup>52, 112, 481</sup> For example, due to the hydrophobic nature of PTFE, too much PTFE in an ES electrode layer would make the electrode layer too hydrophobic, resulting in a difficulty for electrolyte penetration if an aqueous electrolyte is used.<sup>112</sup> Therefore, it is important to optimize the binder content in the electrodes.<sup>112</sup> Paul et al.<sup>482</sup> found the addition of a small amount of PVP (3%) into PTFE binder could significantly increase the wettability of the electrode materials in an aqueous electrolyte. Timperman et al.<sup>279</sup> compared the effects of two different binders on an AC electrode layer. These two binders were PVDF and carboxymethyl cellulose–styrene-Butadiene Rubber (CMC–SBR). They found the wettability of [DIPEA][TFSI] IL electrolyte was higher on PVDF-containing electrodes than on CMC–SBR electrodes while similar wettability was found for both electrodes in the [Pyr][TFSI] IL electrolyte. This difference in electrolyte wettabilities could lead to a difference in electrochemical performance of the electrodes. Liu et al.<sup>483</sup> found the use of Nafion<sup>®</sup> as a binder was beneficial for increasing the power density of a RuO<sub>2</sub> powder-based pseudocapacitor, probably due to its high proton conducting ability. Cao et al.<sup>481</sup> reported the type of the binder could also affect the performance of LIC using LiPF<sub>6</sub>/EC-DMC electrolyte. The use of PTFE as a binder in a negative electrode layer was found to have a beneficial effect in achieving higher energy and power performance when compared to PVDF binder.<sup>481</sup>

To reduce the environmental concern, growing interest has been focused on the development of environmentally friendly (e.g., fluorine-free) binders. Various materials, such as PVP,<sup>484</sup> polyacrylic acid (PAA),<sup>485</sup> and natural cellulose<sup>486</sup> were tested as alternative binders for ES electrode layers. In addition, some ECPs, such as PPy,<sup>487</sup> PEDOT,<sup>488</sup> and PANI,<sup>489</sup> were also explored as the binders for electrode materials. These binders are normally electrically conductive, which are different from the conventional binders (e.g., PVDF and PTFE) which are electrically insulating. Moreover, they can contribute additional pseudocapacitance to the electrode capacitance.

In addition, some work has been devoted to the development of binder-free electrode materials in the literature.<sup>427</sup> If this approach is feasible, some negative effects related to the use of binders, such as an increase in electrode resistance and a reduction of specific surface area, may be avoided.

### 4.3. Separators

The separator is located between the two electrodes in an ES cell to prevent the contact and electron transfer between the negative and positive electrodes. There are several critical requirements for the separators such as: (1) having a minimal resistance for ion transfer within the electrolyte while having a strong electronic insulating capability; (2) having both high chemical and electrochemical stabilities in electrolyte; and (3) having good mechanical strength to provide device durability. Based on these requirements, ES separators are usually made from thin and highly porous film or membrane. Commonly used separator materials are cellulose, polymer membrane and glass fibre. As generally realized, the choice of separator materials depends on the type of electrode, working temperature and ES cell voltage. Although cellulose separators can operate well in organic solvents,<sup>476</sup> they may suffer from degradation in a H<sub>2</sub>SO<sub>4</sub> electrolyte. Bittner et al.<sup>476</sup> found the trace water in the organic electrolyte (TEABF<sub>4</sub>/ACN) could play a role in accelerating the ageing process of EDLCs when a cellulose separator was used. When viscous electrolytes (e.g., IL) were used, the ionic conductivity of the electrolyte in the separator could have a considerable effect on the ES performance through changing the internal resistance (ESR).<sup>490</sup>

Furthermore, the separator's properties such as chemical composition, thickness, porosity, pore size distribution and surface morphology were found to have a noticeable influence on several EDLC performance indicators including polarizability limit, specific capacitance, ESR, characteristic time constant, specific energy and power densities.<sup>490</sup>

In addition to EDLCs, the separator could also affect the performance of pseudocapacitors and hybrid ESs. Liu et al.<sup>491</sup> investigated four different separators for a RuO<sub>2</sub>-based ES with 0.5 M H<sub>2</sub>SO<sub>4</sub> as electrolyte. Among these four separators, Nafion<sup>®</sup> 115 one showed the highest energy density of 31.2 W h kg<sup>-1</sup> at 1 mA cm<sup>-2</sup> while the Celgard<sup>™</sup> separator gave the lowest value of 23.4 W h kg<sup>-1</sup> at the same current density. Cao et al.<sup>481</sup> used a cellulose-based TF40-30 separator for LIC, and found that this separator could give a better discharge capacity retention of LIC than that with Celgard PP 3501 separator. This was probably due to the lower ohmic resistance of cellulose-based TF40-30 separator. When redox-active electrolytes were used for ESs, selecting the appropriate separator could have a positive effect on reducing self-discharge process.<sup>430, 436</sup>

Recently, some new separator materials, such as GO film<sup>492</sup> and eggshell membrane,<sup>493</sup> have been explored for ESs. For instance, Shulga et al.<sup>492</sup> demonstrated that GO film could exhibit a proton conductivity after being permeated with H<sub>2</sub>SO<sub>4</sub> electrolyte, indicating it might be usable as an ES separator.

## 5. Electrolyte performance validation using supercapacitor test cells

Characterizing and validating electrolytes' performance are vital for developing and optimizing their associated ESs. To evaluate the ES performance of an electrolyte, a three-electrode electrochemical cell (Fig. 30A) or two two-electrode cell (Fig. 30B) are commonly used. Some specially designed test cells for evaluating an electrolyte and its associated ES performance have also been fabricated, as shown in Fig. 30(C, D and E) for the sandwiched flexible ES, fiber ES and micro-ES, respectively.

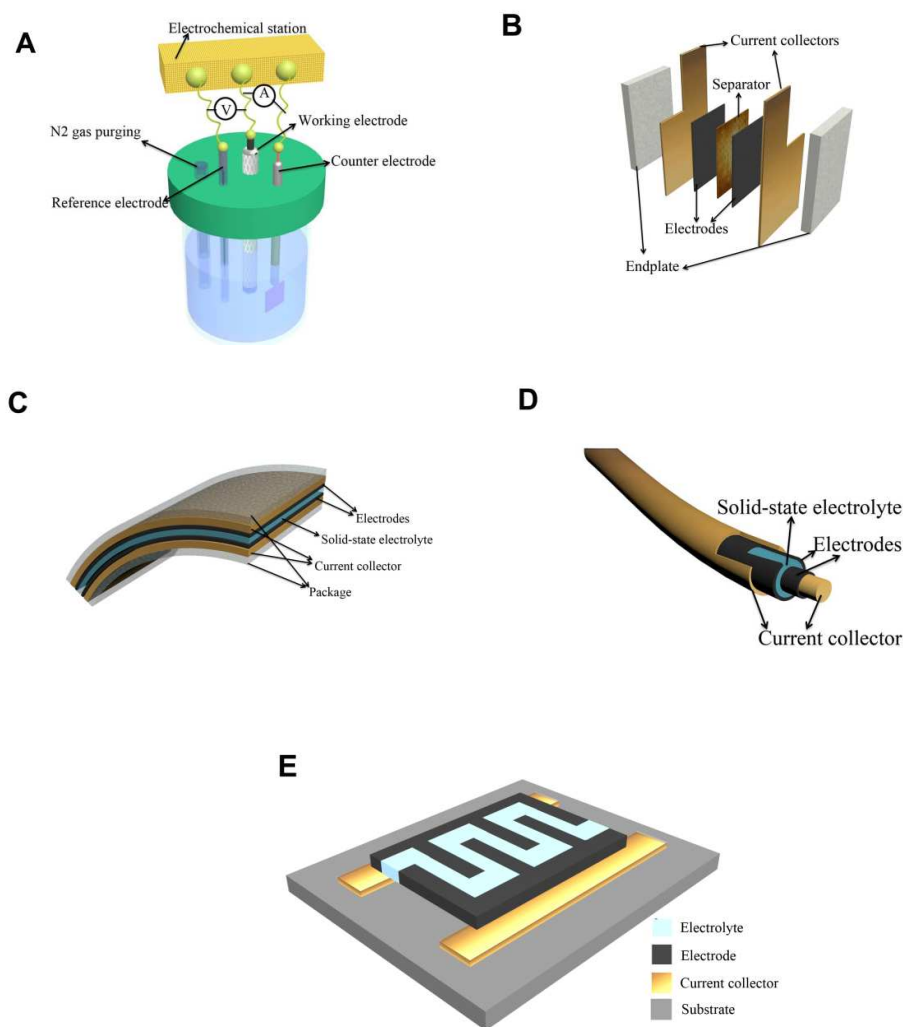


Fig. 30 Schematic diagrams of (A) three-electrode cell, (B) two-electrode cell, (C) sandwiched flexible electrochemical supercapacitor, (D) fiber electrochemical supercapacitor, and (E) micro-electrochemical supercapacitor.

Normally, the three-electrode cell does not require the entire ES assembly. It is

suitable for fast screening and characterizing of electrode materials and electrolytes as well as for probing the fundamental electrochemical processes of the electrolyte and electrode material. The two-electrode cell is closer to the real operating conditions of ESs. Because the specific capacitance of a two-electrode cell is contributed by two capacitive interfaces in series, the capacitance values should be lower than that obtained in a three-electrode cell or half when using a symmetric EDLC.

Several commonly used electrochemical characterization methods such as cyclic voltammetry (CV), galvanostatic charging/discharging (GCD), and electrochemical impedance spectroscopy (EIS) have been widely used to characterize, test and diagnose ES performance in the presence of a targeted electrolyte.<sup>494-496</sup> With the help of these electrochemical techniques, a series of important parameters of ESs, such as capacitance, ESR, energy and power densities, as well as cycle-life, can be measured so the understanding of ES performance of the related electrolyte can be realized. It should be noted that the testing conditions, such as cell configuration, potential (voltage) scan rate in CV, current density in GCD, and voltage range, can affect the measured results (e.g., specific capacitance) of the cell. The specific capacitance achieved at a lower scan rate or current density is commonly higher than that obtained at a higher scan rate or current density. Therefore, to compare the performances of different electrolytes and their associated ESs, the measurement and cell conditions should be controlled at as close to the same conditions as possible.

Due to the determining role of electrolyte's ESPW in ES performance such as both energy and power densities, it is essential to develop accurate quantification methods to measure the ESPW value of the electrolyte being tested. The conventional method of determining the ESPW value is based on the measurement of the electrolyte's cathodic reduction and anodic oxidation limits by linear sweep voltammetry on the smooth working electrode, such as Pt and GC.<sup>26,209,497</sup> As shown in Fig. 31(a), the oxidative and reductive decomposition of an electrolyte can lead to an abrupt increase of the current densities.<sup>497</sup> The applied negative and positive potentials at which the current densities reach critical values are generally defined as the anodic and cathodic limits of the ESPW. It can be seen that the definition of these limits seems to be somewhat arbitrary, which could bring about some uncertainty for the comparison of ESPW values among different electrolytes. Olson et al.<sup>498</sup> demonstrated a method for defining the ESPW limits that seemed to depend less on experimental parameters, allowing more meaningful comparison of data from different investigators. This method involved linear fits in two approximately linear ranges of the current–potential curve. Actually, the electrodes exposed to the electrolyte in ESs are often highly porous, which can give a much larger capacitive current response than that of non-porous electrodes (Fig. 31(b)). Therefore, several studies were devoted to the development of an ESPW determination method for porous electrodes used in ESs.<sup>497,499</sup> For example, Xu et al.<sup>497</sup> reported an improved ESPW quantification method for porous electrodes. In their study, the Faradaic (related to electrolyte decomposition) and capacitive current were isolated.

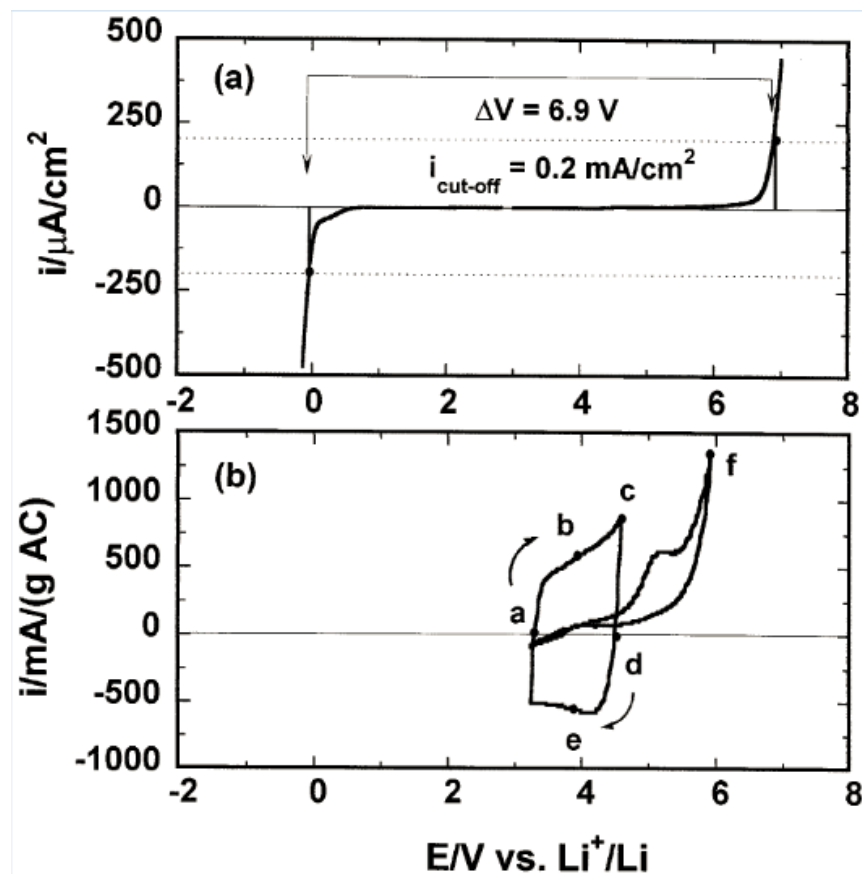


Fig. 31 (a) Cyclic voltammetry and conventional determination of stability limits of a popular non-aqueous electrolyte for a double layer capacitor: 1.0 M  $\text{Et}_3\text{MeNPF}_6$  in EC/DMC (1:1 by wt.) on a non-porous working electrode GC. (b) Cyclic voltammetry of the same electrolyte when a porous composite based on M30 activated carbon (95% with 5% PVDF) is used as the working electrode. Scan rate: 5 mV/s; Li as reference and Pt as counter electrodes. Successive scans were conducted with an interval of 0.25 V between their cut-off potential limits (only sixth and tenth scans are shown). Reprinted from Ref. 497, with permission from Elsevier.

Besides the electrochemical methods, other instrumental techniques such as FTIR and NMR,<sup>176</sup> have also been employed to characterize the properties of electrolytes. In some cases, the cells need to be specially designed to meet the requirements of these experiments.<sup>176</sup> Application of these techniques for investigating the electrolyte has already been discussed in section 3 for specific electrolytes.

## 6. Challenges of electrochemical supercapacitor electrolytes

Enlarging the energy/power densities and enhancing the durability (cycle-life) of electrochemical supercapacitors (ESs) including EDLCs, pseudocapacitors and hybrid capacitors are always a major effort in ES development. Electrolytes have been identified as one of the keys determining components in ES performance. Their



values of ESPW and ionic conductivity, chemical and thermal stabilities, as well as the operating temperature range, have significant effects on both ES performance and practical applications. Although great progress has been made in the field of ES electrolytes, there are still a number of major challenges, which hinder the maturing of the technology and its commercial applications:

(1) *Insufficient ESPW values and their effect on energy density.* The ES's operating cell voltage is largely determined by the ESPW of the electrolyte, which can affect both the energy and power densities (Equations (4) and (5)). Since the energy density is proportional to the square of the cell voltage, electrolytes with higher ESPW values allow increased cell voltage of the ESs, which can significantly improve the energy density. However, this higher cell voltage often results in the deterioration of other properties of electrolytes. For example, although organic electrolyte-based ESs have much higher cell voltages compared with the aqueous electrolyte-based ones, the ionic conductivities of the organic electrolytes are about one magnitude lower than the aqueous electrolyte ones. Although the use of ILs can further increase the cell voltage of ESs up to 4 V, their ionic conductivities are much lower than those of the organic electrolytes. Similarly, electrolytes with wider ESPWs generally have a lower viscosity. In addition, ESs using organic or IL electrolytes commonly show a smaller specific capacitance value compared to those with aqueous electrolytes. It is, therefore, really a challenge to develop ESs with improved energy densities without sacrificing other advantages such as high power densities and durability.

(2) *High ESR values and their effect on power density.* Organic and IL-based electrolytes are favorable for increasing the energy density of ESs. However, due to their lower ionic conductivities, the ESR of organic electrolyte-based ESs can be a magnitude higher than the aqueous electrolyte-based ones.<sup>171</sup> The ESR values of IL electrolyte-based ESs are even higher because of the low ionic conductivities and high viscosity. As a result, the application of electrolytes with higher ESPWs for ESs often leads to increased ESR values and decreased rate and power performance unless the loss of power density due to the increased ESR can be buffered by an increase of the cell operating voltage.

(3) *Impurities in the electrolyte and their effect on ESPW and self-discharge.* Impurities, especially trace amounts of water, can markedly decrease the ESPW values of organic or IL electrolytes. The self-discharge rate and its mechanism are also very sensitive to impurities and residual gas in the electrolytes. Studies have identified, the self-discharge process can be accelerated by certain amounts of metal ion contamination, water, oxygen and so on in the electrolytes.<sup>80, 81, 191</sup>

(4) *Un-optimized matching between the electrolyte and electrode materials and the effect on overall ES performance.* The close-matching between the electrolyte and electrode materials is very important in achieving high-performance ESs. Compared to the extensive research on maximizing the specific capacitance through the matching between electrolyte ion size and porous structure of carbon materials, relatively few studies have focused on the rate and power performance of ESs resulting from optimizing the matching between electrolytes and electrode materials. Since high power density is one of the key advantages of ESs, the matching to improve specific capacitance should not sacrifice power performance. In addition, some different results have also been found in the relationship between pore size and the surface-area-normalized capacitance.<sup>7, 174, 500, 501</sup> For example, Chmiola et al.<sup>7</sup> and Largeot et al.<sup>500</sup> both reported the specific capacitance can increase significantly when the average pore size of the carbon electrode was close to the electrolyte ion size for

IL and TEABF<sub>4</sub>/ACN organic electrolytes (desolvated ion size in the case of organic solvents). However, Centeno et al.<sup>501</sup> studied 28 porous carbons in TEABF<sub>4</sub>/ACN electrolyte and found the specific capacitance was relatively constant between 0.7 and 15 nm. Furthermore, with the development of various new electrolytes such as electrolytes containing multivalent ions, IL mixture, IL-organic solvent mixture and solid-state electrolytes, the optimization of matching between the electrode materials and these electrolytes does not seem to be receiving sufficient emphasis.

(5) *Unfavourable temperature range for ES operation for different practical applications.* Commonly used organic solvents (e.g., ACN and PC) for ESs have a relatively narrow operating temperature range due to high volatility at high temperatures or low viscosity at low temperatures. Although some new electrolytes such as ADN- and IL-based ones with higher temperature limits have been explored, they have other issues. For example, the salt solubility in ADN solvent is low and most IL-based ESs suffer from poor performance at low temperatures.

(6) *High cost of some electrolytes.* Decreasing the cost of ESs is critical for their commercialization. The cost of state of the art ESs is \$10–20 Wh<sup>-1</sup>, which is significantly higher than LIBs with the cost of only \$1–2 Wh<sup>-1</sup>.<sup>502</sup> Although aqueous electrolytes are inexpensive, they generally give a very limited energy density especially in the case of symmetrical ESs due to the low ESPW values. ESs using organic or IL electrolytes have higher operating cell voltages and thus exhibit higher energy and power densities. However, the use of organic electrolytes, especially ILs, significantly increases the cost of ESs. For example, the price of [EMIM][BF<sub>4</sub>] IL is ~\$1328 kg<sup>-1</sup>, which is much higher than the commercial TEABF<sub>4</sub>/ACN organic electrolyte (~\$345 kg<sup>-1</sup> for TEABF<sub>4</sub>).

(7) *Lack of fundamental understanding of the electrolyte process in ES performance for new electrolyte material selection and design, as well as optimization of interaction between the electrode material and electrolyte.* Recently, considerable theoretical and *in-situ* experimental advancements have been achieved. However, in the development of new electrolytes (e.g., ILs and solid-state electrolytes) and new electrode materials, there still exists a challenge for the in-depth fundamental understanding of the charging/discharging mechanisms for these newly developed systems. For example, some controversies exist about the effects of temperature<sup>245</sup> and organic solvent addition<sup>244, 323</sup> on the EDL structure and the capacitance at the IL/electrode interface. DFT studies predicted the capacitance of nanoporous electrodes in an IL could oscillate with increasing pore size,<sup>503</sup> however, direct experimental work is required to confirm this prediction. Besides, there is a lack of a complete understanding of the dynamics of electrolyte ions in more complex electrode structures (e.g., hierarchical porous nanostructures) during the charging/discharging process. Furthermore, compared to the fundamental studies on the EDL charge storage mechanisms, fundamental understanding such as theoretical modeling for pseudocapacitors and hybrid ESs with certain electrolytes is rather limited.<sup>504</sup> Moreover, the dependence of the electrolyte parameters (e.g., ion type and size) on the pseudocapacitive behaviour of electrode materials is not very clear.

(8) *Proper and standardized characterization methods to evaluate the performance of electrolytes for ESs.* With the development of many new electrolytes (e.g., solid-state electrolytes), there is an urgent need to establish standardized

methods suitable to characterize the performance of electrolytes and their associated ESs. Currently, it is difficult to compare the experimental data from different literature since the performance metrics are usually obtained under different conditions. Therefore, it is not easy to identify the candidate electrolytes from different literature. Furthermore, the ES gravimetric capacitance, energy and power densities are generally reported based on the mass of active electrode materials. The electrolyte, however, also contributes a lot to the total mass and cost of ESs, a fact which should not be neglected.

## 7. Summary and possible research directions for overcoming the challenges in

### ES electrolytes

To help facilitate the research and development of electrolytes for ESs, this paper provides a comprehensive overview of the development and recent trends concerning electrolytes for ESs. Various types of electrolytes explored and reported in the literature are summarized and classified into aqueous, organic, ILs, solid-state or quasi-solid-state, and redox-active electrolytes. The effects of the electrolyte properties such as ESPW, ionic conductivity, viscosity, and thermal stability on the ES performance such as the specific capacitance, specific energy and power densities, ESR, rate performance, cycling stability, and temperature performance are reviewed in depth. Principles and methods to design and optimize electrolytes for ESs are given. In particular, the interplay between the electrolytes and electrode materials, including carbon-based and pseudocapacitive electrode materials, are discussed. Additionally, possible interactions between the electrolytes and inactive components, including current collectors, binders, and separators, are reviewed. In spite of considerable achievements in this field, several major challenges still exist such as low energy density, un-optimized matching between newly-developed electrolytes and electrode materials, lack of standard methods to evaluate the performance of electrolytes in ESs, high cost of some electrolytes, and insufficient fundamental understanding of charge storage mechanisms for some newly developed electrolytes in more realistic and complex electrodes. To overcome these challenges, several future research directions are suggested as follows:

(1) *Improving electrolyte's ESPW values to increase the ES's energy density.* Regarding the organic electrolytes, the ESPWs are dependent on the cation and anion of the conducting salt, and the organic solvent including a single solvent or a solvent mixture. Therefore, the improvement of ESPW could be achieved by exploring new organic solvents, new conducting salt or by optimizing/modifying the commonly used organic electrolytes. For example, electrolytes containing organic solvents such as sulfone-based and AND solvents, have shown promising results with higher ESPWs when compared to commercial ACN and PC solvent-based electrolytes. It should be

noted that in most cases, an increase in electrolyte ESPW may lead to the deterioration of other properties such as ionic conductivity and viscosity of electrolytes. To address this issue, all the composition of the electrolyte should be considered. For instance, the combination of a salt with a higher ionic conductivity or solubility and organic solvent(s) with higher ESPW may provide a promising solution. Besides, the use of ILs as electrolytes for ESs is beneficial for increasing the cell voltage and thus the energy density. The studies on ILs for ESs are still at the very beginning, and there are many ILs that have not yet been explored. By rationally designing the cation and anion or using an electrolyte mixture, ILs with higher ESPWs and acceptable ionic conductivities and viscosity may be developed. On the other hand, it is difficult for an electrolyte to meet all the requirements (high ESPW, high ionic conductivity, high thermal stability, low viscosity, low cost and environmental friendliness) at the same time. Some trade-offs may be reasonable in solving the practical problems. We believe the trade-offs strongly depend on the electrolyte and the electrode material as well as the requirements of the ES application.

(2) *Enhancing the charge capacity by utilizing the pseudocapacitive contribution.* Both the electrode materials (pseudocapacitive electrodes) and electrolytes (redox-active electrolytes) can contribute to the pseudocapacitance. In this case, even aqueous electrolyte-based ESs may achieve a significantly higher energy density especially for the hybrid or asymmetric ESs such as LIC. Aqueous electrolyte-based hybrid ESs are highly promising candidates for high-energy-density ESs, due to their attractive advantages such as very low cost, high safety and simplified fabrication procedures (e.g., without complicated and strict drying and purification processes).

(3) *Increasing the purity of the electrolyte.* Since residual impurities in electrolytes can negatively affect the ESPW and also lead to a serious increase in self-discharge, it is highly desirable to develop suitable purification process to decrease the amount of impurities in electrolytes. Considering that extensive experience has already been gained in the field of Li-ion batteries, the purification of organic solvents can be learned from the Li-ion battery industry. Regarding IL-based electrolytes, special attention is suggested to be paid to ILs with hydrophobic anions. This may allow for a low amount of water in the IL and is also beneficial for the long-term stability of the electrolyte.

(4) *Decreasing ESR values to further increase the ES's power density.* Developing electrolytes with high ionic conductivities and low viscosity is beneficial for decreasing the ESR values. Regarding organic electrolytes, this may be achieved by exploring innovative conducting salts such as SBPBF<sub>4</sub>, developing mixtures of organic solvents to decrease the viscosity, optimizing the salt–solvent systems, and so on. In the case of IL electrolytes, the design/selection of proper IL's cation and anion can contribute to increasing ionic conductivity and reducing viscosity of electrolytes. For example, the dicyanamide anion (DCA<sup>−</sup>)-based IL was found to give a smaller ESR compared to both the tetrafluoroborate (BF<sub>4</sub><sup>−</sup>) and bis(trifluoromethylsulfonyl) amide (NTF<sub>2</sub><sup>−</sup>) based IL.<sup>258</sup> The modification (e.g., introduction of the ether bond) of commonly used IL's cation and anion could also decrease ES's ESR.<sup>273</sup>

(5) *Optimizing the matching between the electrolyte and electrode materials to improve the overall performance.* The matching should not only consider the specific capacitance (energy density) but also take into account the power density of ESs. Regarding the specific capacitance, considering that different results have been reported for the relationship between pore size and surface-area-normalized capacitance,<sup>7, 500, 501</sup> more fundamental experiments are required to fully understand this relationship. This would provide the basis for guidance to optimize the matching between the pore size of carbonaceous materials and electrolyte ion size. To address this issue, it is necessary to use more reliable methods to characterize the true surface area of the electrode materials.<sup>501</sup> Furthermore, to increase the ES's specific capacitance (energy density) without sacrificing the power density, further research is required to be devoted to the development of electrodes with special structure such as hierarchical porous structure which could provide a high interfacial area for high capacitance while maintaining efficient ion transport for high power performance.<sup>505, 506</sup>

(6) *Increasing the working temperature range for ES operation.* Depending on the type of electrolytes, different strategies may be explored to widen the operating temperature range of ESs. Regarding aqueous electrolyte, some additives (e.g., ethylene glycol) may be explored to decrease the lower temperature limit.<sup>507</sup> In terms of organic electrolytes, the development of an innovative organic solvent mixture is possible to achieve the electrolyte with a larger working temperature range compared to the single solvent-based electrolytes. In the case of ILs, the exploration of eutectic mixture of ILs together with the development of electrode materials may effectively extend the temperature range, especially on the lower temperature limit of IL-based ESs.<sup>282</sup>

(7) *Further fundamental understanding through both theoretical and experimental investigations.* For the design and optimization of new electrolytes, down-selection of electrolytes with respect to improving ESPW, ionic conductivity, thermal stability and decreasing viscosity, better fundamental understanding by both experimental and theoretical work is definitely required. It is necessary to fundamentally understand the mechanisms of electrolyte ion dynamics, solvation/desolvation (if there is solvent), and the charge storage mechanism in a more realistic electrode structure during the charging/discharging process. This can be achieved using both theoretical modeling (molecular/electronic level) and experimental approaches especially involving *in-situ* characterization methods such as NMR and FTIR spectroelectrochemistry. In particular, special attention is suggested to be paid to the recently-developed electrolytes containing multivalent ions, IL mixture, IL-organic solvent mixtures, and solid-state electrolytes. Furthermore, with the development of pseudocapacitive electrode–electrolyte systems and hybrid ESs, fundamental work on the interaction between the electrolyte and pseudocapacitive or hybrid electrode materials is essential. Such a fundamental understanding will not only provide guidance for choosing or developing innovative electrolytes but also facilitate the development of electrode materials to match specific types of electrolytes. To mitigate the electrolyte degradation, it is also necessary to understand the degradation mechanisms and failure

modes. This can be achieved by both experimental and theoretical modeling approaches. For example, a variety of instrumental analysis methods, especially *in-situ* or on-line characterization methods (e.g., on-line DEMS and Raman microscopy), can be used to characterize the electrolytes during lifetime tests.

(8) *Development of standard methods to evaluate the performance of electrolytes.* With the increasing number of investigations in this area, it is important to develop proper and standardized methods to evaluate and compare the performance of different electrolytes and their associated ESs. It is necessary to know the mass and volume of the electrolyte used when characterizing the performance of ESs. Besides, to evaluate the flexible ESs using solid-state electrolytes, a standard specification and method are required to evaluate the mechanical properties and the performance under applied stress. Furthermore, to speed up the development of new electrolytes, higher output and fast screening methods for evaluating the performance of electrolytes is necessary. When a three-electrode cell is used to evaluate the electrolyte performance, it is suggested to use the electrode (substrate) that is similar to that used in real ESs in some cases, to obtain more realistic performance metrics of the electrolytes for ESs.

#### ACKNOWLEDGMENT

This work was supported by the National Natural Science Foundation for Distinguished Young Scholars (No. 51125016), and the National Natural Science Foundation of China (No. 51472178).

#### References

1. A. Burke, *Electrochim. Acta*, 2007, **53**, 1083-1091.
2. S. Holmberg, A. Perebikovskiy, L. Kulinsky and M. Madou, *Micromachines*, 2014, **5**, 171-203.
3. K. Naoi, S. Ishimoto, J. I. Miyamoto and W. Naoi, *Energ. Environ. Sci.*, 2012, **5**, 9363-9373.
4. M. Lu, F. Beguin and E. Frackowiak, *Supercapacitors: Materials, Systems and Applications*, John Wiley & Sons, 2013.
5. Y. Gogotsi and P. Simon, *Science*, 2011, **334**, 917-918.
6. V. Augustyn, P. Simon and B. Dunn, *Energ. Environ. Sci.*, 2014, **7**, 1597-1614.
7. J. Chmiola, G. Yushin, Y. Gogotsi, C. Portet, P. Simon and P. L. Taberna, *Science*, 2006, **313**, 1760-1763.
8. H. A. Andreas and B. E. Conway, *Electrochim. Acta*, 2006, **51**, 6510-6520.
9. K. Fic, G. Lota, M. Meller and E. Frackowiak, *Energ. Environ. Sci.*, 2012, **5**, 5842-5850.
10. A. Brandt, S. Pohlmann, A. Varzi, A. Balducci and S. Passerini, *MRS Bull.*, 2013, **38**, 554-559.
11. N. A. Choudhury, S. Sampath and A. K. Shukla, *Energ. Environ. Sci.*, 2009, **2**,

- 55-67.
12. H. Gao and K. Lian, *RSC Adv.*, 2014, **4**, 33091-33113.
  13. G. Lota and E. Frackowiak, *Electrochem. Commun.*, 2009, **11**, 87-90.
  14. J. Yan, Q. Wang, T. Wei and Z. J. Fan, *Adv. Energy. Mater.*, 2014, **4**.
  15. F. Béguin, V. Presser, A. Balducci and E. Frackowiak, *Adv. Mater.*, 2014, **26**, 2219-2251.
  16. Y. P. Zhai, Y. Q. Dou, D. Y. Zhao, P. F. Fulvio, R. T. Mayes and S. Dai, *Adv. Mater.*, 2011, **23**, 4828-4850.
  17. G. Wang, L. Zhang and J. Zhang, *Chem. Soc. Rev.*, 2012, **41**, 797-828.
  18. L. L. Zhang and X. S. Zhao, *Chem. Soc. Rev.*, 2009, **38**, 2520-2531.
  19. S. W. Lee, B. M. Gallant, H. R. Byon, P. T. Hammond and Y. Shao-Horn, *Energ. Environ. Sci.*, 2011, **4**, 1972-1985.
  20. A. B. Samui and P. Sivaraman, in *Polymer Electrolytes: Fundamentals and Applications*, 2010, pp. 431-470.
  21. X. Fang and D. Yao, Proceedings of the ASME 2013 International Mechanical Engineering Congress and Exposition, San Diego, California, USA, 2013.
  22. B. E. Conway, *Electrochemical supercapacitors: Scientific fundamentals and technological applications.*, Kluwer Academic/Plenum: New York, 1999.
  23. A. Yu, V. Chabot and J. Zhang, *Electrochemical Supercapacitors for Energy Storage and Delivery: Fundamentals and Applications*, 2013.
  24. A. Burke, *J. Power Sources*, 2000, **91**, 37-50.
  25. A. Burke and M. Miller, *J. Power Sources*, 2011, **196**, 514-522.
  26. M. Ue, K. Ida and S. Mori, *J. Electrochem. Soc.*, 1994, **141**, 2989.
  27. A. Davies and A. Yu, *Can. J. Chem. Eng.*, 2011, **89**, 1342-1357.
  28. G. P. Xiong, C. Z. Meng, R. G. Reifengerger, P. P. Irazoqui and T. S. Fisher, *Electroanalysis*, 2014, **26**, 30-51.
  29. M. Galiński, A. Lewandowski and I. Stępniaik, *Electrochim. Acta*, 2006, **51**, 5567-5580.
  30. J. G. Speight, *Lange's handbook of chemistry (16<sup>th</sup> Edition)*, MCGRAW-HILL, 2005.
  31. A. G. Volkov, S. Paula and D. W. Deamer, *Bioelectrochem. Bioenerg.*, 1997, **42**, 153-160.
  32. E. R. Nightingale, *J. Phys. Chem.*, 1959, **63**, 1381-1387.
  33. M. Y. Kiriukhin and K. D. Collins, *Biophys. Chem.*, 2002, **99**, 155-168.
  34. Y. Mun, C. Jo, T. Hyeon, J. Lee, K. S. Ha, K. W. Jun, S. H. Lee, S. W. Hong, H. I. Lee, S. Yoon and J. Lee, *Carbon*, 2013, **64**, 391-402.
  35. Z. Jin, X. D. Yan, Y. H. Yu and G. J. Zhao, *J. Mater. Chem. A*, 2014, **2**, 11706-11715.
  36. Q. Chen, Y. Hu, C. G. Hu, H. H. Cheng, Z. P. Zhang, H. B. Shao and L. T. Qu, *Phys. Chem. Chem. Phys.*, 2014, **16**, 19307-19313.
  37. D. Jimenez-Cordero, F. Heras, M. A. Gilarranz and E. Raymundo-Pinero, *Carbon*, 2014, **71**, 127-138.
  38. L. F. Chen, Z. H. Huang, H. W. Liang, H. L. Gao and S. H. Yu, *Adv. Funct. Mater.*, 2014, **24**, 5104-5111.

39. D. Hulicova-Jurcakova, A. M. Puziy, O. I. Poddubnaya, F. Suarez-Garcia, J. M. D. Tascon and G. Q. Lu, *J. Am. Chem. Soc.*, 2009, **131**, 5026-5027.
40. M. Jana, P. Khanra, N. C. Murmu, P. Samanta, J. H. Lee and T. Kuila, *Phys. Chem. Chem. Phys.*, 2014, **16**, 7618-7626.
41. L. J. Deng, J. F. Wang, G. Zhu, L. P. Kang, Z. P. Hao, Z. B. Lei, Z. P. Yang and Z. H. Liu, *J. Power Sources*, 2014, **248**, 407-415.
42. X. B. Liu, P. B. Shang, Y. B. Zhang, X. L. Wang, Z. M. Fan, B. X. Wang and Y. Y. Zheng, *J. Mater. Chem. A*, 2014, **2**, 15273-15278.
43. S. S. Shinde, G. S. Gund, D. P. Dubal, S. B. Jambure and C. D. Lokhande, *Electrochim. Acta*, 2014, **119**, 1-10.
44. Q. Wang, J. Yan, Z. J. Fan, T. Wei, M. L. Zhang and X. Y. Jing, *J. Power Sources*, 2014, **247**, 197-203.
45. Z. H. Zhang, Z. F. Zhou, H. R. Peng, Y. Qin and G. C. Li, *Electrochim. Acta*, 2014, **134**, 471-477.
46. Q. Wang, J. Yan, Y. B. Wang, T. Wei, M. L. Zhang, X. Y. Jing and Z. J. Fan, *Carbon*, 2014, **67**, 119-127.
47. H. J. Wang, X. X. Sun, Z. H. Liu and Z. B. Lei, *Nanoscale*, 2014, **6**, 6577-6584.
48. B. S. Mao, Z. H. Wen, Z. Bo, J. B. Chang, X. K. Huang and J. H. Chen, *ACS Appl. Mater. Inter.*, 2014, **6**, 9881-9889.
49. C. Feng, J. F. Zhang, Y. He, C. Zhong, W. B. Hu, L. Liu and Y. D. Deng, *ACS Nano*, 2015, **9**, 1730-1739.
50. L. L. Li, S. J. Peng, Y. L. Cheah, P. F. Teh, J. Wang, G. Wee, Y. W. Ko, C. L. Wong and M. Srinivasan, *Chem.-Eur. J.*, 2013, **19**, 5892-5898.
51. I. I. Misnon, R. A. Aziz, N. K. M. Zain, B. Vidhyadharan, S. G. Krishnan and R. Jose, *Mater. Res. Bull.*, 2014, **57**, 221-230.
52. Q. Abbas, D. Pajak, E. Frackowiak and F. Béguin, *Electrochim. Acta*, 2014, **140**, 132-138.
53. C. Ramasamy, J. P. del Val and M. Anderson, *J. Power Sources*, 2014, **248**, 370-377.
54. M. P. Bichat, E. Raymundo-Piñero and F. Béguin, *Carbon*, 2010, **48**, 4351-4361.
55. L. Demarconnay, E. Raymundo-Piñero and F. Béguin, *Electrochem. Commun.*, 2010, **12**, 1275-1278.
56. S. Dhibar, P. Bhattacharya, G. Hatui, S. Sahoo and C. K. Das, *ACS Sustain. Chem. Eng.*, 2014, **2**, 1114-1127.
57. S. Li, L. Qi, L. Lu and H. Wang, *RSC Adv.*, 2012, **2**, 3298-3308.
58. Y. Lin, X. Y. Wang, G. Qian and J. J. Watkins, *Chem. Mater.*, 2014, **26**, 2128-2137.
59. J. G. Wang, Y. Yang, Z. H. Huang and F. Kang, *J. Power Sources*, 2013, **224**, 86-92.
60. H. Xia, Y. Shirley Meng, G. Yuan, C. Cui and L. Lu, *Electrochem. Solid-State Lett.*, 2012, **15**, A60-A63.
61. L. Zhao, Y. Qiu, J. Yu, X. Deng, C. Dai and X. Bai, *Nanoscale*, 2013, **5**, 4902-4909.



62. K. Torchala, K. Kierzek and J. Machnikowski, *Electrochim. Acta*, 2012, **86**, 260-267.
63. H. Wu, X. Wang, L. Jiang, C. Wu, Q. Zhao, X. Liu, B. Hu and L. Yi, *J. Power Sources*, 2013, **226**, 202-209.
64. X. Zhang, X. Wang, L. Jiang, H. Wu, C. Wu and J. Su, *J. Power Sources*, 2012, **216**, 290-296.
65. H. Oda, A. Yamashita, S. Minoura, M. Okamoto and T. Morimoto, *J. Power Sources*, 2006, **158**, 1510-1516.
66. X. D. Yan, Y. H. Yu and X. P. Yang, *RSC Adv.*, 2014, **4**, 24986-24990.
67. D. Hulicova, M. Kodama and H. Hatori, *Chem. Mater.*, 2006, **18**, 2318-2326.
68. G. Pognon, T. Brousse, L. Demarconnay and D. Belanger, *J. Power Sources*, 2011, **196**, 4117-4122.
69. V. Ruiz, C. Blanco, M. Granda and R. Santamaria, *Electrochim. Acta*, 2008, **54**, 305-310.
70. X. R. Liu and P. G. Pickup, *J. Solid State Electrochem.*, 2010, **14**, 231-240.
71. B. Mendoza-Sánchez, T. Brousse, C. Ramirez-Castro, V. Nicolosi and P. S. Grant, *Electrochim. Acta*, 2013, **91**, 253-260.
72. J. W. Long, D. Belanger, T. Brousse, W. Sugimoto, M. B. Sassin and O. Crosnier, *MRS Bull.*, 2011, **36**, 513-522.
73. P. Perret, Z. Khani, T. Brousse, D. Belanger and D. Guay, *Electrochim. Acta*, 2011, **56**, 8122-8128.
74. Z. Algharaibeh, X. R. Liu and P. G. Pickup, *J. Power Sources*, 2009, **187**, 640-643.
75. D. Salinas-Torres, J. M. Sieben, D. Lozano-Castelló, D. Cazorla-Amorós and E. Morallón, *Electrochim. Acta*, 2013, **89**, 326-333.
76. V. Khomenko, E. Raymundo-Pinero and F. Beguin, *J. Power Sources*, 2010, **195**, 4234-4241.
77. J. P. Zheng, *J. Electrochem. Soc.*, 2003, **150**, A484-A492.
78. P. Perret, T. Brousse, D. Bélanger and D. Guay, *J. Electrochem. Soc.*, 2009, **156**, A645.
79. J. Shen, C. Yang, X. Li and G. Wang, *ACS Appl. Mater. Inter.*, 2013, **5**, 8467-8476.
80. H. A. Andreas, K. Lussier and A. M. Oickle, *J. Power Sources*, 2009, **187**, 275-283.
81. A. M. Oickle and H. A. Andreas, *J. Phys. Chem. C*, 2011, **115**, 4283-4288.
82. J. W. Lang, X. B. Yan, W. W. Liu, R. T. Wang and Q. J. Xue, *J. Power Sources*, 2012, **204**, 220-229.
83. D. W. Wang, F. Li, L. C. Yin, X. Lu, Z. G. Chen, I. R. Gentle, G. Q. Lu and H. M. Cheng, *Chem.-Eur. J.*, 2012, **18**, 5345-5351.
84. C. L. Wang, L. Sun, Y. Zhou, P. Wan, X. Zhang and J. S. Qiu, *Carbon*, 2013, **59**, 537-546.
85. K. Jurewicz, E. Frackowiak and F. Béguin, *Appl. Phys. A-Mater.*, 2004, **78**, 981-987.
86. K. W. Nam and K. B. Kim, *J. Electrochem. Soc.*, 2002, **149**, A346-A354.

87. A. Yuan and Q. Zhang, *Electrochem. Commun.*, 2006, **8**, 1173-1178.
88. X. L. Dong, Z. Y. Guo, Y. F. Song, M. Y. Hou, J. Q. Wang, Y. G. Wang and Y. Y. Xia, *Adv. Funct. Mater.*, 2014, **24**, 3405-3412.
89. R. B. Rakhi, N. A. Alhebshi, D. H. Anjum and H. N. Alshareef, *J. Mater. Chem. A*, 2014, **2**, 16190-16198.
90. D. Choi, G. E. Blomgren and P. N. Kumta, *Adv. Mater.*, 2006, **18**, 1178-1182.
91. J. Joseph, R. Rajagopalan, S. S. Anoop, V. Amruthalakshmi, A. Ajay, S. V. Nair and A. Balakrishnan, *RSC Adv.*, 2014, **4**, 39378-39385.
92. J. T. Mefford, W. G. Hardin, S. Dai, K. P. Johnston and K. J. Stevenson, *Nat. Mater.*, 2014, **13**, 726-732.
93. L. R. Hou, C. Z. Yuan, D. K. Li, L. Yang, L. F. Shen, F. Zhang and X. G. Zhang, *Electrochim. Acta*, 2011, **56**, 7454-7459.
94. C. Z. Yuan, B. Gao, L. H. Su, L. Chen and X. G. Zhang, *J. Electrochem. Soc.*, 2009, **156**, A199-A203.
95. Y. Tian, J. W. Yan, R. Xue and B. L. Yi, *Acta Phys.-Chim. Sin.*, 2011, **27**, 479-485.
96. U. M. Patil, R. R. Salunkhe, K. V. Gurav and C. D. Lokhande, *Appl. Surf. Sci.*, 2008, **255**, 2603-2607.
97. L. Su, L. Gong, H. Lü and Q. Xü, *J. Power Sources*, 2014, **248**, 212-217.
98. X. L. Wang, A. B. Yuan and Y. Q. Wang, *J. Power Sources*, 2007, **172**, 1007-1011.
99. A. I. Inamdar, Y. Kim, S. M. Pawar, J. H. Kim, H. Im and H. Kim, *J. Power Sources*, 2011, **196**, 2393-2397.
100. X. J. Wang, Z. Z. Yan, H. Pang, W. Q. Wang, G. C. Li, Y. H. Ma, H. Zhang, X. X. Li and J. Chen, *Int. J. Electrochem. Sci.*, 2013, **8**, 3768-3785.
101. R. Y. Wang, Q. Li, L. L. Cheng, H. L. Li, B. Y. Wang, X. S. Zhao and P. Z. Guo, *Colloid Surf. A-Physicochem. Eng. Asp.*, 2014, **457**, 94-99.
102. V. D. Nithya, R. K. Selvan, D. Kalpana, L. Vasylechko and C. Sanjeeviraja, *Electrochim. Acta*, 2013, **109**, 720-731.
103. C. Wang, Y. Zhou, L. Sun, P. Wan, X. Zhang and J. Qiu, *J. Power Sources*, 2013, **239**, 81-88.
104. Y. G. Wang, Z. D. Wang and Y. Y. Xia, *Electrochim. Acta*, 2005, **50**, 5641-5646.
105. C. L. Long, T. Wei, J. Yan, L. L. Jiang and Z. J. Fan, *ACS Nano*, 2013, **7**, 11325-11332.
106. L. B. Kong, M. Liu, J. W. Lang, Y. C. Luo and L. Kang, *J. Electrochem. Soc.*, 2009, **156**, A1000-A1004.
107. B. Vidyadharan, R. Abd Aziz, Misnon, II, G. M. A. Kumar, J. Ismail, M. M. Yusoff and R. Jose, *J. Power Sources*, 2014, **270**, 526-535.
108. C. S. Dai, P. Y. Chien, J. Y. Lin, S. W. Chou, W. K. Wu, P. H. Li, K. Y. Wu and T. W. Lin, *ACS Appl. Mater. Inter.*, 2013, **5**, 12168-12174.
109. C. Z. Yuan, B. Gao and X. G. Zhang, *J. Power Sources*, 2007, **173**, 606-612.
110. P. Ratajczak, K. Jurewicz and F. Beguin, *J. Appl. Electrochem.*, 2014, **44**, 475-480.

111. P. Ratajczak, K. Jurewicz, P. Skowron, Q. Abbas and F. Beguin, *Electrochim. Acta*, 2014, **130**, 344-350.
112. K. C. Tsay, L. Zhang and J. Zhang, *Electrochim. Acta*, 2012, **60**, 428-436.
113. J. H. Chae and G. Z. Chen, *Particuology*, 2014, **15**, 9-17.
114. Q. T. Qu, B. Wang, L. C. Yang, Y. Shi, S. Tian and Y. P. Wu, *Electrochem. Commun.*, 2008, **10**, 1652-1655.
115. H. Gao, A. Virya and K. Lian, *Electrochim. Acta*, 2014, **138**, 240-246.
116. H. Y. Lee and J. B. Goodenough, *J. Solid State Chem.*, 1999, **144**, 220-223.
117. S. L. Kuo and N. L. Wu, *J. Electrochem. Soc.*, 2006, **153**, A1317-A1324.
118. C. Xu, B. Li, H. Du, F. Kang and Y. Zeng, *J. Power Sources*, 2008, **184**, 691-694.
119. C. J. Xu, C. G. Wei, B. H. Li, F. Y. Kang and Z. C. Guan, *J. Power Sources*, 2011, **196**, 7854-7859.
120. S. Wen, J. W. Lee, I. H. Yeo, J. Park and S. Mho, *Electrochim. Acta*, 2004, **50**, 849-855.
121. S. Komaba, T. Tsuchikawa, M. Tomita, N. Yabuuchi and A. Ogata, *J. Electrochem. Soc.*, 2013, **160**, A1952-A1961.
122. B. Wang, P. Guo, H. Bi, Q. Li, G. Zhang, R. Wang, J. Liu and X. S. Zhao, *Int. J. Electrochem. Sci.*, 2013, **8**, 8966-8977.
123. Y. U. Jeong and A. Manthiram, *J. Electrochem. Soc.*, 2002, **149**, A1419-A1422.
124. J. Shao, X. Li, Q. Qu and Y. Wu, *J. Power Sources*, 2013, **223**, 56-61.
125. M. Q. Wu, L. P. Zhang, J. H. Gao, C. Xiao, D. M. Wang, A. Chen and S. R. Zhang, *J. Electroanal. Chem.*, 2008, **613**, 125-130.
126. Y. Q. Wang, A. B. Yuan and X. L. Wang, *J. Solid State Electrochem.*, 2008, **12**, 1101-1107.
127. A. Boisset, L. Athouël, J. Jacquemin, P. Porion, T. Brousse and M. Anouti, *J. Phys. Chem. C*, 2013, **117**, 7408-7422.
128. Q. T. Qu, L. L. Liu, Y. P. Wu and R. Holze, *Electrochim. Acta*, 2013, **96**, 8-12.
129. Y. Liu, Y. Jiao, Z. L. Zhang, F. Y. Qu, A. Umar and X. Wu, *ACS Appl. Mater. Inter.*, 2014, **6**, 2174-2184.
130. A. Prakash and D. Bahadur, *ACS Appl. Mater. Inter.*, 2014, **6**, 1394-1405.
131. M. Ammam and J. Fransaer, *Chem. Commun.*, 2012, **48**, 2036-2038.
132. Q. Yang, S. K. Pang and K. C. Yung, *J. Electroanal. Chem.*, 2014, **728**, 140-147.
133. M. S. Hong, Lee, S.H., and Kim, S.W., *Electrochem. Solid-State Lett.*, 2002, **5**, A227.
134. T. Brousse, M. Toupin and D. Belanger, *J. Electrochem. Soc.*, 2004, **151**, A614-A622.
135. G. N. Zhang, L. J. Ren, L. J. Deng, J. F. Wang, L. P. Kang and Z. H. H. Liu, *Mater. Res. Bull.*, 2014, **49**, 577-583.
136. Y. C. Chen, Y. G. Lin, Y. K. Hsu, S. C. Yen, K. H. Chen and L. C. Chen, *Small*, 2014, **10**, 3803-3810.
137. M. Huang, Y. X. Zhang, F. Li, Z. C. Wang, Alamusu, N. Hu, Z. Y. Wen and Q. Liu, *Sci. Rep.*, 2014, **4**.

138. C. H. Wang, H. C. Hsu and J. H. Hu, *J. Power Sources*, 2014, **249**, 1-8.
139. M. Kim and J. Kim, *Phys. Chem. Chem. Phys.*, 2014, **16**, 11323-11336.
140. F. P. Zhao, Y. Y. Wang, X. N. Xu, Y. L. Liu, R. Song, G. Lu and Y. G. Li, *ACS Appl. Mater. Inter.*, 2014, **6**, 11007-11012.
141. W. Shimizu, S. Makino, K. Takahashi, N. Imanishi and W. Sugimoto, *J. Power Sources*, 2013, **241**, 572-577.
142. M. Sevilla and A. B. Fuertes, *ACS Nano*, 2014, **8**, 5069-5078.
143. N. Jung, S. Kwon, D. Lee, D. M. Yoon, Y. M. Park, A. Benayad, J. Y. Choi and J. S. Park, *Adv. Mater.*, 2013, **25**, 6854-6858.
144. R. Francke, D. Cericola, R. Kotz, D. Weingarh and S. R. Waldvogel, *Electrochim. Acta*, 2012, **62**, 372-380.
145. A. Brandt, P. Isken, A. Lex-Balducci and A. Balducci, *J. Power Sources*, 2012, **204**, 213-219.
146. Y. Q. Lai, X. J. Chen, Z. A. Zhang, J. Li and Y. X. Liu, *Electrochim. Acta*, 2011, **56**, 6426-6430.
147. A. Janes, J. Eskusson, T. Thomberg and E. Lust, *J. Electrochem. Soc.*, 2014, **161**, A1284-A1290.
148. E. Perricone, M. Chamas, L. Cointeaux, J. C. Leprêtre, P. Judeinstein, P. Azais, F. Béguin and F. Alloin, *Electrochim. Acta*, 2013, **93**, 1-7.
149. X. W. Yu, D. B. Ruan, C. C. Wu, J. Wang and Z. Q. Shi, *J. Power Sources*, 2014, **265**, 309-316.
150. W. J. Qian, F. X. Sun, Y. H. Xu, L. H. Qiu, C. H. Liu, S. D. Wang and F. Yan, *Energ. Environ. Sci.*, 2014, **7**, 379-386.
151. R. Vali, A. Laheaar, A. Janes and E. Lust, *Electrochim. Acta*, 2014, **121**, 294-300.
152. X. D. Huang, B. Sun, S. Q. Chen and G. X. Wang, *Chem.-Asian J.*, 2014, **9**, 206-211.
153. D. Hanlon, C. Backes, T. M. Higgins, M. Hughes, A. O'Neill, P. King, N. McEvoy, G. S. Duesberg, B. M. Sanchez, H. Pettersson, V. Nicolosi and J. N. Coleman, *Chem. Mater.*, 2014, **26**, 1751-1763.
154. D. Yigit, M. Gullu, T. Yumak and A. Sinag, *J. Mater. Chem. A*, 2014, **2**, 6512-6524.
155. H. Zhang, J. Wang, Y. Chen, Z. Wang and S. Wang, *Electrochim. Acta*, 2013, **105**, 69-74.
156. C. Zheng, J. C. Gao, M. Yoshio, L. Qi and H. Y. Wang, *J. Power Sources*, 2013, **231**, 29-33.
157. C. Zheng, M. Yoshio, L. Qi and H. Y. Wang, *J. Power Sources*, 2014, **260**, 19-26.
158. E. Lim, H. Kim, C. Jo, J. Chun, K. Ku, S. Kim, H. I. Lee, I. S. Nam, S. Yoon, K. Kang and J. Lee, *ACS Nano*, 2014, **8**, 8968-8978.
159. F. Zhang, T. F. Zhang, X. Yang, L. Zhang, K. Leng, Y. Huang and Y. S. Chen, *Energ. Environ. Sci.*, 2013, **6**, 1623-1632.
160. Y. Lei, Z. H. Huang, Y. Yang, W. Shen, Y. Zheng, H. Sun and F. Kang, *Sci. Rep.*, 2013, **3**.

161. S. D. Perera, M. Rudolph, R. G. Mariano, N. Nijem, J. P. Ferraris, Y. J. Chabal and K. J. Balkus, *Nano Energy*, 2013, **2**, 966-975.
162. J. Barthel, H. J. Gores, G. Schmeer and R. Wechter, *Non-aqueous electrolyte solutions in chemistry and modern technology*, Springer Berlin Heidelberg, 1983.
163. J. E. Coetzee, *Commission on Electroanalytical Chemistry International Union of Pure and Applied Chemistry. Recommended methods for purification of solvents and tests for impurities*, New York: Pergamon Press, 1982.
164. *Catalog Handbook of Fine Chemicals*, Aldrich Chemical Co, 1993.
165. M. J. Kelly and W. R. Heineman, *J. Electroanal. Chem.*, 1988, **248**, 441.
166. J. Rosenfarb and J. A. Caruso, *J. Solution Chem.*, 1976, **5**, 345.
167. J. Rosenfarb, M. Martin, C. Prakash and J. A. Caruso, *J. Solution Chem.*, 1976, **5**, 311-318.
168. V. Barranco, M. A. Lillo-Rodenas, A. Linares-Solano, A. Oya, F. Pico, J. Ibañez, F. Agullo-Rueda, J. M. Amarilla and J. M. Rojo, *J. Phys. Chem. C*, 2010, **114**, 10302-10307.
169. J. K. McDonough, A. I. Frolov, V. Presser, J. Niu, C. H. Miller, T. Ubieta, M. V. Fedorov and Y. Gogotsi, *Carbon*, 2012, **50**, 3298-3309.
170. C. M. Yang, Y. J. Kim, M. Endo, H. Kanoh, M. Yudasaka, S. Iijima and K. Kaneko, *J. Am. Chem. Soc.*, 2007, **129**, 20-21.
171. S. Vaquero, R. Díaz, M. Anderson, J. Palma and R. Marcilla, *Electrochim. Acta*, 2012, **86**, 241-247.
172. D. E. Jiang and J. Z. Wu, *J. Phys. Chem. Lett.*, 2013, **4**, 1260-1267.
173. A. Takana, Iiyama, T., Ohba, T., Ozeki, S., Urita, K., Fujimori, T., Kanoh, H., and Kaneko, K., *J. Am. Chem. Soc.*, 2010, **132**, 2112.
174. D. E. Jiang, Z. Jin, D. Henderson and J. Wu, *J. Phys. Chem. Lett.*, 2012, **3**, 1727-1731.
175. L. Yang, B. H. Fishbine, A. Migliori and L. R. Pratt, *J. Am. Chem. Soc.*, 2009, **131**, 12373-12376.
176. F. Blanc, M. Leskes and C. P. Grey, *Acc. Chem. Res.*, 2013, **46**, 1952-1963.
177. H. Wang, T. K. J. Koster, N. M. Trease, J. Segalini, P. L. Taberna, P. Simon, Y. Gogotsi and C. P. Grey, *J. Am. Chem. Soc.*, 2011, **133**, 19270-19273.
178. M. Deschamps, E. Gilbert, P. Azais, E. Raymundo-Piñero, M. R. Ammar, P. Simon, D. Massiot and F. Béguin, *Nat. Mater.*, 2013, **12**, 351-358.
179. H. Wang, A. C. Forse, J. M. Griffin, N. M. Trease, L. Trognko, P. L. Taberna, P. Simon and C. P. Grey, *J. Am. Chem. Soc.*, 2013, **135**, 18968-18980.
180. M. D. Levi, G. Salitra, N. Levy, D. Aurbach and J. Maier, *Nat. Mater.*, 2009, **8**, 872-875.
181. S. Boukhalifa, D. Gordon, L. L. He, Y. B. Melnichenko, N. Nitta, A. Magasinski and G. Yushin, *ACS Nano*, 2014, **8**, 2495-2503.
182. F. Bonhomme, J. C. Lassègues and L. Servant, *J. Electrochem. Soc.*, 2001, **148**, E450-E458.
183. A. C. Forse, J. M. Griffin, H. Wang, N. M. Trease, V. Presser, Y. Gogotsi, P. Simon and C. P. Grey, *Phys. Chem. Chem. Phys.*, 2013, **15**, 7722-7730.

184. P. Kurzweil and M. Chwistek, *J. Power Sources*, 2008, **176**, 555-567.
185. H. Maeshima, H. Moriwake, A. Kuwabara and C. A. J. Fisher, *J. Electrochem. Soc.*, 2010, **157**, A696-A701.
186. H. Maeshima, H. Moriwake, A. Kuwabara, C. A. J. Fisher and I. Tanaka, *J. Electrochem. Soc.*, 2014, **161**, G7-G14.
187. Y. A. Shuichi Ishimoto, Masanori Shinya, and Katsuhiko Naoia, *J. Electrochem. Soc.*, 2009, **156**.
188. L. J. Hardwick, M. Hahn, P. Ruch, M. Holzapfel, W. Scheifele, H. Buqa, F. Krumeich, P. Novák and R. Kötz, *Electrochim. Acta*, 2006, **52**, 675-680.
189. R. Kötz, M. Hahn and R. Gally, *J. Power Sources*, 2006, **154**, 550-555.
190. E. J. Brandon, W. C. West, M. C. Smart, L. D. Whitcanack and G. A. Plett, *J. Power Sources*, 2007, **170**, 225-232.
191. B. W. Ricketts and C. Ton-That, *J. Power Sources*, 2000, **89**, 64-69.
192. Q. Zhang, J. Rong, D. Ma and B. Wei, *Energ. Environ. Sci.*, 2011, **4**, 2152-2159.
193. M. Y. Cho, M. H. Kim, H. K. Kim, K. B. Kim, J. R. Yoon and K. C. Roh, *Electrochem. Commun.*, 2014, **47**, 5-8.
194. Y. Cai, B. T. Zhao, J. Wang and Z. P. Shao, *J. Power Sources*, 2014, **253**, 80-89.
195. W. H. Qu, F. Han, A. H. Lu, C. Xing, M. Qiao and W. C. Li, *J. Mater. Chem. A*, 2014, **2**, 6549-6557.
196. G. G. Amatucci, F. Badway, A. Du Pasquier and T. Zheng, *J. Electrochem. Soc.*, 2001, **148**, A930.
197. D.-W. Wang, H.-T. Fang, F. Li, Z.-G. Chen, Q.-S. Zhong, G. Q. Lu and H.-M. Cheng, *Adv. Funct. Mater.*, 2008, **18**, 3787-3793.
198. J. S. Bonso, A. Rahy, S. D. Perera, N. Nour, O. Seitz, Y. J. Chabal, K. J. Balkus Jr, J. P. Ferraris and D. J. Yang, *J. Power Sources*, 2012, **203**, 227-232.
199. P. Sivaraman, A. R. Bhattacharyya, S. P. Mishra, A. P. Thakur, K. Shashidhara and A. B. Samui, *Electrochim. Acta*, 2013, **94**, 182-191.
200. P. H. Smith, T. N. Tran, T. L. Jiang and J. Chung, *J. Power Sources*, 2013, **243**, 982-992.
201. C. H. Lee, F. Xu and C. Jung, *Electrochim. Acta*, 2014, **131**, 240-244.
202. K. Xu, *Chem. Rev.*, 2004, **104**, 4303-4417.
203. P. Simon and Y. Gogotsi, *Acc. Chem. Res.*, 2013, **46**, 1094-1103.
204. M. Ue, *Electrochemistry*, 2007, **75**, 565-572.
205. K. Naoi, *Fuel Cells*, 2010, **10**, 825-833.
206. P. Liu, M. Verbrugge and S. Soukiazian, *J. Power Sources*, 2006, **156**, 712-718.
207. M. Arulepp, L. Permann, J. Leis, A. Perkson, K. Rumma, A. Janes and E. Lust, *J. Power Sources*, 2004, **133**, 320-328.
208. M. S. Ding, K. Xu, J. P. Zheng and T. R. Jow, *J. Power Sources*, 2004, **138**, 340-350.
209. M. Ue, M. Takeda, M. Takehara and S. Mori, *J. Electrochem. Soc.*, 1997, **144**, 2684-2688.
210. K. Chiba, T. Ueda, Y. Yamaguchi, Y. Oki, F. Saiki and K. Naoi, *J. Electrochem. Soc.*, 2011, **158**, A1320-A1327.

211. K. Suzuki, M. Shin-Ya, Y. Ono, T. Matsumoto, N. Nanbu, M. Takehara, M. Ue and Y. Sasaki, *Electrochemistry*, 2007, **75**, 611-614.
212. K. Chiba, T. Ueda, Y. Yamaguchi, Y. Oki, F. Shimodate and K. Naoi, *J. Electrochem. Soc.*, 2011, **158**, A872-A882.
213. A. Janes, T. Thomberg, J. Eskusson and E. Lust, *J. Electrochem. Soc.*, 2013, **160**, A1025-A1030.
214. S. F. Tian, L. Qi, M. Yoshio and H. Y. Wang, *J. Power Sources*, 2014, **256**, 404-409.
215. A. Laheear, H. Kurig, A. Janes and E. Lust, *Electrochim. Acta*, 2009, **54**, 4587-4594.
216. A. Janes and E. Lust, *J. Electroanal. Chem.*, 2006, **588**, 285-295.
217. E. Perricone, M. Chamas, J. C. Leprêtre, P. Judeinstein, P. Azais, E. Raymundo-Pinero, F. Béguin and F. Alloin, *J. Power Sources*, 2013, **239**, 217-224.
218. J. P. Zheng and T. R. Jow, *J. Electrochem. Soc.*, 1997, **144**, 2417-2420.
219. M. UE, *Electrochemistry*, 2007, 555.
220. K. Xu, M. S. Ding and T. R. Jow, *J. Electrochem. Soc.*, 2001, **148**, A267-A274.
221. A. R. Koh, B. Hwang, K. C. Roh and K. Kim, *Phys. Chem. Chem. Phys.*, 2014, **16**, 15146-15151.
222. A. Jänes, H. Kurig, T. Romann and E. Lust, *Electrochem. Commun.*, 2010, **12**, 535-539.
223. Y. Yokoyama, N. Shimosaka, H. Matsumoto, M. Yoshio and T. Ishiharaa, *Electrochem. Solid St.*, 2008, **11**, A72-A75.
224. K. Chiba, T. Ueda and H. Yamamoto, *Electrochemistry*, 2007, **75**, 664-667.
225. K. Chiba, T. Ueda and H. Yamamoto, *Electrochemistry*, 2007, **75**, 668-671.
226. H. Kurig, A. Janes and E. Lust, *J. Mater. Res.*, 2010, **25**, 1447-1450.
227. T. Ebina, H. Uno, S. Ishizawa, N. Nanbu and Y. Sasaki, *Chem. Lett.*, 2005, **34**, 1014-1015.
228. N. Nanbu, T. Ebina, H. Uno, S. Ishizawa and Y. Sasaki, *Electrochim. Acta*, 2006, **52**, 1763-1770.
229. N. Nambu, R. Takahashi, K. Suzuki and Y. Sasaki, *Electrochemistry*, 2013, **81**, 811-813.
230. Q. Li, X. X. Zuo, J. S. Liu, X. Xiao, D. Shu and J. M. Nan, *Electrochim. Acta*, 2011, **58**, 330-335.
231. A. Laheäär, A. Jänes and E. Lust, *Electrochim. Acta*, 2011, **56**, 9048-9055.
232. R. Chandrasekaran, M. Koh, A. Yamauchi and M. Ishikawa, *J. Power Sources*, 2010, **195**, 662-666.
233. R. D. Rogers and G. A. Voth, *Acc. Chem. Res.*, 2007, **40**, 1077-1078.
234. M. Armand, F. Endres, D. R. MacFarlane, H. Ohno and B. Scrosati, *Nat. Mater.*, 2009, **8**, 621-629.
235. P. Wasserscheid and T. Welton, *Ionic liquids in synthesis*, Wiley-VCH Verlag GmbH & Co. KGaA, 2002.
236. M. Freemantle, *Chemical & Engineering News Archive*, 1998, **76**, 32-37.
237. A. Lewandowski and M. Galinski, *J. Power Sources*, 2007, **173**, 822-828.

238. A. Lewandowski, A. Olejniczak, M. Galinski and I. Stepniak, *J. Power Sources*, 2010, **195**, 5814-5819.
239. J. G. Huddleston, A. E. Visser, W. M. Reichert, H. D. Willauer, G. A. Broker and R. D. Rogers, *Green Chem.*, 2001, **3**, 156-164.
240. Z. B. Zhou, H. Matsumoto and K. Tatsumi, *Chem.-Eur. J.*, 2004, **10**, 6581-6591.
241. Y. Chen, X. Zhang, D. Zhang, P. Yu and Y. Ma, *Carbon*, 2011, **49**, 573-580.
242. B. Xu, F. Wu, R. J. Chen, G. P. Cao, S. Chen, Z. M. Zhou and Y. S. Yang, *Electrochem. Commun.*, 2008, **10**, 795-797.
243. C. Merlet, B. Rotenberg, P. A. Madden, P. L. Taberna, P. Simon, Y. Gogotsi and M. Salanne, *Nat. Mater.*, 2012, **11**, 306-310.
244. G. Feng, J. Huang, B. G. Sumpter, V. Meunier and R. Qiao, *Phys. Chem. Chem. Phys.*, 2011, **13**, 14723-14734.
245. M. V. Fedorov and A. A. Kornyshev, *Chem. Rev.*, 2014, **114**, 2978-3036.
246. R. Burt, G. Birkett and X. S. Zhao, *Phys. Chem. Chem. Phys.*, 2014, **16**, 6519-6538.
247. G. Feng, S. Li, V. Presser and P. T. Cummings, *J. Phys. Chem. Lett.*, 2013, **4**, 3367-3376.
248. S. Baldelli, *Acc. Chem. Res.*, 2008, **41**, 421-431.
249. M. Kunze, E. Paillard, S. Jeong, G. B. Appetecchi, M. Schönhoff, M. Winter and S. Passerini, *J. Phys. Chem. C*, 2011, **115**, 19431-19436.
250. M. Kunze, S. Jeong, E. Paillard, M. Schönhoff, M. Winter and S. Passerini, *Adv. Energy. Mater.*, 2011, **1**, 274-281.
251. T. Romann, O. Oll, P. Pikma, H. Tamme and E. Lust, *Electrochim. Acta*, 2014, **125**, 183-190.
252. J. Kruusma, A. Tonisoo, R. Parna, E. Nommiste and E. Lust, *J. Electrochem. Soc.*, 2014, **161**, A1266-A1277.
253. G. H. Sun, K. X. Li and C. G. Sun, *J. Power Sources*, 2006, **162**, 1444-1450.
254. N. Handa, T. Sugimoto, M. Yamagata, M. Kikuta, M. Kono and M. Ishikawa, *J. Power Sources*, 2008, **185**, 1585-1588.
255. G. P. Pandey and S. A. Hashmi, *Bull. Mater. Sci.*, 2013, **36**, 729-733.
256. K. Matsumoto and R. Hagiwara, *J. Electrochem. Soc.*, 2010, **157**, A578-A581.
257. H. Kurig, M. Vestli, K. Tönurist, A. Jänes and E. Lust, *J. Electrochem. Soc.*, 2012, **159**, A944-A951.
258. M. Shi, S. Kou and X. Yan, *ChemSusChem*, 2014.
259. C. Kong, W. Qian, C. Zheng, Y. Yu, C. Cui and F. Wei, *Chem. Commun.*, 2013, **49**, 10727-10729.
260. I. Murayama, N. Yoshimoto, M. Egashira, M. Morita, Y. Kobayashi and M. Ishikawa, *Electrochemistry*, 2005, **73**, 600-602.
261. H. Matsumoto, H. Kageyama and Y. Miyazaki, *Electrochemistry*, 2003, **71**, 1058-1060.
262. R. S. Borges, H. Ribeiro, R. L. Lavall and G. G. Silva, *J. Solid State Electrochem.*, 2012, **16**, 3573-3580.
263. L. G. Bettini, M. Galluzzi, A. Podestà, P. Milani and P. Piseri, *Carbon*, 2013,



- 59**, 212-220.
264. M. Lazzari, F. Soavi and M. Mastragostino, *J. Power Sources*, 2008, **178**, 490-496.
265. M. Lazzari, F. Soavi and M. Mastragostino, *J. Electrochem. Soc.*, 2009, **156**, A661-A666.
266. C. Arbizzani, M. Bisio, D. Cericola, M. Lazzari, F. Soavi and M. Mastragostino, *J. Power Sources*, 2008, **185**, 1575-1579.
267. T. Sato, G. Masuda and K. Takagi, *Electrochim. Acta*, 2004, **49**, 3603-3611.
268. Y.-J. Kim, Y. Matsuzawa, S. Ozaki, K. C. Park, C. Kim, M. Endo, H. Yoshida, G. Masuda, T. Sato and M. S. Dresselhaus, *J. Electrochem. Soc.*, 2005, **152**, A710.
269. A. Senda, K. Matsumoto, T. Nohira and R. Hagiwara, *J. Power Sources*, 2010, **195**, 4414-4417.
270. M. Anouti, L. Timperman, M. El Hilali, A. Boisset and H. Galiano, *J. Phys. Chem. C*, 2012, **116**, 9412-9418.
271. S. Pohlmann, T. Olyschläger, P. Goodrich, J. Alvarez Vicente, J. Jacquemin and A. Balducci, *J. Power Sources*, 2014, **273**, 931-936.
272. F. B. Sillars, S. I. Fletcher, M. Mirzaeian and P. J. Hall, *Phys. Chem. Chem. Phys.*, 2012, **14**, 6094-6100.
273. A. J. R. Rennie, N. Sanchez-Ramirez, R. M. Torresi and P. J. Hall, *J. Phys. Chem. Lett.*, 2013, **4**, 2970-2974.
274. K. R. Seddon, A. Stark and M. J. Torres, *Pure Appl. Chem.*, 2000, **72**, 2275-2287.
275. G. H. Lane, *Electrochim. Acta*, 2012, **83**, 513-528.
276. W. Y. Tsai, R. Lin, S. Murali, L. Li Zhang, J. K. McDonough, R. S. Ruoff, P. L. Taberna, Y. Gogotsi and P. Simon, *Nano Energy*, 2013, **2**, 403-411.
277. L. Demarconnay, E. G. Calvo, L. Timperman, M. Anouti, D. Lemordant, E. Raymundo-Piñero, A. Arenillas, J. A. Menéndez and F. Béguin, *Electrochim. Acta*, 2013, **108**, 361-368.
278. L. Timperman, P. Skowron, A. Boisset, H. Galiano, D. Lemordant, E. Frackowiak, F. Beguin and M. Anouti, *Phys. Chem. Chem. Phys.*, 2012, **14**, 8199-8207.
279. L. Timperman, F. Beguin, E. Frackowiak and M. Anouti, *J. Electrochem. Soc.*, 2014, **161**, A228-A238.
280. A. Brandt, J. Pires, M. Anouti and A. Balducci, *Electrochim. Acta*, 2013, **108**, 226-231.
281. W. Xu and C. A. Angell, *Science*, 2003, **302**, 422-425.
282. R. Y. Lin, P. L. Taberna, S. Fantini, V. Presser, C. R. Perez, F. Malbosc, N. L. Rupesinghe, K. B. K. Teo, Y. Gogotsi and P. Simon, *J. Phys. Chem. Lett.*, 2011, **2**, 2396-2401.
283. S. Li, G. Feng, P. F. Fulvio, P. C. Hillesheim, C. Liao, S. Dai and P. T. Cummings, *J. Phys. Chem. Lett.*, 2012, **3**, 2465-2469.
284. D. Rochefort and A.-L. Pont, *Electrochem. Commun.*, 2006, **8**, 1539-1543.
285. L. Mayrand-Provencher, S. X. Lin, D. Lazzarini and D. Rochefort, *J. Power*

- Sources*, 2010, **195**, 5114-5121.
286. F. W. Richey and Y. A. Elabd, *J. Electrochem. Soc.*, 2013, **160**, A862-A868.
287. M. T. Lee, W. T. Tsai, H. F. Cheng, I. W. Sun and J. K. Chang, *J. Power Sources*, 2013, **233**, 28-33.
288. Y. S. Li, I. W. Sun, J. K. Chang, C. J. Su and M. T. Lee, *J. Mater. Chem.*, 2012, **22**, 6274-6279.
289. T. M. Benedetti, V. R. Goncales, S. I. C. de Torresi and R. M. Torresi, *J. Power Sources*, 2013, **239**, 1-8.
290. M. T. Lee, Y. S. Li, I. W. Sun and J. K. Chang, *J. Power Sources*, 2014, **246**, 269-276.
291. J. K. Chang, M. T. Lee, C. W. Cheng, W. T. Tsai, M. J. Deng and I. W. Sun, *Electrochem. Solid St.*, 2009, **12**, A19-A22.
292. J. K. Chang, M. T. Lee, W. T. Tsai, M. J. Deng and I. W. Sun, *Chem. Mater.*, 2009, **21**, 2688-2695.
293. C. A. C. Ruiz, D. Belanger and D. Rochefort, *J. Phys. Chem. C*, 2013, **117**, 20397-20405.
294. J. S. Shaikh, R. C. Pawar, R. S. Devan, Y. R. Ma, P. P. Salvi, S. S. Kolekar and P. S. Patil, *Electrochim. Acta*, 2011, **56**, 2127-2134.
295. F. Fabregat-Santiago, H. Randriamahazaka, A. Zaban, J. Garcia-Cañadas, G. Garcia-Belmonte and J. Bisquert, *Phys. Chem. Chem. Phys.*, 2006, **8**, 1827-1833.
296. S. X. Sun, J. W. Lang, R. T. Wang, L. B. Kong, X. C. Li and X. B. Yan, *J. Mater. Chem. A*, 2014, **2**, 14550-14556.
297. N. Kobayashi, T. Sakumoto, S. Mori, H. Ogata, K. C. Park, K. Takeuchi and M. Endo, *Electrochim. Acta*, 2013, **105**, 455-461.
298. N. Fechler, G. A. Tiruye, R. Marcilla and M. Antonietti, *RSC Adv.*, 2014, **4**, 26981-26989.
299. C. Arbizzani, F. Soavi and M. Mastragostino, *J. Power Sources*, 2006, **162**, 735-737.
300. W. Chen, R. B. Rakhi and H. N. Alshareef, *J. Mater. Chem. A*, 2013, **1**, 3315-3324.
301. K. Wang, J. Huang and Z. Wei, *J. Phys. Chem. C*, 2010, **114**, 8062-8067.
302. A. Balducci, F. Soavi and M. Mastragostino, *Applied Physics A: Materials Science and Processing*, 2006, **82**, 627-632.
303. D. Aradilla, G. Bidan, P. Gentile, P. Weathers, F. Thissandier, V. Ruiz, P. Gomez-Romero, T. J. S. Schubert, H. Sahin and S. Sadki, *RSC Adv.*, 2014, **4**, 26462-26467.
304. X. Zhang, D. Zhao, Y. Zhao, P. Tang, Y. Shen, C. Xu, H. Li and Y. Xiao, *J. Mater. Chem. A*, 2013, **1**, 3706-3712.
305. A. B. McEwen, S. F. McDevitt and V. R. Koch, *J. Electrochem. Soc.*, 1997, **144**, L84-L86.
306. A. Orita, K. Kamijima and M. Yoshida, *J. Power Sources*, 2010, **195**, 7471-7479.
307. R. Lin, P. Huang, J. Segalini, C. Largeot, P. L. Taberna, J. Chmiola, Y. Gogotsi

- and P. Simon, *Electrochim. Acta*, 2009, **54**, 7025-7032.
308. F. Ghamouss, A. Brugere and J. Jacquemin, *J. Phys. Chem. C*, 2014, **118**, 14107-14123.
309. R. Palm, H. Kurig, K. Tonurist, A. Janes and E. Lust, *J. Electrochem. Soc.*, 2013, **160**, A1741-A1745.
310. V. Ruiz, T. Huynh, S. R. Sivakkumar and A. G. Pandolfo, *RSC Adv.*, 2012, **2**, 5591-5598.
311. S. Pohlmann, R. S. Kuhnel, T. A. Centeno and A. Balducci, *ChemElectroChem*, 2014, **1**, 1301-1311.
312. A. Krause and A. Balducci, *Electrochem. Commun.*, 2011, **13**, 814-817.
313. T. Abdallah, D. Lemordant and B. Claude-Montigny, *J. Power Sources*, 2012, **201**, 353-359.
314. A. Brandt, C. Ramirez-Castro, M. Anouti and A. Balducci, *J. Mater. Chem. A*, 2013, **1**, 12669-12678.
315. E. Frackowiak, G. Lota and J. Pernak, *Appl. Phys. Lett.*, 2005, **86**, 1-3.
316. A. Lewandowski and A. Olejniczak, *J. Power Sources*, 2007, **172**, 487-492.
317. K. Yuyama, G. Masuda, H. Yoshida and T. Sato, *J. Power Sources*, 2006, **162**, 1401-1408.
318. A. Orita, K. Kamijima, M. Yoshida and L. Yang, *J. Power Sources*, 2010, **195**, 6970-6976.
319. A. Brandt and A. Balducci, *J. Power Sources*, 2014, **250**, 343-351.
320. L. Timperman, H. Galiano, D. Lemordant and M. Anouti, *Electrochem. Commun.*, 2011, **13**, 1112-1115.
321. M. Anouti and L. Timperman, *Phys. Chem. Chem. Phys.*, 2013, **15**, 6539-6548.
322. E. Coadou, L. Timperman, J. Jacquemin, H. Galiano, C. Hardacre and M. Anouti, *J. Phys. Chem. C*, 2013, **117**, 10315-10325.
323. Y. Shim, Y. Jung and H. J. Kim, *J. Phys. Chem. C*, 2011, **115**, 23574-23583.
324. B. E. Francisco, C. M. Jones, S. H. Lee and C. R. Stoldt, *Appl. Phys. Lett.*, 2012, **100**.
325. A. S. Ulihin, Y. G. Mateyshina and N. F. Uvarov, *Solid State Ionics*, 2013, **251**, 62-65.
326. A. A. Łatoszyńska, G. Z. Zukowska, I. A. Rutkowska, P. L. Taberna, P. Simon, P. J. Kulesza and W. Wieczorek, *J. Power Sources*, 2014, **274**, 1147-1154.
327. L. Q. Fan, J. Zhong, J. H. Wu, J. M. Lin and Y. F. Huang, *J. Mater. Chem. A*, 2014, **2**, 9011-9014.
328. M. L. Verma, M. Minakshi and N. K. Singh, *Electrochim. Acta*, 2014, **137**, 497-503.
329. R. C. Agrawal and G. P. Pandey, *J. Phys. D: Appl. Phys.*, 2008, **41**.
330. J. Duay, E. Gillette, R. Liu and S. B. Lee, *Phys. Chem. Chem. Phys.*, 2012, **14**, 3329-3337.
331. C. W. Huang, C. A. Wu, S. S. Hou, P. L. Kuo, C. T. Hsieh and H. S. Teng, *Adv. Funct. Mater.*, 2012, **22**, 4677-4685.
332. Y. N. Sudhakar, M. Selvakumar and D. K. Bhat, *Ionics*, 2013, **19**, 277-285.
333. C. Ramasamy, J. P. del Vel and M. Anderson, *J. Solid State Electrochem.*, 2014,

- 18**, 2217-2223.
334. X. F. Wang, B. Liu, Q. F. Wang, W. F. Song, X. J. Hou, D. Chen, Y. B. Cheng and G. Z. Shen, *Adv. Mater.*, 2013, **25**, 1479-1486.
335. Z. Q. Niu, H. B. Dong, B. W. Zhu, J. Z. Li, H. H. Hng, W. Y. Zhou, X. D. Chen and S. S. Xie, *Adv. Mater.*, 2013, **25**, 1058-1064.
336. G. Sun, J. An, C. K. Chua, H. Pang, J. Zhang and P. Chen, *Electrochem. Commun.*, 2015, **51**, 33-36.
337. S. Liu, J. Xie, H. Li, Y. Wang, H. Y. Yang, T. Zhu, S. Zhang, G. Cao and X. Zhao, *J. Mater. Chem. A*, 2014, **2**, 18125-18131.
338. W. P. Si, C. L. Yan, Y. Chen, S. Oswald, L. Y. Han and O. G. Schmidt, *Energ. Environ. Sci.*, 2013, **6**, 3218-3223.
339. C. Z. Meng, J. Maeng, S. W. M. John and P. P. Irazoqui, *Adv. Energy. Mater.*, 2014, **4**.
340. L. Kou, T. Q. Huang, B. N. Zheng, Y. Han, X. L. Zhao, K. Gopalsamy, H. Y. Sun and C. Gao, *Nat. Commun.*, 2014, **5**.
341. G. Sun, J. Liu, X. Zhang, X. Wang, H. Li, Y. Yu, W. Huang, H. Zhang and P. Chen, *Angew. Chem. Int. Edit.*, 2014, **53**, 12576-12580.
342. T. Chen, H. S. Peng, M. Durstock and L. M. Dai, *Sci. Rep.*, 2014, **4**.
343. L. Peng, X. Peng, B. Liu, C. Wu, Y. Xie and G. Yu, *Nano Lett.*, 2013, **13**, 2151-2157.
344. J. Ren, W. Y. Bai, G. Z. Guan, Y. Zhang and H. S. Peng, *Adv. Mater.*, 2013, **25**, 5965-5970.
345. L. Yuan, B. Yao, B. Hu, K. Huo, W. Chen and J. Zhou, *Energ. Environ. Sci.*, 2013, **6**, 470-476.
346. X. F. Wang, B. Liu, R. Liu, Q. F. Wang, X. J. Hou, D. Chen, R. M. Wang and G. Z. Shen, *Angewandte Chemie-International Edition*, 2014, **53**, 1849-1853.
347. H. J. Fei, C. Y. Yang, H. Bao and G. C. Wang, *J. Power Sources*, 2014, **266**, 488-495.
348. M. Kaempgen, C. K. Chan, J. Ma, Y. Cui and G. Gruner, *Nano Lett.*, 2009, **9**, 1872-1876.
349. C. Zhou and J. P. Liu, *Nanotechnology*, 2014, **25**.
350. G. M. Wang, H. Y. Wang, X. H. Lu, Y. C. Ling, M. H. Yu, T. Zhai, Y. X. Tong and Y. Li, *Adv. Mater.*, 2014, **26**, 2676-2682.
351. Y. Xu, Z. Lin, X. Huang, Y. Wang, Y. Huang and X. Duan, *Adv. Mater.*, 2013, **25**, 5779-5784.
352. G. Huang, C. Hou, Y. Shao, B. Zhu, B. Jia, H. Wang, Q. Zhang and Y. Li, *Nano Energy*, 2015, **12**, 26-32.
353. H. F. Ju, W. L. Song and L. Z. Fan, *J. Mater. Chem. A*, 2014, **2**, 10895-10903.
354. Q. Chen, X. M. Li, X. B. Zang, Y. C. Cao, Y. J. He, P. X. Li, K. L. Wang, J. Q. Wei, D. H. Wu and H. W. Zhu, *RSC Adv.*, 2014, **4**, 36253-36256.
355. H. Gao and K. Lian, *J. Electrochem. Soc.*, 2013, **160**, A505-A510.
356. C. S. Lim, K. H. Teoh, C. W. Liew and S. Ramesh, *Mater. Chem. Phys.*, 2014, **143**, 661-667.
357. C. S. Lim, K. H. Teoh, C. W. Liew and S. Ramesh, *Ionics*, 2014, **20**, 251-258.

358. Y. F. Huang, P. F. Wu, M. Q. Zhang, W. H. Ruan and E. P. Giannelis, *Electrochim. Acta*, 2014, **132**, 103-111.
359. M. Rosi, F. Iskandar, M. Abdullah and Khairurrijal, *Int. J. Electrochem. Sci.*, 2014, **9**, 4251-4256.
360. H. Gao, J. Li and K. Lian, *RSC Adv.*, 2014, **4**, 21332-21339.
361. T. M. Dinh, A. Achour, S. Vizireanu, G. Dinescu, L. Nistor, K. Armstrong, D. Guay and D. Pech, *Nano Energy*, 2014, **10**, 288-294.
362. H. M. Zheng, T. Zhai, M. H. Yu, S. L. Xie, C. L. Liang, W. X. Zhao, S. C. I. Wang, Z. S. Zhang and X. H. Lu, *J. Mater. Chem. C*, 2013, **1**, 225-229.
363. H. Gao, Y. J. Ting, N. P. Kherani and K. Lian, *J. Power Sources*, 2013, **222**, 301-304.
364. L. L. Liu, Z. Q. Niu, L. Zhang, W. Y. Zhou, X. D. Chen and S. S. Xie, *Adv. Mater.*, 2014, **26**, 4855-4862.
365. Y. Huang, J. Tao, W. Meng, M. Zhu, Y. Huang, Y. Fu, Y. Gao and C. Zhi, *Nano Energy*, 2015, **11**, 518-525.
366. N. Kurra, J. Park and H. N. Alshareef, *J. Mater. Chem. A*, 2014, **2**, 17058-17065.
367. W. L. Yang, Z. Gao, J. Ma, X. M. Zhang, J. Wang and J. Y. Liu, *J. Mater. Chem. A*, 2014, **2**, 1448-1457.
368. J. Zhao, J. Chen, S. Xu, M. Shao, D. Yan, M. Wei, D. G. Evans and X. Duan, *J. Mater. Chem. A*, 2013, **1**, 8836-8843.
369. Y. B. Xie and X. Q. Fang, *Electrochim. Acta*, 2014, **120**, 273-283.
370. G. M. Wang, X. H. Lu, Y. C. Ling, T. Zhai, H. Y. Wang, Y. X. Tong and Y. Li, *ACS Nano*, 2012, **6**, 10296-10302.
371. Y. J. Kang, H. Chung and W. Kim, *Synth. Met.*, 2013, **166**, 40-44.
372. M. Sawangphruk, P. Srimuk, P. Chiochan, A. Krittayavathananon, S. Luanwuthi and J. Limtrakul, *Carbon*, 2013, **60**, 109-116.
373. K. Y. Zhang, H. Chen, X. Wang, D. L. Guo, C. G. Hu, S. X. Wang, J. L. Sun and Q. Leng, *J. Power Sources*, 2014, **268**, 522-532.
374. P. Yang, X. Xiao, Y. Li, Y. Ding, P. Qiang, X. Tan, W. Mai, Z. Lin, W. Wu, T. Li, H. Jin, P. Liu, J. Zhou, C. P. Wong and Z. L. Wang, *ACS Nano*, 2013, **7**, 2617-2626.
375. C. Z. Wu, X. L. Lu, L. L. Peng, K. Xu, X. Peng, J. L. Huang, G. H. Yu and Y. Xie, *Nat. Commun.*, 2013, **4**, 7.
376. X. H. Lu, M. H. Yu, T. Zhai, G. M. Wang, S. L. Xie, T. Y. Liu, C. L. Liang, Y. X. Tong and Y. Li, *Nano Lett.*, 2013, **13**, 2628-2633.
377. T. Qian, N. Xu, J. Zhou, T. Yang, X. Liu, X. Shen, J. Liang and C. Yan, *J. Mater. Chem. A*, 2015, **3**, 488-493.
378. X. Xiao, X. Peng, H. Y. Jin, T. Q. Li, C. C. Zhang, B. Gao, B. Hu, K. F. Huo and J. Zhou, *Adv. Mater.*, 2013, **25**, 5091-5097.
379. K. M. Kim, J. H. Nam, Y. G. Lee, W. I. Cho and J. M. Ko, *Curr. Appl. Phys.*, 2013, **13**, 1702-1706.
380. J. M. Ko, J. H. Nam, J. H. Won and K. M. Kim, *Synth. Met.*, 2014, **189**, 152-156.

381. H. S. Nam, N. L. Wu, K. T. Lee, K. M. Kim, C. G. Yeom, L. R. Hepowit, J. M. Ko and J. D. Kim, *J. Electrochem. Soc.*, 2012, **159**, A899-A903.
382. K. M. Kim, M. Latifatu, Y. G. Lee, J. M. Ko, J. H. Kim and W. I. Cho, *J. Electroceram.*, 2014, **32**, 146-153.
383. C. Y. Yang, J. L. Shen, C. Y. Wang, H. J. Fei, H. Bao and G. C. Wang, *J. Mater. Chem. A*, 2014, **2**, 1458-1464.
384. K. Shimamoto, K. Tadanaga and M. Tatsumisago, *Electrochim. Acta*, 2013, **109**, 651-655.
385. C. K. Subramaniam and G. Boopalan, *Appl. Phys. A-Mater.*, 2014, **116**, 887-891.
386. C. Huang and P. S. Grant, *Sci. Rep.*, 2013, **3**.
387. C. Ramasamy, J. Palma and M. Anderson, *J. Solid State Electrochem.*, 2014, **18**, 2903-2911.
388. P. M. DiCarmine, T. B. Schon, T. M. McCormick, P. P. Klein and D. S. Seferos, *J. Phys. Chem. C*, 2014, **118**, 8295-8307.
389. R. Yuksel, Z. Sarioba, A. Cirpan, P. Hiralal and H. E. Unalan, *ACS Appl. Mater. Inter.*, 2014, **6**, 15434-15439.
390. K. F. Chiu and S. H. Su, *Thin Solid Films*, 2013, **544**, 144-147.
391. M. F. Hsueh, C. W. Huang, C. A. Wu, P. L. Kuo and H. Teng, *J. Phys. Chem. C*, 2013, **117**, 16751-16758.
392. S. N. Syahidah and S. R. Majid, *Electrochim. Acta*, 2013, **112**, 678-685.
393. Y. D. Chiou, D. S. Tsai, H. H. Lam, C. H. Chang, K. Y. Lee and Y. S. Huang, *Nanoscale*, 2013, **5**, 8122-8129.
394. M. Schroeder, P. Isken, M. Winter, S. Passerini, A. Lex-Balducci and A. Balducci, *J. Electrochem. Soc.*, 2013, **160**, A1753-A1758.
395. J. Rodríguez, E. Navarrete, E. A. Dalchiele, L. Sánchez, J. R. Ramos-Barrado and F. Martín, *J. Power Sources*, 2013, **237**, 270-276.
396. A. Jain and S. K. Tripathi, *Ionics*, 2013, **19**, 549-557.
397. G. Ayalneh Tiruye, D. Muñoz-Torrero, J. Palma, M. Anderson and R. Marcilla, *J. Power Sources*, 2015, **279**, 472-480.
398. S. Wang, B. Hsia, C. Carraro and R. Maboudian, *J. Mater. Chem. A*, 2014, **2**, 7997-8002.
399. G. P. Pandey and S. A. Hashmi, *J. Mater. Chem. A*, 2013, **1**, 3372-3378.
400. Y. Gao, Y. S. Zhou, M. Qian, H. M. Li, J. Redepenning, L. S. Fan, X. N. He, W. Xiong, X. Huang, M. Majhour-Samani, L. Jiang and Y. F. Lu, *RSC Adv.*, 2013, **3**, 20613-20618.
401. G. P. Pandey, A. C. Rastogi and C. R. Westgate, *J. Power Sources*, 2014, **245**, 857-865.
402. S. S. A. Hashmi, *J. Solid State Electrochem.*, 2014, **18**, 465-475.
403. P. Tamilarasan and S. Ramaprabhu, *Mater. Chem. Phys.*, 2014, **148**, 48-56.
404. Y. Lim, J. Yoon, J. Yun, D. Kim, S. Y. Hong, S. J. Lee, G. Zi and J. S. Ha, *ACS Nano*, 2014, **8**, 11639-11650.
405. C. W. Liew, S. Ramesh and A. K. Arof, *Int. J. Hydrogen Energy*, 2014, **39**, 2953-2963.

406. S. Ketabi and K. Lian, *Electrochim. Acta*, 2013, **103**, 174-178.
407. M. Suleman, Y. Kumar and S. A. Hashmi, *J. Phys. Chem. B*, 2013, **117**, 7436-7443.
408. M. Yamagata, K. Soeda, S. Ikebe, S. Yamazaki and M. Ishikawa, *Electrochim. Acta*, 2013, **100**, 275-280.
409. L. Yang, J. Hu, G. Lei and H. Liu, *Chem. Eng. J.*, 2014, **258**, 320-326.
410. G. P. Pandey, A. C. Rastogi and C. R. Westgate, *Electrochemical Capacitors*, 2013, **50**, 145-151.
411. G. P. Pandey and S. A. Hashmi, *J. Power Sources*, 2013, **243**, 211-218.
412. X. H. Liu, Z. B. Wen, D. B. Wu, H. L. Wang, J. H. Yang and Q. G. Wang, *J. Mater. Chem. A*, 2014, **2**, 11569-11573.
413. R. Taniki, K. Matsumoto, T. Nohira and R. Hagiwara, *J. Power Sources*, 2014, **245**, 758-763.
414. M. F. Shukur, R. Ithnin and M. F. Z. Kadir, *Electrochim. Acta*, 2014, **136**, 204-216.
415. Y. N. Sudhakar and M. Selvakumar, *Electrochim. Acta*, 2012, **78**, 398-405.
416. H. J. Woo, C. W. Liew, S. R. Majid and A. K. Arof, *High Perform. Polym.*, 2014, **26**, 637-640.
417. N. Shirshova, A. Bismarck, S. Carreyette, Q. P. V. Fontana, E. S. Greenhalgh, P. Jacobsson, P. Johansson, M. J. Marczewski, G. Kalinka, A. R. J. Kucernak, J. Scheers, M. S. P. Shaffer, J. H. G. Steinke and M. Wienrich, *J. Mater. Chem. A*, 2013, **1**, 15300-15309.
418. A. S. Westover, J. W. Tian, S. Bernath, L. Oakes, R. Edwards, F. N. Shabab, S. Chatterjee, A. V. Anilkumar and C. L. Pint, *Nano Lett.*, 2014, **14**, 3197-3202.
419. Q. Zhang, K. Scrafford, M. T. Li, Z. Y. Cao, Z. H. Xia, P. M. Ajayan and B. Q. Wei, *Nano Lett.*, 2014, **14**, 1938-1943.
420. W. Gao, N. Singh, L. Song, Z. Liu, A. L. M. Reddy, L. Ci, R. Vajtai, Q. Zhang, B. Wei and P. M. Ajayan, *Nat. Nanotech.*, 2011, **6**, 496-500.
421. K. Fic, E. Frackowiak and F. Béguin, *J. Mater. Chem.*, 2012, **22**, 24213-24223.
422. G. Lota, K. Fic and E. Frackowiak, *Electrochem. Commun.*, 2011, **13**, 38-41.
423. E. Frackowiak, K. Fic, M. Meller and G. Lota, *ChemSusChem*, 2012, **5**, 1181-1185.
424. J. Suarez-Guevara, V. Ruiz and P. Gomez-Romero, *J. Mater. Chem. A*, 2014, **2**, 1014-1021.
425. K. Lian and C. M. Li, *Electrochem. Solid St.*, 2009, **12**, A10-A12.
426. Q. F. Tian and K. Lian, *Electrochem. Solid St.*, 2010, **13**, A4-A6.
427. L. Q. Mai, A. Minhas-Khan, X. Tian, K. M. Hercule, Y. L. Zhao, X. Lin and X. Xu, *Nat. Commun.*, 2013, **4**, 1-7.
428. I. Tanahashi, *Electrochem. Solid St.*, 2005, **8**, A627-A629.
429. S. Roldán, M. Granda, R. Menéndez, R. Santamaría and C. Blanco, *J. Phys. Chem. C*, 2011, **115**, 17606-17611.
430. L. B. Chen, H. Bai, Z. F. Huang and L. Li, *Energ. Environ. Sci.*, 2014, **7**, 1750-1759.
431. S. Roldán, M. Granda, R. Menéndez, R. Santamaría and C. Blanco,

- Electrochim. Acta*, 2012, **83**, 241-246.
432. S. Roldan, Z. Gonzalez, C. Blanco, M. Granda, R. Menendez and R. Santamaria, *Electrochim. Acta*, 2011, **56**, 3401-3405.
433. J. Wu, H. Yu, L. Fan, G. Luo, J. Lin and M. Huang, *J. Mater. Chem.*, 2012, **22**, 19025-19030.
434. H. Yu, L. Fan, J. Wu, Y. Lin, M. Huang, J. Lin and Z. Lan, *RSC Adv.*, 2012, **2**, 6736-6740.
435. G. Lota and G. Milczarek, *Electrochem. Commun.*, 2011, **13**, 470-473.
436. L. B. Chen, Y. R. Chen, J. F. Wu, J. W. Wang, H. Bai and L. Li, *J. Mater. Chem. A*, 2014, **2**, 10526-10531.
437. K. Wasinski, M. Walkowiak and G. Lota, *J. Power Sources*, 2014, **255**, 230-234.
438. S. Maiti, A. Pramanik and S. Mahanty, *ACS Appl. Mater. Inter.*, 2014, **6**, 10754-10762.
439. C. M. Zhao, W. T. Zheng, X. Wang, H. B. Zhang, X. Q. Cui and H. X. Wang, *Sci. Rep.*, 2013, **3**.
440. S. T. Senthilkumar, R. Kalai Selvan, M. Ulaganathan and J. S. Melo, *Electrochim. Acta*, 2014, **115**, 518-524.
441. H. Xie, Y. H. Zhu, Y. H. Wu, Z. L. Wu and E. H. Liu, *Mater. Res. Bull.*, 2014, **50**, 303-306.
442. W. Chen, R. B. Rakhi and H. N. Alshareef, *Nanoscale*, 2013, **5**, 4134-4138.
443. C. M. Ionica-Bousquet, W. J. Casteel Jr, R. M. Pearlstein, G. GirishKumar, G. P. Pez, P. Gómez-Romero, M. R. Palacín and D. Muñoz-Rojas, *Electrochem. Commun.*, 2010, **12**, 636-639.
444. R. Taniki, K. Matsumoto, T. Nohira and R. Hagiwara, *J. Electrochem. Soc.*, 2013, **160**, A734-A738.
445. T. Tooming, T. Thomborg, L. Siinor, K. Tonurist, A. Janes and E. Lust, *J. Electrochem. Soc.*, 2014, **161**, A222-A227.
446. S. Yamazaki, T. Ito, M. Yamagata and M. Ishikawa, *Electrochim. Acta*, 2012, **86**, 294-297.
447. J. Zhou, Y. Yin, A. N. Mansour and X. Zhou, *Electrochem. Solid-State Lett.*, 2011, **14**, A25-A28.
448. Y. Yin, J. Zhou, A. N. Mansour and X. Zhou, *J. Power Sources*, 2011, **196**, 5997-6002.
449. G. Ma, J. Li, K. Sun, H. Peng, J. Mu and Z. Lei, *J. Power Sources*, 2014, **256**, 281-287.
450. S. T. Senthilkumar, R. K. Selvan, J. S. Melo and C. Sanjeeviraja, *ACS Appl. Mater. Inter.*, 2013, **5**, 10541-10550.
451. S. T. Senthilkumar, R. K. Selvan, N. Ponpandian and J. S. Melo, *RSC Adv.*, 2012, **2**, 8937-8940.
452. G. F. Ma, E. K. Feng, K. J. Sun, H. Peng, J. J. Li and Z. Q. Lei, *Electrochim. Acta*, 2014, **135**, 461-466.
453. H. Yu, J. Wu, L. Fan, Y. Lin, K. Xu, Z. Tang, C. Cheng, S. Tang, J. Lin, M. Huang and Z. Lan, *J. Power Sources*, 2012, **198**, 402-407.



454. F. D. Yu, M. L. Huang, J. H. Wu, Z. Y. Qiu, L. Q. Fan, J. M. Lin and Y. B. Lin, *J. Appl. Polym. Sci.*, 2014, **131**.
455. A. N. Mansour, J. J. Zhou and X. Y. Zhou, *J. Power Sources*, 2014, **245**, 270-276.
456. J. Zhou, J. Cai, S. Cai, X. Zhou and A. N. Mansour, *J. Power Sources*, 2011, **196**, 10479-10483.
457. I. Ryu, M. Yang, H. Kwon, H. K. Park, Y. R. Do, S. B. Lee and S. Yim, *Langmuir*, 2014, **30**, 1704-1709.
458. H. W. Cho, L. R. Hepowit, H. S. Nam, S. H. Kim, Y. M. Lee, J. H. Kim, K. M. Kim and J. M. Ko, *Synth. Met.*, 2012, **162**, 410-413.
459. B. H. Wee and J. D. Hong, *Langmuir*, 2014, **30**, 5267-5275.
460. Y. S. Yun, M. E. Lee, M. J. Joo and H. J. Jin, *J. Power Sources*, 2014, **246**, 540-547.
461. X. F. Gong, J. P. Cheng, F. Liu, L. Zhang and X. B. Zhang, *J. Power Sources*, 2014, **267**, 610-616.
462. W. Xing, S. Z. Qiao, X. Z. Wu, X. L. Gao, J. Zhou, S. P. Zhuo, S. B. Hartono and D. Hulicova-Jurcakova, *J. Power Sources*, 2011, **196**, 4123-4127.
463. F. Xiang, J. Zhong, N. Y. Gu, R. Mukherjee, I. K. Oh, N. Koratkar and Z. Y. Yang, *Carbon*, 2014, **75**, 201-208.
464. R. Shah, X. F. Zhang and S. Talapatra, *Nanotechnology*, 2009, **20**, 5.
465. N. A. Alhebshi, R. B. Rakhi and H. N. Alshareef, *J. Mater. Chem. A*, 2013, **1**, 14897-14903.
466. R. F. Zhou, C. Z. Meng, F. Zhu, Q. Q. Li, C. H. Liu, S. S. Fan and K. L. Jiang, *Nanotechnology*, 2010, **21**.
467. J. Xu, Q. Wang, X. Wang, Q. Xiang, B. Liang, D. Chen and G. Shen, *ACS Nano*, 2013, **7**, 5453-5462.
468. L. Huang, D. C. Chen, Y. Ding, Z. L. Wang, Z. Z. Zeng and M. L. Liu, *ACS Appl. Mater. Inter.*, 2013, **5**, 11159-11162.
469. J. Ji, L. L. Zhang, H. Ji, Y. Li, X. Zhao, X. Bai, X. Fan, F. Zhang and R. S. Ruoff, *ACS Nano*, 2013, **7**, 6237-6243.
470. J. W. Xiao, S. X. Yang, L. Wan, F. Xiao and S. Wang, *J. Power Sources*, 2014, **245**, 1027-1034.
471. Z. J. Su, C. Yang, B. H. Xie, Z. Y. Lin, Z. X. Zhang, J. P. Liu, B. H. Li, F. Y. Kang and C. P. Wong, *Energ. Environ. Sci.*, 2014, **7**, 2652-2659.
472. Z. Q. Wang, Z. S. Li, J. Y. Feng, S. C. Yan, W. J. Luo, J. G. Liu, T. Yu and Z. G. Zou, *Phys. Chem. Chem. Phys.*, 2014, **16**, 8521-8528.
473. J. S. Kim, S. S. Shin, H. S. Han, L. S. Oh, D. H. Kim, J. H. Kim, K. S. Hong and J. Y. Kim, *ACS Appl. Mater. Inter.*, 2014, **6**, 268-274.
474. H. Zhou and Y. R. Zhang, *J. Phys. Chem. C*, 2014, **118**, 5626-5636.
475. J. Liu, F. Mirri, M. Notarianni, M. Pasquali and N. Motta, *J. Power Sources*, 2014, **274**, 823-830.
476. A. M. Bittner, M. Zhu, Y. Yang, H. F. Waibel, M. Konuma, U. Starke and C. J. Weber, *J. Power Sources*, 2012, **203**, 262-273.
477. R. S. Kühnel, J. Reiter, S. Jeong, S. Passerini and A. Balducci, *Electrochem.*

- Commun.*, 2014, **38**, 117-119.
478. R. S. Kühnel and A. Balducci, *J. Power Sources*, 2014, **249**, 163-171.
479. M. Meller, J. Menzel, K. Fic, D. Gastol and E. Frackowiak, *Solid State Ionics*, 2014, **264**, 61-67.
480. Y. W. Cheng, S. T. Lu, H. B. Zhang, C. V. Varanasi and J. Liu, *Nano Lett.*, 2012, **12**, 4206-4211.
481. W. J. Cao, Y. X. Li, B. Fitch, J. Shih, T. Doung and J. Zheng, *J. Power Sources*, 2014, **268**, 841-847.
482. S. Paul, K. S. Choi, D. J. Lee, P. Sudhagar and Y. S. Kang, *Electrochim. Acta*, 2012, **78**, 649-655.
483. X. Liu and P. G. Pickup, *J. Power Sources*, 2008, **176**, 410-416.
484. M. Aslan, D. Weingarth, N. Jackel, J. S. Atchison, I. Grobelsek and V. Presser, *J. Power Sources*, 2014, **266**, 374-383.
485. K. T. Lee, C. B. Tsai, W. H. Ho and N. L. Wu, *Electrochem. Commun.*, 2010, **12**, 886-889.
486. A. Varzi, A. Balducci and S. Passerini, *J. Electrochem. Soc.*, 2014, **161**, A368-A375.
487. H. Lee, H. Kim, M. S. Cho, J. Choi and Y. Lee, *Electrochim. Acta*, 2011, **56**, 7460-7466.
488. C. Lei, P. Wilson and C. Lekakou, *J. Power Sources*, 2011, **196**, 7823-7827.
489. M. Kang, J. E. Lee, H. W. Shim, M. S. Jeong, W. B. Im and H. Yoon, *RSC Adv.*, 2014, **4**, 27939-27945.
490. K. Tonurist, T. Thomberg, A. Janes, I. Kink and E. Lust, *Electrochem. Commun.*, 2012, **22**, 77-80.
491. X. R. Liu and P. G. Pickup, *Energ. Environ. Sci.*, 2008, **1**, 494-500.
492. Y. M. Shulga, S. A. Baskakov, V. A. Smirnov, N. Y. Shulga, K. G. Belay and G. L. Gutsev, *J. Power Sources*, 2014, **245**, 33-36.
493. H. J. Yu, Q. Q. Tang, J. H. Wu, Y. Z. Lin, L. Q. Fan, M. L. Huang, J. M. Lin, Y. Li and F. D. Yu, *J. Power Sources*, 2012, **206**, 463-468.
494. N. Devillers, S. Jemei, M. C. Pera, D. Bienaime and F. Gustin, *J. Power Sources*, 2014, **246**, 596-608.
495. A. Burke and M. Miller, *Electrochim. Acta*, 2010, **55**, 7538-7548.
496. M. D. Stoller and R. S. Ruoff, *Energ. Environ. Sci.*, 2010, **3**, 1294-1301.
497. K. Xu, M. S. Ding and T. R. Jow, *Electrochim. Acta*, 2001, **46**, 1823-1827.
498. E. J. Olson and P. Buhlmann, *J. Electrochem. Soc.*, 2012, **160**, A320-A323.
499. D. Weingarth, H. Noh, A. Foelske-Schmitz, A. Wokaun and R. Kotz, *Electrochim. Acta*, 2013, **103**, 119-124.
500. C. Largeot, C. Portet, J. Chmiola, P. L. Taberna, Y. Gogotsi and P. Simon, *J. Am. Chem. Soc.*, 2008, **130**, 2730-+.
501. T. A. Centeno, O. Sereda and F. Stoeckli, *Phys. Chem. Chem. Phys.*, 2011, **13**, 12403-12406.
502. J. R. Miller and A. F. Burke, *Electrochem. Soc. Interface*, 2008, **17**, 53-57.
503. D. E. Jiang, Z. Jin and J. Wu, *Nano Lett.*, 2011, **11**, 5373-5377.
504. V. Ozolinš, F. Zhou and M. Asta, *Acc. Chem. Res.*, 2013, **46**, 1084-1093.

505. H. Zhong, F. Xu, Z. Li, R. Fu and D. Wu, *Nanoscale*, 2013, **5**, 4678-4682.
506. H. C. Huang, C. W. Huang, C. T. Hsieh and H. Teng, *J. Mater. Chem. A*, 2014, **2**, 14963-14972.
507. A. J. Roberts, A. F. D. De Namor and R. C. T. Slade, *Phys. Chem. Chem. Phys.*, 2013, **15**, 3518-3526.